Università di Pisa

Facoltà di Scienze Matematiche, Fisiche e Naturali

Corso di Laurea Magistrale in Fisica

A Field Theoretical Approach to Stationarity in Reaction-Diffusion Processes

Candidato:
Simone Cenci

Relatori:
Dr. Gunnar Pruessner
Prof. Ettore Vicari

Anno accademico 2014/2015

Alla mia famiglia

CONTENTS

ACKNOWLEDGEMENTS

INTRODUCTION

The fast and exciting growth of interest in the study of complex systems emerges from the necessity to develop techniques for estabilishing an understanding of how, in systems made of many interacting units, the systemic collective behaviour is related to the dynamics of the collection of the components.
Since the focus is on similarity between different macroscopic systems, complexity science is inevitably a cross disciplinary field. This latter peculiarity makes the, relatively new discipline a beautiful and challenging field of research.

In this context statistical mechanics is an unequalled tool which allow a rigorous approach to the problem. It is fascinating how the very same techniques that have been developed for the study of physical systems, and in particular systems that exhibit a second-oder phase transition, can be applied in many other fields such as biology, population dynamics, economy, etc...

The work of this thesis has been carried out in the department of mathematics at Imperial College London under the supervision of Dr. Gunnar Pruessner and in collaboration with Dr. Chiu Fan Lee, in the department of bioengineering. The aim of the project is to devise a general method to characterise the stationary state in finite mesoscopic systems, subjected to particular microscopic, local dynamics. Specifically, we have investigated, by means of field-theoretic techniques, the non-universal properties of a class of *reaction-diffusion systems*. These are stochastic models that, as it will be explained in more detail later on, can be used to describe a plethora of different phenomena, ranging from condensed matter physics to biology, ecology, just to quote few of them.
To make the stochastic process accessible to field-theoretic methods we have taken the *Doi-Peliti* formalism which provides an exact description of the process in terms of a field theory. Furthermore, alongside the analytical approach we have investigated the system by means of numerical simulations in C.

The thesis is organised as follow:

- In the first chapter, we will give an overview of stochastic processes, equilibrium and non-equilibrium statistical mechanics. To offer an insight into the world of reaction-diffusion processes we will give some example of models that can be undesrtood in terms of such systems. All the figures of the chapter have been generated by numerical simulations in C.

- In the second chapter, we will introduce the model which was under investigation in this project and the Doi-Peliti formalism. We will discuss the main features of the formalism and we will derive the master equation which describe the temporal evolution of the probability distribution for the abovementioned model. In the last section we will focus on the mapping of the master equation into a field theory.

- In the third chapter, which is the core of the thesis, we will present the analytical results that we have obtained by means of a diagrammatic expansion. In order to check the quality of the loop expansion, we will compare the latter with numerical simulations. The last part of the chapter is devoted to the introduction and the preliminary results for a model that will be investigated in future works (i.e. *the Brusselator*).

- In the fourth and last chapter, we will present the numerical results, dwelling on details of the simulations.

Works related with this thesis:

- Imperial College London, Centre for Complexity Science, internal seminar:
  Talk: *A field theoretical approach to stationarity in reaction-diffusion processes.* 25/06/2015

- S. Cenci,G. Pruessner,C.F. Lee:
  Poster: *A field theoretical approach to non-universal properties of the contact process with diffusion.* Physics of Emergent Behavior, Science Museum, London 09-10/07/2015

CHAPTER 1

NON-EQUILIBRIUM STATISTICAL MECHANICS

In this chapter we will describe some of the most important features of stochastic processes and non-equilibrium statistical mechanics. In the last section we will discuss and give examples of reaction-diffusion processes which are the main subject of this thesis.

1.1 Stochastic Processes

When dealing with complex systems random behavior is a common feature as, in most of the situations, the details of the microscopic behavior, in principle specified by the microscopic Hamiltonian of the system, are not fully understood [1]. For this reason statistical mechanics become so important nowadays and its applicability has gone well beyond the domain of physics making the subject of vital importance for a wide range of disciplines.

1.1.1 Markov Processes

A number of important notions associated with stochastic processes are conveniently introduced using the specific example of the discrete-time Markov process [2]. Let us consider a physical system which at time t is in a given configuration $\omega \in \Omega$ with Ω being the set of all possible configurations. At time $t+1$ the system will evolve in a new configuration ω' with a transition probability[1] $\Gamma(\omega \to \omega')$. In a Markov process a configuration at time $t+1$ depends only on the configuration of the system at the previous time t. Specifically, let $X(t)$ be a stochastic process taking value in a countable state space $\mathcal{T}$, where $\mathcal{T}$ can either be the integer $\mathbb{Z}$ (discrete time) or the real axis $\mathbb{R}$ (continuous time). Calling $X(t_i) = \omega_i$, the

---

[1]Note that in discrete time Markov processes we deal with transition probabilties not rates
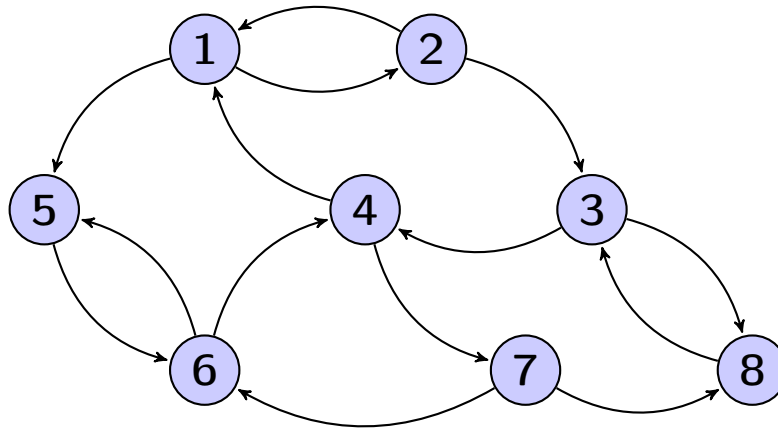
Figure 1.1: Graphical representation of a stochastic process. In the figure are pictured only the allowed transitions (i.e. $\Gamma(\omega \to \omega') \neq 0$).

stochastic process is said to be a Markov process if:

$$P(\omega_{n+1}|\omega_1, \ldots, \omega_n) = P(\omega_{n+1}|\omega_n) \tag{1.1}$$

Where $t_1 < t_2 < \cdots < t_n < t_{n+1}$ [4].

There is a convinient graphical representation of a discrete time Markov process in terms of *directed graphs*, a digraph $G(V, E)$ is a finite, non empty set V, together with a set E that contains ordered pairs of distinct elements of V [3]. In what follow the graph is constructed by drawing a vertex which represent a possible configuration of the system (elements of the set V) and a directed edge from one vertex to another whenever the transition probability between the two is not zero (Figure 1.1).

For a general set of transition probabilities there may be more than one sequence of transitions (directed path) that leads from an initial configuration ω_0 to a specified configuration ω_t at time t. Each of these sequences form a realisation of the stochastic process.

The set of all the configurations, the transition rates and the initial conditions fully define the stochastic model [1]. Note that the graph is far from being *fully connected* as jumps between very different configurations are usually impossible.

In the study of a stochastic system we are mainly interested in the conditional probability $P(\omega_n, t_n|\omega_{n-1}, t_{n-1})$ to find the system in ω_n at time t_n given that at time t_{n-1} was in the configuration ω_{n-1}.

From now on the probability distribution will be deonted by $P_t(\omega)$ with the normalisation condition $\sum_{\omega \in \Omega} P_t(\omega) = 1 \ \forall t$

1.1.2   The Master Equation

Let us now consider a continuous-time Markov process, this is defined in terms of transition rates $R(\omega \to \omega')$. In a continuos time process we assume that in the limit $dt \to 0$ (where dt is an infinitesimal time step) only one transition can occur and the probability of this transition is $R(\omega \to \omega')dt$ [2].

The evolution of the system's configuration is generally unpredictable due to its stochastic nature whereas the temporal evolution of the probability distribution is predictable and given by the *master equation*.

The master equation is a linear partial differantial equation that express the rate at which a system moves between states labelled by $\{\omega\}$. At time t, let the system be in state ω with probability $P_t(\omega)$ and consider the time derivative of such a probability. The change in P is due to transitions into and out of the state ω [34]. The generic form of a master equation is:

$$\frac{\partial P_t(\omega)}{\partial t} = \sum_{\omega' \neq \omega} R(\omega' \to \omega)P_t(\omega') - R(\omega \to \omega')P_t(\omega) \qquad (1.2)$$

This equation can be seen as a flow in the configuration space, the first term on the right hand side describes the rate at which the probability flows into the configuration ω, it is referred to as the *gain term* and contribute to the master equation with a positive sign. The other term describe the outflow to other configurations, it is often called the *loss term* and appears with a negative sign.

The terms that appear in the master equation are rates and, in contrast to the probabilities, their numerical value depends upon the unit of time and may be larger than one. Rescaling all rates of a system by the same factor it is equivalent to a change of the time scale, this strategy is usually adopted in the implementation of numerical simulations, see chapter 4.

Since the temporal change of $P_t(\omega)$ is fully determined by the actual probability distribution at time t, the master equation describes a Markov process.

Let N be the number of possible configurations, by casting the probability distribution into a vector that, using the Dirac notation, we denote by $|P_t\rangle$:

$$|P_t\rangle = \begin{pmatrix} P_t(\omega_1) \\ P_t(\omega_2) \\ \dots \\ P_t(\omega_N) \end{pmatrix} \qquad (1.3)$$

we can rewrite the master equation in a more compact form:

$$\partial_t |P_t\rangle = -\mathcal{L} |P_t\rangle \qquad (1.4)$$

Since the probability distribution is usually refered to as the state of the system the vector $|P_t\rangle$ is often called *state vector*. $|P_t\rangle \in V$ with V being a real vector space with dimension $d = N$ [5]. Furthemore, as the elements of V are positive

and sum up to one the actual *state space* V is a subset of $\mathbb{R}^N$.

The operator $\mathcal{L}$ is the *Liouville* operator which in the *canonical configuration basis* is defined by the matrx elements:

$$\langle \omega' | \mathcal{L} | \omega \rangle = -R(\omega \to \omega') + \delta_{\omega,\omega'} \sum_{\omega''} R(\omega \to \omega'') \tag{1.5}$$

Given an initial probability distribution $|P_0\rangle$ we can write a formal solution: $|P_t\rangle = e^{-\mathcal{L}t} |P_0\rangle$.
To find the solution we need to diagonalise the Liouville operator i.e. we need to solve the eigenvalue problem:

$$\mathcal{L} |k\rangle = k |k\rangle \tag{1.6}$$

expanding the initial state as a linear combination of eigenvectors : $|P_0\rangle = \sum_k a_k |k\rangle$ the formal solution che be written as [5]:

$$|P_t\rangle = e^{-\mathcal{L}t} \sum_k a_k |k\rangle = \sum_k a_k e^{-\mathcal{L}t} |k\rangle = \sum_k a_k e^{-\lambda_k t} |k\rangle \tag{1.7}$$

Even though the master equation has been rewritten in a much more elegant and compact form, its solution is still not trivial as the diagonalisation of the Liouville operator is generally a complicated task. In order to solve the master equation one usually adopt approximation schemes such as the Van Kampen system size expansion or the Kramers-Moyal expansion.
A much more fascinating method for dealing with the master equation is the *Doi-Peliti* formalism, which will be presented in detail in the next chapter. Nevertheless, it is interesting to make a further remark: the gain (+) and loss (-) terms in the master equation correspond to the non diagonal and diagonal elements of the Liouville oeprator, which, given the minus sign in front of its definition, has (negative) positive (non) diagonal elements. Furthermore, the sum over all columns of $\mathcal{L}$ is zero, a matrix having these propeties is refered to as *intesity matrix*.
Intesity matrices have at least one eigenvector with eigenvalue zero [5], given the solution (1.7) the state that correspond to the eigenvalue zero is the only one that survive for $t \to \infty$. Such a state is refered to as *the stationary state* and it is often denoted by $|P_\infty\rangle$, from now on by stationarity we mean a state with *time-independent* probability distribution. It is important to remark that the concept of stationarity has not to be confused with the notion of *thermal equilibrium*, the latter is a much stronger constrain and the two do not necessary come together.

Before ending this section we would like to make a note.
Stochastic processes with continuous time evolve by *asynchronous dynamics* i.e. transitions from a state ω into another state ω' occur spontaneously at a given rate $R(\omega \to \omega') \geq 0$ [1]. On the other hand, discrete time processes evolve by

synchronous dynamic, i.e. all lattice sites are simultaneously update according to certain transition probabilities $\Gamma(\omega \to \omega') \in [0,1]$. The temporal evolution of the probability distribution of the former is capture by equation (1.2), wheares if the time variable t is a discrete quantity the corresponding master equation is a linear recurrence relation:

$$P_{t+1}(\omega) = P_t(\omega) + \sum_{\omega'} \Gamma(\omega' \to \omega)P_t(\omega') - \sum_{\omega'} \Gamma(\omega \to \omega')P_t(\omega) \qquad (1.8)$$

It is interesting to note (see [1]) that in both cases the dynamic rules are simplified descriptions of a much more complex physical process. Therefore, in the description of a physical system we cannot say *a priori* which of the two dynamics is more suitable. The choice of the dynamic procedure should depend on the specific physical system under consideration. Very often both variants display essentially the same physical properties. In some cases, however, they lead to different results.

1.1.3 The Detailed Balance

In the last part of this section we want to discuss a concept that assumes a fundamental role in any discussion of equilibrium and non-equilibrium statistical physics i.e. *the detailed balance*
Let us consider a stationary (i.e. time independent) probability distribution $P^*(\omega)$, the master equation reads:

$$\sum_{\omega' \neq \omega} R(\omega' \to \omega)P^*(\omega') - R(\omega \to \omega')P^*(\omega) = 0 \qquad \forall \omega \in \Omega \qquad (1.9)$$

because of the time independece of P^*. Equation (1.9) states that the sum of all transitions per unit time into any state ω must be balanced by the sum of all transitions into ω' [6]. The detailed balance is a much stronger condition: a process is said to obey the detailed balance if the probability current between pairs of configurations compense each others, i.e. if each term in the summation (1.9) is zero [2, 9]:

$$R(\omega' \to \omega)P^*(\omega') = R(\omega \to \omega')P^*(\omega) \qquad (1.10)$$

A proof of this statement can be found in [6] in a closed, isolated and finite classical system.

As pointed out in [1] and graphically depicted in figure 1.2, even though the detailed balance imply stationarity the *vice versa* is not generally true, non-equilibrium stationary states will be investigated in the following chapters and are the main topics of this thesis.
Condition (1.10) gives a method through which the stationary probability distribution can be obtained efficiently from the transition rates. The power of equilibrium
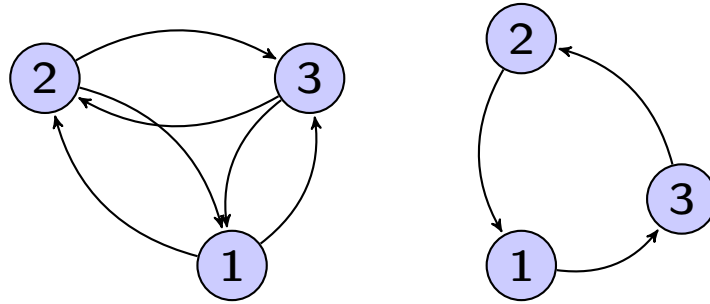
Figure 1.2: Detailed balance imply stationarity but the opposite is not generally true

statistical mechanics rely precisely on this condition which allow the probability of a particular state to be represented by the *Boltzmann-Gibbs distribution* [12]. On the other hand, in the absence of detailed balance one does not have a general means to calculate the steady-state probability distribution.

We can give a definition of a nonequilibrium system as one whose microscopic transition rates do not satisfy detailed balance [2].

It is now worth it to underline a distinction in the terminology. Systems governed by a Hamiltonian which relax back to an equilibrium state (where the detailed balance is restored) are usually referred to as *out of equilibrium*, their importance lies in the presence of a dynamics and thus in the presence of a notion of *time*.

On the other hand, *far from equilibrium systems* are always out of equilibrium, they never relax to a state that obey detailed balance[12].

A particularly interesting class of far from equilibrium systems are those who exhibits an *absorbing state phase transition*. A discussion of this systems will be presented later on in this chapter.

1.2   Equilibrium and non-equilibrium statistical mechanics

As outlined above, for systems at thermal equilibrium we can rely on the Boltzmann-Gibbs stationary probability distribution $P_{eq}(\omega) = \frac{1}{Z} e^{-E(\omega)/K_B T}$ from which, in principle, we can extract the expectation value of any time-independent observables. However, in most cases, such a calculation is an unwieldy task and an exact solution cannot be found. In order to deal with such cumbersome systems, powerful and fascinating techniques have been developed [1].

Systems that exhibits collective behavior of the microscopic degree of freedom on large scales , such as those observed in second order phase transitions, are particularly interesting to investigate. Plenty of captivating phenomena arise in such systems and, in the domain of equilibrium physics, a vast and beautiful literature can be found, see for example: [15, 17, 51].

Before going into the description of *non-equilibrium systems* we review few basics concepts which have been deeply investigated in equilibrium statistical mechanics,

namely: *universality* and *scale invariance*.

1.2.1   Scale invariance and universality in equilibrium statistical mechanics

The concept of *universality* was originally introduced by the experimentalists in order to describe the observation that many different physical systems behave in the very same way near a continuous phase transition. In particular, it was observed that some quantites, like the critical temperature, depend sensitively upon the details of the interaction, whereas other observables, like for example the *critical exponents*, depend only on a small number of general feature (dimension and symmetries of the system) [8]. The latter are usually called *universal properties* of the system.
An explanation of the physical origin of universality has been found in the framework of the Renormalisation Group (RG) which is probably the most successful tool to study the statistical mechanics of phase transitions.

There is not a unique definition for the Renormalisation Group, the name itself is slightly misleading as the mathematical structure of the procedure is not that of a group [17]. The basis idea of RG is re-expressing the parameters which define a problem in terms of some others while keeping unchanged those physical aspects of the problem which are of interest [19]. All the RG methods end up with mathematical equations describing renormalisation group flows in a parameter space. The essence of renormalisation group theory is the analysis of these flows. In the context of equilibrium critical behaviour, this general aspect of the renormalisation group appears most directly in the method of real space renormalisation [19].

The RG is a set of symmetry transformations operating on a space of parameters, we will call this parameters K ($K = (K_1, K_2, \ldots, K_n)$) and we define a RG transformation $\mathbf{R}_s$ as follow:

$$K' = \mathbf{R}_s K \tag{1.11}$$

An assumption has to be made, *the parameters $(K_1, K_2, \ldots)$ are analytic functions of the temperature* and the new parameters $K'_1, K'_2, \ldots$ are analytic function of the K_i [19]. A point, in the parameter space, which is invariant under $\mathbf{R}_s$ is refered to as *fixed point*:

$$K^* = \mathbf{R}_s K^* \tag{1.12}$$

For example in the Ising model the T-dependece enters in the parameters through K_1 and the *critical point* is at $K_1 = K_{1c} \sim 0.44$ corresponding to a temperature $T = T_c = 2.27 J/k$ [15].

A fixed point is physically significant bacause the system become invariant under scale transformation, thus the correlation length of the system is either 0 or ∞. The latter is the one we are interested in, as the divergence of the correlation length, and the resulting appearence of scale-invariant structures, is the hallmark of critical phenomena.

As an example we can again take the Ising model, let us consider a ferromagnetic material a $T > T_c$.

In the absence of magnetic fields the system will be made of clusters of up-spins and clusters of down-spins. Their average size will be of the order of the correlation length ξ which is the tipical distance over which the microscopic variables are correlated. Decreasing the temperature toward T_c the size of the clusters and the correlation length will increase. Precisely at the critical point we oberve clusters of all size with up-spin islands immerse in a sea of down-spins and so on and so forth [10].

At this temperature fluctuactions extend over regions of all possible dimensions and the system has not scale of length i.e. at the critical point the system is invariant under scale transformation [15]. A fundamental hypotesis in the theory of critical phenomena is the *scaling hypotesis* which states that, close to criticality, the only characteristic length is the correlation length and all the other quantities are expressed as function of ξ. Since experimental observations show that ξ diverges at criticality the system at the critical point has not characteristic length, i.e. it exhibits scale invariance [10].

In the parameter space it is possible to define a *critical surface* of the fixed point K^* which is that particular subspace in which all points have the property:

$$\lim_{s \to \infty} \mathbf{R}_s K = K^* \tag{1.13}$$

the long distance properties of each system corresponding to a point on this surface will be controlled by the fixed point.

Thanks to the assumption of the analyticity of the K_i , we can linearise the RG transformation about the fixed point and perform a linear stability analysis.

For a point near K^* we can write: $K = K^* + \delta K$, equation (1.11) can be written as:

$$\delta K' = \mathbf{R}_s^l \delta K + h.o.t. \tag{1.14}$$

In a linear approximation we ignore higher order terms and $\mathbf{R}_s^l$ is a linear operator. Let K_a be the ath entry of K, then:

$$(\mathbf{R}_s^l)_{ab} = \frac{\partial K_a'}{\partial K_b}|_{K=K^*} \implies \delta K_a' \sim \sum_b (\mathbf{R}_s^l)_{ab} \delta K_b \tag{1.15}$$

The eigenvalues of the matrix that represent RG near the fixed point are related to the critical exponents that correspond to that fixed point.

The fundamental hypotesis linking the RG to the theory of critical phenomena is that *the point in the parameter space representing a system at a critical point lies on the critical surface* [17]. Different materials at the critical point can be represented by different point on the same critical surface. Thus, as the critical exponents are properties of RG in the neighbouring of a fixed point these material will share the same critical exponents.

A *universality class* consists of all those critical models wich flow into a particular fixed point, to each class will correspond a different fixed point.

The concept of universality class can be extended to non-equilibrium phase transitions but a general classification is still needed.

1.2.2 Non-equilibrium systems

In nature thermal equilibrium is rather an exception than a rule, hence understanding the non-equilibrium dynamics of physical systems is currently one of the most challenging problems in statistical physics. In contrast with equilibrium systems, where a description in terms of probabilities of the micro-states can be given by means of the Boltzamm-Gibbs probability distribution, in non equilibrium such a formalism does not yet exist [18].

A common way of approaching such systems is to write down either a master equation for the probability distribution or, alternatively, a stochastic *Langevin equation* for some average of physical observables [8]. Nevertheless, the solution of the former is rarely feasible [9] and the latter is not longer fully microscopic but can be seen as a sort of *coarse-grained* description on a mesoscopic level. Thus, the discussion of non equilibrium behaviour is usually formulated in terms of phenomenological models.

Since nonequilibrium systems do not require detailed balance, they exhibit a potentially richer behavior than equilibrium systems. However, compared to equilibrium statistical mechanics, the theoretical understanding of nonequilibrium processes is still at its beginning [1].

Non-equilibrium phenomena are, for example, encountered where an external current flow thorough to the system keeping it away from thermal equilibrium. Examples of these kind of systems are: a resistor in a electric circuit (where even if a stationary state is reached its probability distribution will no longer be given by the Gibbs ensamble), catalytic reactions, surface growth, and many other phenomena with a flow of energy or particles through the system [1].

For what concern systems that exhibit a *collective behaviour* over large scales (such as systems that undergo a continuous phase transition) most of what is known in equilibrium can be extendend to the non equilibrium case. On the other hand,

these systems present new fascinating behaviours that cannot be observed in equilibrium and some constrains, such as the necessity of *fine-tune* a control parameter in order to reach a critical domain, can be relaxed. This is, for example, the case of systems that exhibit *self-organised criticality* [8].

The concept of universality that, as outlined above, assume a central role in equilibrium critical phenomena can be applied to non-equilibrium systems as well. However, the universality classes of nonequilibrium critical phenomena are expected to be even more diverse as they are governed by various symmetry properties of the evolution dynamics. On the other hand, the experimental evidence for universality of nonequilibrium phase transitions is still very poor, calling for intensified experimental efforts [1].

A class of systems that are currently intesively studied by theoretical physicists is the one that undergoes a phase transition into an *absorbing state*. As suggested by the definition, an absorbing state is a configuration that, once has been reached by the dynamics, it can never be left. It is clear that such systems are intrisically non in equilbirium as the detailed balance can never be satisfied, i.e. there is no rate with which the system can escape from the absorbing state [13]. Famous examples of non-equilibrium systems which posses an *absorbing configuration* are: chemical reactions [8], the voter model [20, 21] and the contact process [22, 23].

A transition between an *active* and an absorbing state is called *absorbing phase transition*. Just like in equilibrium critical phenomena, absorbing phase transitions exhibits universal features determinated by symmetry properties and conservation laws which allow one to define universality classes. In contrast with equilibrium phase transitions only few classes of transition into absorbing state are known. This lack of knowledge leaves space to many interesting investigations in order to specify all the possible universality classes.

The milstone of second order absorbing non-equilibrium phase transition is *directed percolation*. DP is the biggest universality class (so far known) of non-equilibrium critical phenomena[2] and, given its importance, is usually refered to as the Ising model of non-equilibrium physics. Nevertheless, despite its key role in non-equilibrium physics, directed percolation is one of the very few critical phenomena which cannot be solved exactly in one spatial dimension [8]. Although is easy to define, its critical behavior is highly nontrivial, this is the reasons why DP continues to fascinate theoretical physicists.

Also, even if many models have been studied and found to belong to the DP universality class it is really difficult to observe DP behaviour in experimental studied. Recently, directed percolation has captured the attention and the interest of experimentalists (see for example [11]) letting us hope that the joint work of theoretical physicists and experimentalists can enrich our knowledge.

---

[2]By biggest universality class we mean that most of the non-equilibrium models that have been investigated so far belong to DP.

1.3   Reaction Diffusion Processes

Interacting particle systems, such as those that are usually refered to as *reaction diffusion processes* are a classical example of non equilibrium statistical mechanics. These are stochastic models for chemical reactions in which particles are carried around by diffusion and, upon encounter another particle or spontaneously, they undergo certein kind of reactions.

Beyond their applications in chemistry, reaction diffusion models are frequently utilized to describe a multitude of phenomena in many disciplines such as: physics, ecology, population dynamics, economy, sociology, biology,....

These model are defined in terms of probabilisitc transition rules, the involved objects (atoms, molecules, individual, opinions,...) are interpreted as species and do not carry a mass nor an internal momentum [8].

As an example, in physics one encounter Reaction Diffusion models in *molecular beam epitaxy* [5]. In such experiments one exposes a solid-state surface in a *UV* chamber to a beam of incident particles evaporating from a thermal source. Some of these atoms land on the surface, forming a deposition layer. The actual microscopic processes depend on various parameters such as the temperature and the involved materials. Typically the deposited atoms diffuse for some time on the surface until they find another atom, forming an immobile deposition layer. With advanced microscopy techniques it is possible to track the motion of the individual atoms on the surface in real time. It has been observed that the motion is discontinuous, i.e. the atoms jump instantaneously from a given position on the lattice to a neighboring one (just like a random walker). Furthermore, these jumps occur spontaneously, indicating that the events of jumping are totally random. In fact, the jumps are not caused by quantum-mechanical tunneling, rather they are thermally induced by lattice vibrations. Since thermal fluctuations are fully chaotic, they can be considered as some kind of random noise, triggering diffusive moves of the atoms [5].

Other physical systems in which we find RD processes are: domain wall interaction in magnets, interface dynamics in growth models, percolation of water through porous rocks, electric current in a diluited network, just to quote some of them.

Given the broad range of applicability of RD models we will try to be as general as possible. Atoms, molecules, bacteria, opinions, individual, chemical reactants, etc ..., are generally called *particles* and are labelled by capital letters $A, B, C, \ldots$, where each letter represent a particular species. Particles are free to move in the continuum or in any kind of lattice (with fractal or integer dimenion) or network. They propagate hopping to nearest neighbours and with prescribed reaction rates they undergo species transormation (transmutation), annihilation, coagulation, ... The reactions are usually depicted as follow:

- $A + A \rightarrow A$ Coagulation

- $A + A \rightarrow \emptyset$ Annihilation

- $A \rightarrow A + A$ Branching

- $\emptyset \rightarrow A$ Spontaneus creation

- $A \rightarrow \emptyset$ Extinction

- $A \rightarrow B$ Transmutation
  . . .
  . . .
  . . .

where $\emptyset$ denotes any inert species and the dots can be filled with any reaction one can immagine.

The competition between the reactions and diffusion introduce two different regimes [39]: at sufficiently high particles densities the characteristic time scales of the dynamics will be governed by the reaction rate and the system is called *reaction-limited*. On the other hand, at very low densities reaction that need the presence of at least two particles, occours only once the two are brought in their vicinity by the hopping, such systems are refered to as: *diffusion-limited*.

In general, from some random initial state the system will evolve toward a stationary state with a particular stationary probability distribution. In most of the cases this will not be given by the Gibbs mesuare as the dynamics do not satisfy the detailed balance (it need to be remarked that this is the general scenario but is not always the case). The steady state can be an active state with fluctuactions of the number of particles, it can be an absorbing state with no particels at all or it can be an absorbing state with only one particle and hence no fluctuations (e.g. we can think about a system that from a initial distribution of particles that diffuse and coagulate, it is clear that once we are left with one particle in a closed system we are in a trivial steady state).

Even if the stationary state is *trivial* the approach to such a state could be critical, reaction diffusion models give us the possibility to explore non equilibrium phase transitions.

1.3.1   Mean field theory and role of fluctuations

In many cases the macroscopic properties of a reaction-diffusion process can be predicted by solving the corresponding mean field theory [39]. Let us take the example of chemistry, the simplest mean field approximation is known as the *law of mass action*: for a given temperature the rate of a reaction is assumed to be proportional to the product of concentrations of the reacting substances (note that this approach assumes that the particles are homogeneously distributed). It therefore ignores any spatial correlations as well as instabilities with respect to inhomogeneous perturbations. Thus, the homogeneous mean field approximation is expected to hold on scales where diffusive mixing is strong enough to wipe out spatial structures. Especially in higher dimensions, where diffusive mixing is more efficient, the mean field approximation provides a good description. It becomes exact in infinitely many dimensions,where all particles can be considered as being

neighbored [1].

A general mean field equation reads:

$$\partial_t a(\mathbf{x}, t) = D\nabla^2 a(\mathbf{x}, t) + f(\mathbf{x}, t) \tag{1.16}$$

Where D is the diffusion constant, $a(\mathbf{x}, t)$ is the local density and $f(\mathbf{x}, t)$ is a function that specify the reactions and its form depends upon the particluar model under investigation.

As an example of mean field theory we can consider the *coagulation* process $A + A \to A$ that occours with rate μ in an inhomogeneous system with a local density at time t denoted by $a(\mathbf{x}, t)$ [44]. The probability of a reaction is assumed to be proportional to $a^2(\mathbf{x}, t)$ and the local density is assumed to be slowly varying on the scale of the lattice size. Such a description neglects correlations bewteen the reactants, the corresponding rate equation is:

$$\partial_t a(\mathbf{x}, t) = D\nabla^2 a(\mathbf{x}, t) - \mu a^2(\mathbf{x}, t) \tag{1.17}$$

In certain chemical reactions with several particle species the diffusive term may have a destabilizing influence, see for example section (1.3.3). The study of mean-field instabilities is the starting point for the theory of pattern formation which has become an important field of statistical physics and biology.

The mean field theory has the huge disadvantage that ingore fluctuaction effects and spatial correlations. This is a big problem especially in low dimensional systems where fluctuations may play an important role and are able to entirely change the physical properties of a given reaction-diffusion system [44].

The influence of fluctuations on the mean field results can be observe experimentally, as an example let us consider the experiment described in [1] on *laser-induced* excitons in TMMC (tetramethylammonium manganese trichloride). This is a crystal consisting of parallel manganese chloride chains in which laser-induced electronic excitations of the Mn^{2+} ions diffuse around the chain. The chains are separated by large tetramethylammonium ions so that the excange of excitons between the chains is suppressed and the system can be regarded as a one dimensional chain. When two excitons (quasi particles) meet at the same lattice site the Mn^{2+} ion is excited to twice the excitation energy and the relax back to its original state producing a phonon.

The process can be described in term of the coagulation reaction $A + A \to A +$ heat on a one dimensional regular lattice and the concentration of *quasi particles* is observed to decay with a power law behavior: $a(\mathbf{x}, t) \sim t^{-\delta}$ with $\delta = 0.48(3)$ [1]. To compare with the analytical results, the mean field theory predict $\delta = 1$ whereas the *Interparticle distribution functions* technique[3] predict $\delta = 0.5$ [1].

---

[3]The IPDF technique is a method usually employed in systems with fermionic symmetry and is implemented by writing a master equation for the probability that an arbitrary chosen interval of size L contains no particles, details can be found in [14] and [1].

It is clear that in order to provide an exact description of the process we need to go beyond the mean field theory and include a mathematical description of stochastic fluctuations. As this will be the subject of the next chapter we will now continue the review by giving some specific example of RD processes. In the following we will describe a theoretical model that belong to the universality class of *directed percolation*, namely: *the contact process*. In the last section of this chapter we will describe a model, in the contest of *evolutionary game theory*, which exhibits many interesting features, such as absorbing phase transition and pattern formation.

1.3.2 The Contact Process

The contact process, proposed by T.E. Harris in 1974 [22], is a toy model for the spreading of a disease. The model is not exactly soluble but many properties such as its critical parameter have been estabilshed rigorously by means of numerical simulations [23]. Given its importance in non equilibrium phase transitions this model is the starting point for developing new methods for non equilibrium problems expecially for what concern numerical simulations.

The contact process is defined on a d-dimensional square lattice whose sites can be either active (healthy) or inactive (infected). Infected sites are said to be occupied by a particle whereas healthy sites are empty. The disease spreads through nearest neighbour upon contact[4] i.e. an occupied site infects a nearest neigbour at rate λ/q (where q is the coordination number) and recover at unitary rate. Since an individual must have an infected nearest neighbour in order to get the disease, it is clear that the disease-free state is an absorbing state. The active phase and the absorbing state are separeted by a second order non-equilibrium phase transition that belong to the universality class of directed percolation. The order parameenter is the density as a function of time and the critical point λ_c depends upon the dimension of the system, for example $\lambda_c = 3.297848(22)$ in $d = 1$ and $\lambda_c = 1.64877(3)$ in $d = 2$ [8]

Although the CP is a continuous time Markov process a discrete time formulation is often employed in simulations [23]. There are several efficient computational implementations of the contact process, all equivalent with respect to the universal behavior at the phase transition; a classical example is the one describe by [23]. The simulation starts at time $t = 0$ with a given initial distribution of infected individuals, normally it either starts with a fully occupied lattice or with a single infected site placed randomly in the system. It is convinient to keep track of the infected sites by creating a list of occupied sites and at each time step update every element on the list with the following rules:
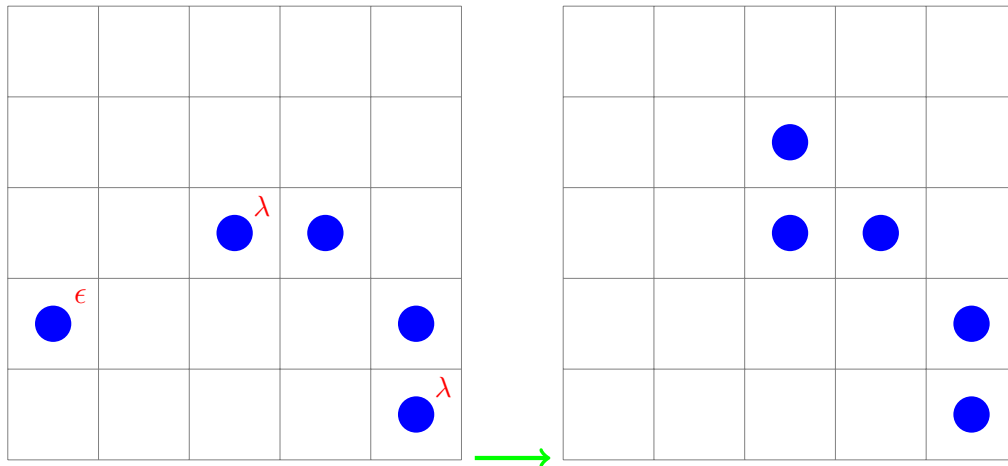
---

[4]This is the reason of the model's name

Figure 1.3: Graphical represenation of the contact process on a two-dimensional lattice in terms of *reaction-diffusion processes*. Infected sites try to infect a random nearest neighbour and they either succeed, if the target is an healty site, or fail, if the target is an infected site. With rate ϵ a site spontaneously heal.

- with proability $\frac{\lambda}{1+\lambda}$ the infected individual try to infect one of its nearest neighbour, it succeeds only if the random chosen neighbour is healty.

- with probability $1 - \frac{\lambda}{1+\lambda}$ the infected individual spontaneously heals

The time increment associated with this event is $1/N_{occ}$ where N_{occ} is the number of elements on the list.

An example of how to implement the contact process in C on a two dimensional lattice with periodic boundary conditions is given by the following lines of code:

```
for(i=Active_list.size-1; i>=0;  i--){

  if(ranMT()<lambda/(1.+lambda)){
    rnd=(int)(ranMT()*4);
    rndNNx=Active_list.data[i].x+increment[rnd].x+LENGTH;
    rndNNx%=LENGTH;
    rndNNy=Active_list.data[i].y+increment[rnd].y+LENGTH;
    rndNNy%=LENGTH;
    if(site[rndNNx][rndNNy].count==0){
      POPULATE(rndNNx, rndNNy);
    }
  }
  else {
    site[Active_list.data[i].x][Active_list.data[i].y].count=0;
    POP(Active_list.data[i]);
  }
}
```

Where $POPULATE$ is a function-like macro that add an element to the list and increments the occupation number of the site $rndNNx, rndNNy$ and POP is a function-like macro that delete the element from the list.

The choice of the initial conditions depends upon the particular observable we are going to measure, for example if we are interested in the critical exponent of the decay of the density as a function of time it is convinient to start the simulation with a fully occupied (infected) lattice. On the other hand, if we are interested in the survival probability [29], which is the probability that an active cluster survives at time t when starting from a single site seed at time 0 the initial condition must bee a single infected site [5].
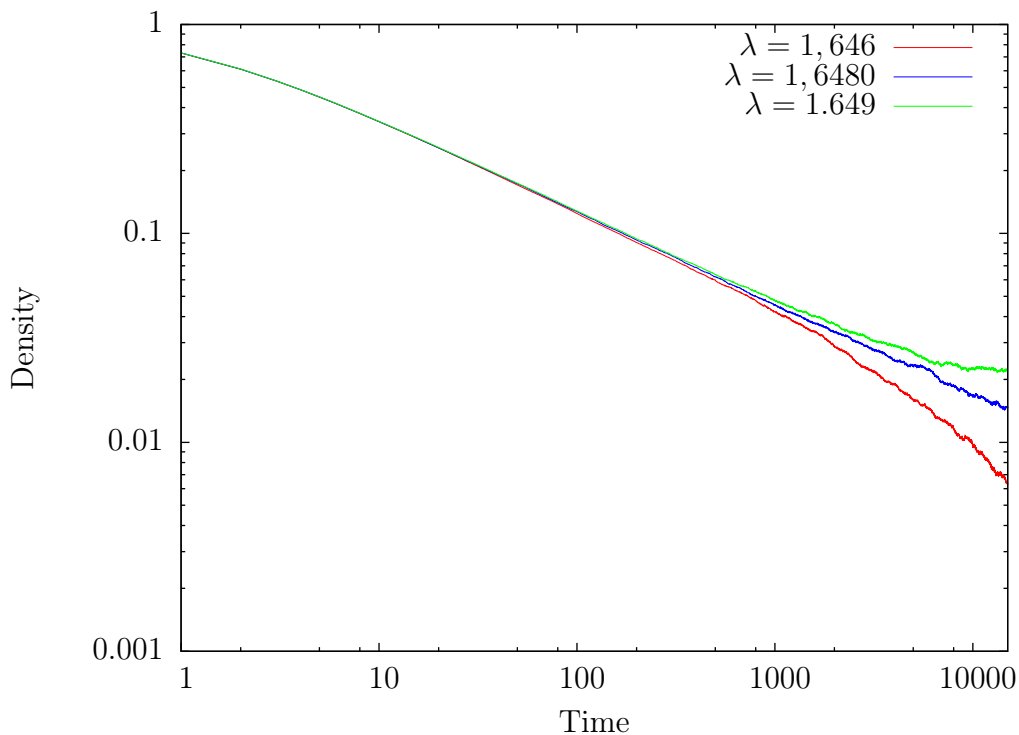

Figure 1.4: Critical decay of the density in the contact process in a 1000X1000 square lattice. Critical point (Blue line ——): $\lambda = 1.6480(1)$. The data are averaged over 800 realisation of the process. In the literature [28] $\lambda_c = 1,64874(2)$.

The simplest analytical approach to the contact process is a mean field approximation. Let $a(\mathbf{x}, t)$ be the density at time t on a d-dimensional space, assuming spatial homogeneity the equation of motion for $a(t)$ becomes [23]:

$$\frac{da(t)}{dt} = (\lambda - 1)a(t) - \lambda a^2(t) \tag{1.18}$$

For $\lambda \leq 1$ the only stationary solution is the vacuum $\bar{a} = 0$. On the other hand for

---

[5]A discussion about initial conditions in numerical simulations will be given in the last chapter: *Numerical Simulations*

$\lambda > 1$ there is an active stationary state with $\bar{a} = 1 - 1/\lambda$; $\lambda_c = 1$ marks the mean field critical point. Near the critical point the order parameter follow a power law with exponent δ, the mean field theory predict $\delta = 1$ (Numerical simulations give $\delta = 0.159464(6)$ in $d = 1$, $\delta = 0.4505 \pm 0.0010$ in $d = 2$ [8]).

The mean field theory is quantitatively wrong regarding both the critical exponents and the critical point for $d < d_c = 4$, which is the *upper critical dimension* of the theory[6]. The main error in the mean field approach lies in neglecting completely any fluctuations and spatial correlations, treating different sites as independent when in reality they are highly correlated.

The existence of a phase transition in the contact process has been proven by Ligget T.M. 1985 [24] and Durret R. [25], whereas Bezuidenhout and Grimmett [26] proved that the transition is continuous. This assertion are valid for dimensions equal or greater than one in an infinte system [23](in a finte system the probability to reach the absorbing state is almost one for any value of the parameters).

The standard contact process has one absorbing state: a completely empty lattice. However, it is easy to imagine similar models that present many (or infinitely many) absorbing states. One of them is the *Pair-Contact Process* [27] defined on a d-dimensional lattice as follow:for each attempted update a pair of adjacent sites is randomly chosen. If both of the sites are occupied they annihilate with probability p and with probability $1 - p$ another adjacent site get the infection (provided that the randomly chosen target site is empty).

Solitary particles are not allowed to wonder around so that a state with no pairs of infected site is absorbing (as no one is able to infect a nearest neighbour or spontaneously heal); the order parameter of the Pair contact process is the density of pair of particles, in the thermodinamic limit the number of possible absorbing configuration tend to infinity.

The pair contact process still belong to the Directed Percolation universality class even if the *DP-conjecture* formulated by Janssen and Grassberger cannot be applied as the model exhibits infinitely many absorbing configurations [8]:

- the model displays a continuous phase transition from a fluctuating active phase into a unique absorbing state

- the transition is characterised by a non-negative one-component order parameter

- the dynamic rules are short-ranged

- the system has no special attributes such as unconventional symmetries, conservation laws, or quenched randomness.

If one add diffusion of single particles on top of the previous model, the number of possible absorbing configurations become two: the empty lattice and a lattice

---

[6]Dimension above which fluctuactions are not strong enough to be able to change the mean field predictions.

with only one particle that wonder around without having any possibility to undergo any kind of reaction. This model is know as *Pair-Contact Process with Diffusion* and it is of great interest as is still not really understood whether it belongs to the DP universality class or represent a new kind of universality class for absorbing phase transition [8].

1.3.3   Rock-Paper-Scissor Games

We now move to a model which exhibits an absorbing phase transition which does not belong to the directed percolation universality class: *Rock-Paper-Scissor games.*
Evolutionary game theory, nonlinear dynamics, and the theory of stochastic processes provides the mathematical tools for a deeper understanding of ecological systems. These are complex assemblies of large numbers of individuals, interacting competitively under multifaceted environmental conditions [30]. There is a lot of interest at the moment in understanding how species compete between each others, what cause the extiction of one species and the survival of another and how the local microscopic interaction between individuals leads to the formation of self-oraganised spatial patterns and other kind of social behavior.
Spatial distribution of individuals, their mutual interaction and the possibility to migrate (mobility) are common features of real ecosystems. This is true for species of any size and nature: from bacteria in a Petri dishes to elephant in a forest [30]. *Mobility* assume a particuarly important role in the dynamical evolution of real ecosystems. Low values of mobility, which is the capability of an individual or a species to spread around the system, lead to the formation of spatial patterns like spirals in myxobacteria aggregation. On the other hand, high value of mobility make the spatial distribution irrelevant, the population is said to be *well-mixed*[7] and one would not observe pattern formation.

A study on how mobility influence biodiversity in Rock-Paper-Scissor games can be found in [32], whereas a review on evolutionary game theories can be found in [30].
To give a specific example on how reaction-diffusion processes can be used to investigate biological and ecological systems we consider a well known spatial game with cyclic dominance: *Rock-Paper-Scissor*, sometimes called *cyclic Lotka-Volterra model.*

   The model is defined in the very same way one would expect from the name: species are labelled by capital letters, A,B,C,... and the cyclic dynamical rules are: A kill B (Paper wraps rock), B kill C (scissor cuts paper) and C kill A (rock smashes scissor). Mobility is implemented by switch the position between two neighbouring individuals, see figure (1.5) for a graphical representation of the dynamical rules captured by the following reactions:

---

[7]In a well-mixed system individual's diffusion rate is so large that one can assume that each individual interact with everyone else at the same time, i.e. is a mean field picture[30]
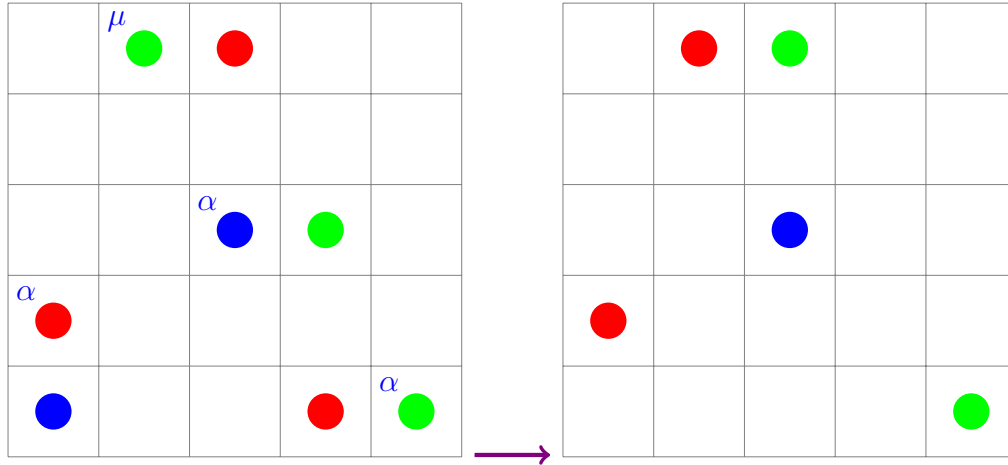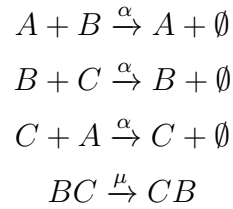
Figure 1.5: Graphical representation of the dynamical rules: A=blue species, B=green species, C=red species

$$A + B \xrightarrow{\alpha} A + \emptyset$$
$$B + C \xrightarrow{\alpha} B + \emptyset$$
$$C + A \xrightarrow{\alpha} C + \emptyset$$
$$BC \xrightarrow{\mu} CB$$

The last reaction is the mobility (diffusion or switching) and occurs with the same rate for each species. At each time step a pair of nearest neighbour sites are randomly selected and one of the above-mentioned reaction occours, if the nearest neighbour is an empty site the individual can leave an offspring with rate σ, i.e.:

$$A + \emptyset \xrightarrow{\sigma} A + A$$
$$B + \emptyset \xrightarrow{\sigma} B + B$$
$$C + \emptyset \xrightarrow{\sigma} C + C$$
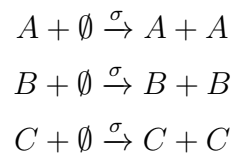
Writing the density of each species as a vector: $\vec{a}(\mathbf{x}, t) = (a(\mathbf{x}, t), b(\mathbf{x}, t), c(\mathbf{x}, t))$, the rate equations read:

$$\partial_t \vec{a}(\mathbf{x}, t) = D\nabla^2 \vec{a}(\mathbf{x}, t) + F(\vec{a}) \tag{1.19}$$

where $F(\vec{a})$ is given by:

$$F(a(\mathbf{x}, t)) = a(\mathbf{x}, t))[\sigma(1 - n) - \alpha c(\mathbf{x}, t))] \tag{1.20}$$
$$F(b(\mathbf{x}, t)) = b(\mathbf{x}, t))[\sigma(1 - n) - \alpha a(\mathbf{x}, t))]$$

$$F(c(\mathbf{x}, t)) = c(\mathbf{x}, t))[\sigma(1 - n) - \alpha b(\mathbf{x}, t))]$$

where n is the total density.

Mobility in this model is an *exchange* of position between two nearest neighbours, such a process lead to a macroscopic diffusion constant $D = \frac{\mu}{2L^2}$ with $L =$ linear system size [30].
On the one hand mobility is responsible for the formation and evolution of spiral patterns, the latter can be observed by solving the PDE. On the other hand in order to properly invastigate the non-equilibrium phase transition into an *absorbing state* one has to take into account the stochastic nature of the problem. This can be done, in the usual way, by writing down a stochastic Langevin equation (SPDE) or a master equation. However, this chapter is just an introduction to reaction-diffusion processes and we will not go into the details of the calculations, the interested reader can find a fantastic treatise in [30].

One can extend the same dynamics to an arbitrary number of species, see figure (1.6), and implement simple numerical simulations. Setting $\alpha = \sigma = 1$ one can use the mobility as parameter to tune. The observables that one can study are, for example, the evolution of self-organised spatial pattern formation or the conditions for coexistence between species (or, equivalently, the dominance of one over the others, phase transition into an absorbing state), see figure (1.7).
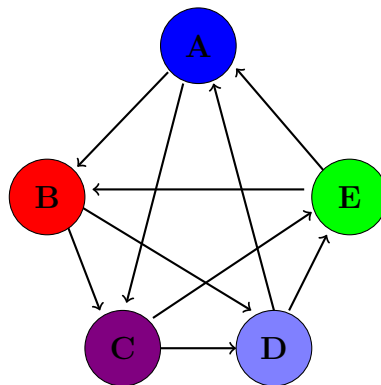

Figure 1.6: Interaction network which describe the dynamical rules for the five species RPS game. The direction of the arrows specify who is dominant, for example in the graphs above A kill B and A is killed by D

Depending upon the value of the mobility rate, the ecosystem will be either stable, i.e. the species coexist and biodiversity is sustained during the temporal evolution, or unstable, i.e. one species take over the whole enviroment. Given the symmetry in the reaction rates (all the α_i and σ_i are the same, just like in a proper fair battle) the species that will survive is subject to a random process.
The model can be investigated in more details by letting the fantasy take over and

adding all kind of reactions that one can immagine occour in a natural ecosystem or a biological model. For example one can add spontaneous mutation from one species to another, this operation is a support for biodiversity and it has been observed in *E.coli* bacteria and side-blotched lizards *Uta stansburiana* [31].

Increasing the number of competinig species, features like formation of defensive alliance (i.e. subgroups of species protect each others from an external invasion) have been observed [31]

1.4   Final remarks

Reaction-diffusion processes are of great interest nowadays and the reason is twofold: firstly, they can be used for a phenomenological study of real systems in many disciplines (as we have seen in the previous two examples). Secondly, RD processes are a classical example of non-equilibrium statistical mechanics and they can be used as toy models on which one can investigate the new and still poorly undesrtood features of non-equilibrium phase transitions.

Frequently a mean field theory is not able to capture the interesting features of these kind of processes even away from the critical transitions. The reason being that fluctuations strongly influence the behavior of the system. In the interesting limit of small systems, strong fluctuations in the number of particles makes standard techniques to solve the master equation, such as the Van Kampen's system size expansion, fail. For this reasons new techniques for the computation of universal and non-universal quantites, of reaction-diffusion systems, are needed.

A new method to investigate *non-universal properties* of the stationary state of reaction diffusion models will be developed in the following chapters starting from techniques widely used for the investigation of systems in the critical domain.

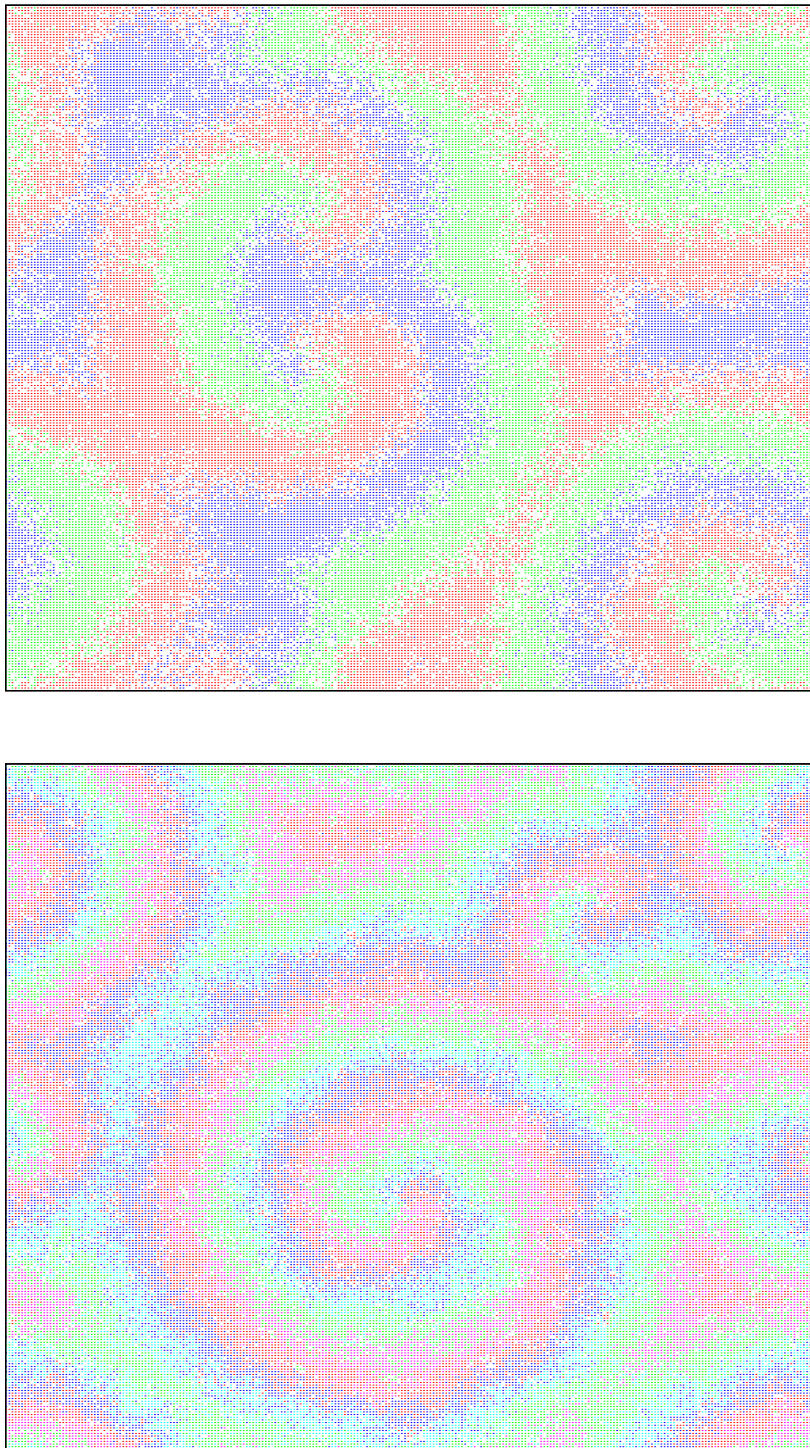Figure 1.7: Numerical simulations in a two dimensional regular lattice, L=128, for the three and five species cyclic Lotka-Volterra model with low value of mobility. Increasing the mobility rate jeopardize biodiversity and break the patterns that one can observe in the figures.

CHAPTER 2

DOI-PELITI FORMALISM

In this section we will introduce the model which is the object of this thesis. We will derive the master equation and we will discuss the *Doi-peliti* formalism, which provide an exact description of the process in term of a field theory.

We will then show in detail how to map the stochastic system under investigation into a field theory which will be the starting point for the calculation of the next chapter.

2.1 Fock Space Representation for Stochastic Interacting Particle Systems

In the following we will consider the *on-site reactions*:

$$A \xrightarrow{\sigma} A + A \qquad Branching \tag{2.1}$$

$$A + A \xrightarrow{\mu} A \qquad Coagulation \tag{2.2}$$

$$A \xrightarrow{\epsilon} \emptyset \qquad Extinction \tag{2.3}$$

The first two reactions occour with rates σ and μ with, in general, $\mu \neq \sigma$ whereas spontaneous extinction occours with rate ϵ. Moreover, particles diffuse to a nearest neighbour with hopping rate h.

The model has many similarity with the contact process but in the present case diffusion is explicit, instead of being mediated by the branching process. Furthermore, more then one particle is admitted on each lattice site and the role of carrying capacity is played by the coagulation process which is absent in the standard contact process.
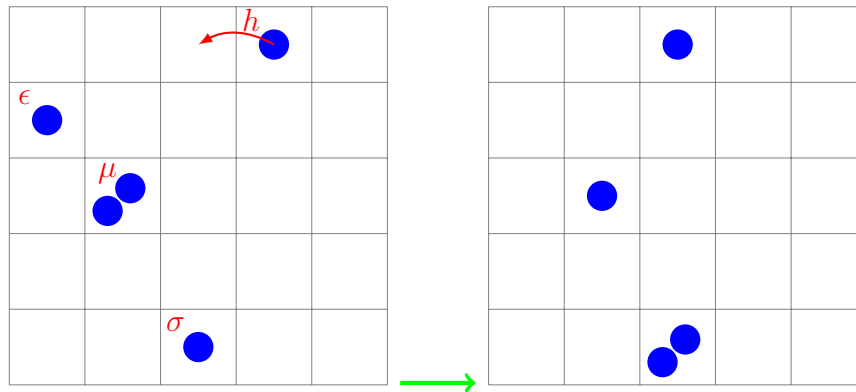
Figure 2.1: Graphical representation of the process on a two dimensional regular lattice. Extinction rate=ϵ, coagulation rate=μ and branching rate=σ.

The system reaches an active stationary state for some values of the reaction rates and shows a second order non-equilibrium phase transition to an *absorbing* state, when the parameters are fine-tuned to their critical value.

As usual, the temporal evolution of the system's configuration probability is described by a master equation which is a linear partial differential equation that describe the flow of probability into and away from the configuration of the system at time t. The latter is specified by the occupation number (number of particles) of the sites on the lattice. The configuration probability than is a function of time and a string of integers.

$$\{n\} = (n(\mathbf{m}), n(\mathbf{n}), ...) \tag{2.4}$$

Where from now on the notation: $n(\mathbf{m})$ stands for having n particles on the site $\mathbf{m}$ on a d-dimensional lattice.

The configurations $\{n\}$ of the system can be considered as vectors $|n\rangle = |n(\mathbf{m})\rangle \otimes |n(\mathbf{n})\rangle \otimes \ldots$ of a Hilbert space H which is the tensor product of a Hilber space for each site [35].

While it has long been recognised that the methods of quantum field theory extend far beyond their original domain of application to, for example, many body quantum systems in condensed matter physics, it is less well appreciated that they also provide a powerful tool for analysing classical statistical systems far from equilibrium [33]. Also, even though in recent years the interest towards the application of field theoretical techniques to interacting classical systems considerably increased, this is limitated in the characterisation of universal properties.
In this work we will apply those techniques but with the aim of characterise non-universal quantities at stationarity.

Any stochastic process involving particle motion and chemical reactions is encapsulated in changing the occupation number variables by integer amounts, thus the number of particles of a given type is not exactly know and changes during the evolution of the system. In order to track the integer occupation number changes a well established trick ([36, 37, 38]) consist in introducing ladder operators:

$$\hat{a}\,|n\rangle = n\,|n-1\rangle \qquad\qquad \hat{a}^{\dagger}\,|n\rangle = |n+1\rangle \qquad\qquad (2.5)$$

Creation and annihilation operators acting on each site are defined by $\hat{a}(\mathbf{m})^{\dagger}$ and $\hat{a}(\mathbf{m})$. This is an adaptation of the second quantized Fock space representation but the normalisation convention is different from standard quantum mechanics. The annihilation and creation operators satisfies the commutation rules:

$$[\hat{a}(\mathbf{n}), \hat{a}^{\dagger}(\mathbf{m})] = \delta_{\mathbf{n},\mathbf{m}} \qquad [\hat{a}(\mathbf{n}), \hat{a}(\mathbf{m})] = [\hat{a}^{\dagger}(\mathbf{n}), \hat{a}^{\dagger}(\mathbf{m})] = 0 \qquad\qquad (2.6)$$

In general, when dealing with systems made up of many different species, we can introduce an annihilation and creation operator for each species ($\hat{b}, \hat{b}^{\dagger}$ etc.), operators pertaining to different species commute i.e. $[\hat{a}(\mathbf{m}), \hat{b}(\mathbf{n})] = [\hat{a}(\mathbf{m}), \hat{b}^{\dagger}(\mathbf{n})] = 0$.

The 'vacuum' state is indicated by $|0\rangle$ and stands for a completely empty lattice. Starting from an empty lattice, on each lattice site, the state vector is constructed by hitting the vacuum with as many creation operators as many particles occupy the site:

$$|n(\mathbf{n})\rangle = \hat{a}^{\dagger}(\mathbf{n})^{n(\mathbf{n})}\,|0\rangle \qquad\qquad (2.7)$$

The presence of a vacuum state is the stregth point of the Doi-Peliti formalism as it sets a lower bound (i.e. zero) in the number of particles that the system can host. This feature is not present in the standard method for solving the chemical master equation, such as the Linear Noise Approximation (LNA, Van Kampen's systems size expansion) and Kramer-Moyal expansion. The consequence is that using those techniques one would risk to end up with negative populations (negative density) due to large fluctuations [40]. This is particularly true in low density systems which are of great interest, particularly in biology and microbiology. The Doi-Peliti formalism allows an exact description of the system in terms of a field theory and it can be employed for the characterisation of processes that involve an arbitrary small number of particles.

It is possible to associate a state in the Fock space with a set of probabilty at time t [34]:

$$|\Psi(t)\rangle = \sum_{\{n\}} P(\{n\}, t) \prod_{\mathbf{m}} (\hat{a}^{\dagger}(\mathbf{m}))^{n(\mathbf{m})}\,|0\rangle \qquad\qquad (2.8)$$

This is the state vector of the entire system. Note that the definition above differ from standard quantum mechanics, this feature will be discussed in section (2.2.1).

In system made of many, non inhert, different species ($n(\mathbf{n})$ species A, $m(\mathbf{m})$ species B, ...) a configuration is constructed from the vacuum as follow:

$$|n, m, \dots\rangle = \prod_{\mathbf{m}} (\hat{a}(\mathbf{m})^\dagger)^{n(\mathbf{m})} (\hat{b}^\dagger(\mathbf{m}))^{m(\mathbf{m})} \dots |0\rangle \qquad (2.9)$$

In what follow we will take, as initial configuration, an uncorrelated Poissonian distribution with initial mean density n_0:

$$|\Psi(0)\rangle = e^{-n_0 \sum_{\mathbf{m}} (\hat{a}^\dagger(\mathbf{m})-1)} |0\rangle \qquad (2.10)$$

Let us now prove a relation which will be important later on in the calculation of the expectation values of the observables:

$$e^{\hat{a}} f(\hat{a}^\dagger) = f(\hat{a}^\dagger + 1) e^{\hat{a}} \qquad (2.11)$$

In what follow we will assume $f(\hat{a}^\dagger)$ to be polynomial (i.e. we assume $f(\hat{a}^\dagger) = \hat{a}^{\dagger m}$). Since $e^{\hat{a}} = \sum_n \frac{\hat{a}^n}{n!}$ it is convinient to calculate $\hat{a}^n \hat{a}^{\dagger m}$ first.
We can prove the relation above by induction, let us start with $n = 3, m = 1$:

$$\hat{a}\hat{a}\hat{a}\hat{a}^\dagger = \hat{a}\hat{a}(\hat{a}^\dagger\hat{a} + 1) = \hat{a}\hat{a}\hat{a}^\dagger\hat{a} + \hat{a}\hat{a} = \hat{a}(\hat{a}^\dagger\hat{a} + 1)\hat{a} + \hat{a}\hat{a} = \hat{a}\hat{a}^\dagger\hat{a}\hat{a} + 2\hat{a}\hat{a} =$$
$$= (\hat{a}^\dagger\hat{a} + 1)\hat{a}\hat{a} + 2\hat{a}\hat{a} = \hat{a}^\dagger\hat{a}^3 + 3\hat{a}^2 \quad (2.12)$$

It is now straightforward to extend this calculation for any n and obtain the reccurent relation: $\hat{a}^n \hat{a}^\dagger = \hat{a}^\dagger \hat{a}^n + n\hat{a}^{n-1}$.
For $m = 1$ we then obtain the expected result:

$$e^{\hat{a}} \hat{a}^\dagger = \sum_n \frac{\hat{a}^n}{n!} \hat{a}^\dagger = \sum_n \hat{a}^\dagger \frac{1}{n!} \hat{a}^n + \sum_n \frac{n}{n!} \hat{a}^{n-1} = \hat{a}^\dagger e^{\hat{a}} + e^{\hat{a}} = (\hat{a}^\dagger + 1) e^{\hat{a}} \qquad (2.13)$$

We now have to prove that the same hold for any m, for $m = 2$ we have

$$\hat{a}^n \hat{a}^\dagger \hat{a}^\dagger = \hat{a}^\dagger \hat{a}^n \hat{a}^\dagger + n\hat{a}^{n-1} \hat{a}^\dagger = \hat{a}^\dagger (\hat{a}^\dagger \hat{a}^n + n\hat{a}^{n-1}) + n(\hat{a}^\dagger \hat{a}^{n-1} + (n-1)\hat{a}^{n-2}) =$$
$$= \hat{a}^{\dagger 2} \hat{a}^n + 2n\hat{a}^\dagger \hat{a}^{n-1} + n(n-1)\hat{a}^{n-2} \quad (2.14)$$

which again give us the right result:

$$e^{\hat{a}}\hat{a}^{\dagger 2} = \sum_n \frac{1}{n!}\hat{a}^n \hat{a}^{\dagger 2} = \sum_n \{\hat{a}^{\dagger 2}\frac{1}{n!}\hat{a}^n + 2n\hat{a}^\dagger \frac{1}{n!}\hat{a}^{n-1} + \frac{n(n-1)}{n!}\hat{a}^{n-2}\} =$$
$$= \hat{a}^{\dagger 2}e^{\hat{a}} + 2\hat{a}^\dagger e^{\hat{a}} + e^{\hat{a}} = (\hat{a}^\dagger + 1)^2 e^{\hat{a}} \quad (2.15)$$

It is now just a matter of straightforward algebra to continue for any m.

As a consequence the following identity holds:

$$\langle 0| \, e^{\hat{a}}\hat{a}^\dagger = \langle 0| \, e^{\hat{a}} \quad (2.16)$$

Which is now straightforward to prove as $\langle 0| \, e^{\hat{a}}\hat{a}^\dagger = \langle 0| \, \hat{a}^\dagger e^{\hat{a}} + \langle 0| \, e^{\hat{a}}$ and the action of $\hat{a}^\dagger$ on an empty bra gives zero.

2.2 Master equation

In order to write down the master equation we have to consider how each reaction that occours in the system contribute to the temporal evolution of the probability distribution $P(\{n\}, t)$ of finding the system at time t in the configuration $\{n\}$.

$$\frac{\partial P(\{n\}, t)}{\partial t} = \frac{h}{q} \sum_{\langle \mathbf{m}, \mathbf{n} \rangle} \underbrace{[(n(\mathbf{m}) + 1)P(..., n(\mathbf{m}) + 1, n(\mathbf{n}) - 1, ..., t) - n(\mathbf{m})P(\{n\}, t)}_{Diffusion} +$$
$$\underbrace{+(n(\mathbf{n}) + 1)P(..., n(\mathbf{n}) + 1, n(\mathbf{m}) - 1, ..., t) - n(\mathbf{n})P(\{n\}, t)]}_{Diffusion} +$$
$$+\mu \sum_{\mathbf{m}} \underbrace{[n(\mathbf{m})(n(\mathbf{m}) + 1)P(..., n(\mathbf{m}) + 1, ..., t) - n(\mathbf{m})(n(\mathbf{m}) - 1)P(\{n\}, t)]}_{A+A \rightarrow A} +$$
$$+\sigma \sum_{\mathbf{m}} \underbrace{(n(\mathbf{m}) - 1)P(..., n(\mathbf{m}) - 1, ..., t) - n(\mathbf{m})P(\{n\}, t)}_{A \rightarrow A+A} +$$
$$\epsilon \sum_{\mathbf{m}} \underbrace{(n(\mathbf{m}) + 1)P(..., n(\mathbf{m}) + 1, ..., t) - n(\mathbf{m})P(\{n\}, t)}_{A \rightarrow \emptyset} \quad (2.17)$$

By means of the Doi-Peliti formalism we can rewrite the master equation in a more compact form which is usually referred to as *imaginary time Schrödinger equation.*

In order to perform the mapping we have to multiply each term on the right by the ket $|n\rangle$ and sum over all the configurations $\{n\}$ Performing this operation, on the left hand site we obtain $\frac{\partial|\Psi(t)\rangle}{\partial t}$. On the right hand side things are a bit more complicated and require more attention.

In the following calculations we are going to take the master equation term by term on a single lattice site so that we do not have to carry the summation over $\mathbf{m}$ throughout the calculation.

- Coagulation, gain term:

$$\mu \sum_{\{n\}} n(\mathbf{m})(n(\mathbf{m}) + 1)P(..., n(\mathbf{m}) + 1, ...t)\,|n\rangle =$$
$$= \mu \sum_{\{n\}} P(..., n(\mathbf{m}) + 1, ...t)\hat{a}^\dagger(\mathbf{m})\hat{a}(\mathbf{m})\hat{a}(\mathbf{m})\,|n + 1\rangle \quad (2.18)$$

The right hand side can be rewritten as:

$$\mu \sum_{\{n\}} P(..., n(\mathbf{m}) + 1, ...t)\hat{a}^\dagger(\mathbf{m})\hat{a}(\mathbf{m})\hat{a}(\mathbf{m})\,|n + 1\rangle =$$
$$= \mu \sum_{\{n\}} P(..., n(\mathbf{m}), ...t)\hat{a}^\dagger(\mathbf{m})\hat{a}(\mathbf{m})\hat{a}(\mathbf{m})\,|n\rangle \quad (2.19)$$

Which, given the definition of $|\Psi(t)\rangle$ is the same as:

$$\mu \sum_{\{n\}} P(..., n(\mathbf{m}), ...t)\hat{a}^\dagger(\mathbf{m})\hat{a}(\mathbf{m})\hat{a}(\mathbf{m})\,|n\rangle = \hat{a}^\dagger(\mathbf{m})\hat{a}(\mathbf{m})\hat{a}(\mathbf{m})\,|\Psi(t)\rangle \quad (2.20)$$

The loss term is easier:

$$\mu \sum_{\{n\}} n(\mathbf{m})(n(\mathbf{m}) - 1)P(..., n(\mathbf{m}), ...t)\,|n\rangle =$$
$$= \mu \sum_{\{n\}} P(..., n(\mathbf{m}), ...t)\hat{a}^\dagger(\mathbf{m})\hat{a}^\dagger(\mathbf{m})\hat{a}(\mathbf{m})\hat{a}(\mathbf{m})\,|n\rangle \quad (2.21)$$

Which is:

$$\mu \sum_{\{n\}} P(..., n(\mathbf{m}), ...t)\hat{a}^\dagger(\mathbf{m})\hat{a}^\dagger(\mathbf{m})\hat{a}(\mathbf{m})\hat{a}(\mathbf{m})\,|n\rangle = \mu\hat{a}^\dagger(\mathbf{m})\hat{a}^\dagger(\mathbf{m})\hat{a}(\mathbf{m})\hat{a}(\mathbf{m})\,|\Psi(t)\rangle$$
$$(2.22)$$

- Branching, gain term:

$$\sigma \sum_{\{n\}} (n(\mathbf{m}) - 1)P(..., n(\mathbf{m}) - 1, ..., t) \,|n\rangle =$$

$$= \sigma \sum_{\{n\}} P(..., n(\mathbf{m})-1, ..., t)\hat{a}^\dagger(\mathbf{m})\hat{a}^\dagger(\mathbf{m})\hat{a}(\mathbf{m}) \,|n - 1\rangle = \sigma\hat{a}^\dagger(\mathbf{m})\hat{a}^\dagger(\mathbf{m})\hat{a}(\mathbf{m}) \,|\Psi(t)\rangle$$

$$(2.23)$$

loss term:

$$\sigma \sum_{\{n\}} n(\mathbf{m})P(\{n\}, t) \,|n\rangle = \sigma \sum_{\{n\}} P(\{n\}, t)\hat{a}^\dagger(\mathbf{m})\hat{a}(\mathbf{m}) \,|n\rangle = \sigma\hat{a}^\dagger(\mathbf{m})\hat{a}(\mathbf{m}) \,|\Psi(t)\rangle$$

$$(2.24)$$

- For the diffusion we need a pair of annihilation and creation operators for each lattice site $\mathbf{m}, \mathbf{n}$. First term:

$$\frac{h}{q} \sum_{\{n\}} (n(\mathbf{m}) + 1)P(..., n(\mathbf{m}) + 1, n(\mathbf{n}) - 1, ..., t) \,|n(\mathbf{m})n(\mathbf{n})\rangle =$$

$$= \frac{h}{q} \sum_{\{n\}} P(..., n(\mathbf{m}) + 1, n(\mathbf{n}) - 1, ..., t)\hat{a}^\dagger(\mathbf{n})\hat{a}(\mathbf{m}) \,|n(\mathbf{m}) + 1, n(\mathbf{n}) - 1\rangle =$$

$$= \frac{h}{q}\hat{a}^\dagger(\mathbf{n})\hat{a}(\mathbf{m}) \,|\Psi(t)\rangle \quad (2.25)$$

The second term is the same as the one of the branching $\frac{h}{q}\hat{a}^\dagger(\mathbf{m})\hat{a}(\mathbf{m}) \,|\Psi(t)\rangle$.

- Extinction, first term:

$$\epsilon \sum_{\{n\}} (n(\mathbf{m})+1)P(..., n(\mathbf{m})+1, ..., t) \,|n\rangle = \epsilon \sum_{\{n\}} P(..., n(\mathbf{m})+1, ..., t)\hat{a}(\mathbf{m}) \,|n + 1\rangle =$$

$$= \epsilon\hat{a}(\mathbf{m}) \,|\Psi(t)\rangle \quad (2.26)$$

The second term is the same as the one in the branching and the diffusion: $\epsilon\hat{a}^\dagger(\mathbf{m})\hat{a}(\mathbf{m}) \,|\Psi(t)\rangle$

We can finally write down the master equation in terms of the ladder operators and the state vector:

$$\frac{\partial \left| \Psi(t) \right\rangle}{\partial t} = -[\underbrace{\frac{h}{q} \sum_{\langle \mathbf{m},\mathbf{n} \rangle} (\hat{a}^\dagger(\mathbf{m}) - \hat{a}^\dagger(\mathbf{n}))(\hat{a}(\mathbf{m}) - \hat{a}(\mathbf{n}))}_{Diffusion} +$$

$$+ \underbrace{\mu \sum_{\mathbf{m}} (\hat{a}^\dagger(\mathbf{m})\hat{a}^\dagger(\mathbf{m})\hat{a}(\mathbf{m})\hat{a}(\mathbf{m}) - \hat{a}^\dagger(\mathbf{m})\hat{a}(\mathbf{m})\hat{a}(\mathbf{m}))}_{Coagulation} +$$

$$+ \underbrace{\sigma \sum_{\mathbf{m}} (\hat{a}^\dagger(\mathbf{m})\hat{a}(\mathbf{m}) - \hat{a}^\dagger(\mathbf{m})\hat{a}^\dagger(\mathbf{m})\hat{a}(\mathbf{m}))}_{Branching} +$$

$$+ \underbrace{\epsilon \sum_{\mathbf{m}} \hat{a}^\dagger(\mathbf{m})\hat{a}(\mathbf{m}) - \hat{a}(\mathbf{m})}_{Extinction}] \left| \Psi(t) \right\rangle \quad (2.27)$$

We now have a neat reformulation of the master equation which is the starting point for the formulation of the *field theory*.

The object between square bracket is generally refered to as *pseudo-Hamiltonian*, *quasi-Hamiltonian* or *Liouville operator*:

$$\hat{H} = \frac{h}{q} \sum_{\langle \mathbf{m},\mathbf{n} \rangle} (\hat{a}^\dagger(\mathbf{m}) - \hat{a}^\dagger(\mathbf{n}))(\hat{a}(\mathbf{m}) - \hat{a}(\mathbf{n})) +$$

$$+ \mu \sum_{\mathbf{m}} (\hat{a}^\dagger(\mathbf{m})\hat{a}^\dagger(\mathbf{m})\hat{a}(\mathbf{m})\hat{a}(\mathbf{m}) - \hat{a}^\dagger(\mathbf{m})\hat{a}(\mathbf{m})\hat{a}(\mathbf{m})) +$$

$$+ \sigma \sum_{\mathbf{m}} (\hat{a}^\dagger(\mathbf{m})\hat{a}(\mathbf{m}) - \hat{a}^\dagger(\mathbf{m})\hat{a}^\dagger(\mathbf{m})\hat{a}(\mathbf{m}) + \epsilon \sum_{\mathbf{m}} \hat{a}^\dagger(\mathbf{m})\hat{a}(\mathbf{m}) - \hat{a}(\mathbf{m})) \quad (2.28)$$

Note that the *quasi-Hamiltonian* is normal ordered so that its expectation value on the vacuum is zero.

The equation above can be written in a more compact form:

$$\frac{\partial |\Psi(t)\rangle}{\partial t} = -\hat{H} \left| \Psi(t) \right\rangle \quad (2.29)$$

which is formally solved by:

$$\left| \Psi(t) \right\rangle = e^{-\hat{H}t} \left| \Psi(0) \right\rangle \quad (2.30)$$

This is of course a formal solution, the right way to procede, in order to extract

expectation value of the observables, will be illustrated in section 2.3.

Let us now make a little note that in many cases can make life easier. There is a quicker way to write down the pseudo-Hamiltonian in system without an explicit carrying capacity (i.e. limitation on the number of particles per site, see the end of the next section) [44].

For a general reaction $kA \rightarrow lA$ we have to assign a pair of,normal ordered, creation and an annihilation operators for each reactant, this term comes with a positive sign, then we assign a creation operator for each product and an annihilation operator for each reactant, this term comes with negative sign. For example, the coagulation reaction $A + A \rightarrow A$, following these rules will contribute to the pseudo-Hamiltonian with a term $\hat{a}^\dagger \hat{a}^\dagger \hat{a} \hat{a} - \hat{a}^\dagger \hat{a} \hat{a}$. The branching process $A \rightarrow A + A$ will contribute with a term $\hat{a}^\dagger \hat{a} - \hat{a}^\dagger \hat{a}^\dagger \hat{a}$ and so on so forth.

The extension to a system with many species is again straightforward, we just need to assign an annihilation and creation operator for each species (i.e. $B \rightarrow (\hat{b}, \hat{b}^\dagger)$ etc...) and apply the same set of rules.

2.2.1 Differences With Quantum Mechanics and Observables

There are three main differences between the Doi-Peliti formalism and ordinary quantum mechanics as pointed out in [34], obviously this is not surprising as it has always to be kept in mind that we are dealing with an entirely classical system.

The first difference is the imaginary unity i in the Schrödinger equation, but this is familiar from euclidean formulations of conventional quantum theories.
The second difference lies in the quasi-Hamiltonian which, in most of the situations, is not Hermitian in this formalism. Nevertheless, if a system satisfied detailed balance it can be proved that the quasi-Hamilonian can be made symmetric and real by a similarity transformation. Anyway, complex eigenvalues correspond to oscillating states which have been observed in some chemical reactions [34].

The third difference is the most relevant for our purpose and it appears clear when one look carefully at the definition of the state vector given above. We can not rely on the standard quantum-mechanical expression for the expectation value of an observable $\hat{O}$: $\langle \hat{O}(t) \rangle = \langle \Psi(t)|\hat{O}|\Psi(t) \rangle$ as it would be bilinear in $P(\{n\}, t)$. Instead, given an observable that is expressible as a function of the occupation number, its expectation value is:

$$\langle O(t) \rangle = \sum_{\{n\}} O(\{n\}) P(\{n\}, t) \tag{2.31}$$

Expressing the operator $\hat{O}$ as a function of the creation and annihilation oper-

ators $O(\hat{a}^\dagger, \hat{a})$, the expectation value reads:

$$\langle O(t) \rangle = \langle P|O(\hat{a}^\dagger, \hat{a})|\Psi(t)\rangle = \langle P|O(\hat{a}^\dagger, \hat{a})e^{-\hat{H}t}|\Psi(0)\rangle \tag{2.32}$$

Where the *projection state* is defined as follow:

$$\langle P| = \langle 0| \, e^{\sum_{\mathbf{m}} \hat{a}(\mathbf{m})} \tag{2.33}$$

Note that $\langle P|\Psi(0)\rangle = 1$ if the initial state corresponds to the probability distribution. Since we know, from the definition of the vector state, that setting $\hat{O} = 1$ we have:

$$\langle P|\Psi(t)\rangle = \langle P|e^{-\hat{H}t}|\Psi(0)\rangle = 1 \tag{2.34}$$

for any value of t, the condition $\langle P| \, \hat{H}(\hat{a}^\dagger, \hat{a}) = 0$ must be fulfilled in order o preserv probability conservation. This can be easily seen by expanding the exponential:

$$1 = \langle P|e^{-\hat{H}t}|\Psi(0)\rangle = \underbrace{\langle P|\Psi(0)\rangle}_{=1} - \langle P|\hat{H}t|\Psi(0)\rangle + \dots \tag{2.35}$$

thus the second and all the following terms on the rigth hand side, which are power of $\hat{H}$, have to be zero.

We know recall equation (2.11): upon commuting the factor $e^{\sum_{\mathbf{m}} \hat{a}(\mathbf{m})}$ in the projection state with the creation operator, the latter is shifted by 1: $\hat{a}^\dagger \to 1 + \hat{a}^\dagger$. Conservation of probability (eq (2.35)) is then guaranted if $H(\{\hat{a}^\dagger \to 1\}, \{\hat{a}\}) = 0$ i.e. if we set to one all the creation operators in the quasi-hamiltonian the latter has to vanish, note that the quasi-Hamiltonian of our system fulfill this condition. Also, because of the identity (2.16), any operator $\hat{O}$ corresponding to an observable can be expressed entirely in terms of annihilation operators by commuting to the left all the creation operators. Once all the $\hat{a}^\dagger$ are on the left hand side of the annihilation operators they commute with the exponential of the projection state and equation (2.16) shows that the overall effect is that we do not have creation operator in the expression of the observables [39].
This results in a new operator, but one which yields the same expectation value [43].

Another consequece of such a shift is that the initial state (equation (2.10)) becomes:

$$|\tilde{\Psi}(0)\rangle = e^{n_0 \sum_{\mathbf{m}} \hat{a}^\dagger(\mathbf{m})} \tag{2.36}$$

As an example let us take the expectation value of the number of particels $\bar{n}$:

$$\bar{n} = \langle 0|e^{\hat{a}}\hat{a}^{\dagger}\hat{a}e^{-\hat{H}t}|\Psi(0)\rangle \tag{2.37}$$

We can commute $e^{\hat{a}}$ with $\hat{a}^{\dagger}$ on the left, as a consequence of equation (2.11) and the action of the creation operator on the $\langle 0|$ being zero we have:

$$\bar{n} = \langle 0|e^{\hat{a}}\hat{a}e^{\hat{H}t}|\Psi(0)\rangle \tag{2.38}$$

The hamiltonian with all the creation operator shifted $\hat{a}^{\dagger} \rightarrow 1 + \hat{a}^{\dagger}$ is known in the literature as the *Doi-shifted Hamiltonian* [34]. For our purpose it is convinient to introduce this shift later on at the field level.

Before going into the detail of the field theory it is interesting to make a remark: in all we have done so far we have assumed that there is not restriction in the number of particle that a site can host, this is the equivalent of a *bosonic* representation. However, if there is a limit in the number of particles per lattice site (this is refered to as *carrying capacity* in the ecology literature [39]) an analogous formalism with Pauli spin matrices is often used [43]. This is particularly useful in one-dimension, where the resulting second quantized representation can be mapped into a quantum spin-chain system, which is often integrable.
Another way of dealing with carrying capacity is to consider the fermionic case on a lattice with a particular connectivity [42], this can be done by means of a suitable reformulation of the master equation.

2.3   The Field Theory

A field theory is a system whose degrees of freedom are distributed throughout space [41]. In reaction-diffusion systems, by means of the Doi-Peliti reformulation of the master equation, a field theory can be formualated via the very same path integral techniques as developed for quantum many particle systems. However, given the classical nature of the process and the deriving differences bewteen DP and standard quantum mechanics, in the mapping of the master equation into a field theory there are some subtleties that make the derivation worth to be explored in detail.
In order to write down the action it is convinient to start introducing choerent states i.e. an eigenstate of the annihilation operator $\hat{a}\,|\phi\rangle = \phi\,|\phi\rangle$ with complex eigenvalue ϕ [44, 47]. A base formed by coherent states is overcomplete and they can be used to form a resolution for the identity operator, which take the form:

$$\mathbb{1} = \int_{\mathbb{C}} \frac{d\phi^* d\phi}{\pi} e^{-\phi^*\phi} e^{\phi\hat{a}^{\dagger}}\,|0\rangle\,\langle 0|\,e^{\phi^*\hat{a}} \tag{2.39}$$

It is easy to show that the expression above is effectively an identity:

$$\int_{\mathbb{C}} \frac{d\phi^* d\phi}{\pi} e^{-\phi^*\phi} e^{\phi\hat{a}^\dagger} |0\rangle \langle 0| e^{\phi^*\hat{a}} = \int_{\mathbb{C}} \frac{d\phi^* d\phi}{\pi} e^{-\phi^*\phi} \sum_{n,m} \frac{\phi^n (\hat{a}^\dagger)^n}{n!} |0\rangle \langle 0| \frac{(\phi^*)^m \hat{a}^m}{m!} =$$

$$= \sum_{n,m} \underbrace{\int_{\mathbb{C}} \frac{d\phi^* d\phi}{\pi} e^{-\phi^*\phi} \phi^n (\phi^*)^m}_{\odot} \frac{(\hat{a}^\dagger)^n}{n!} |0\rangle \langle 0| \frac{\hat{a}^m}{m!} \quad (2.40)$$

By means of the substitution: $\phi = re^{i\theta}$ we get:

$$\bigodot = \int_0^\infty dr \int_0^{2\pi} \frac{d\theta}{\pi} r r^{m+n} e^{-r^2} e^{-i(m-n)\theta} = \int_0^\infty \frac{dr}{\pi} 2\pi r^{m+n+1} e^{-r^2} \delta_{m,n} = \quad (2.41)$$

$$= 2 \int_0^\infty dr r^{n+m+1} e^{-r^2} \delta_{n,m} = n! \delta_{n,m} \quad (2.42)$$

The last equality arise from the definition of the gamma function. Inserting this expression in the identity we have:

$$\mathbb{1} = \sum_{n,m} \delta_{m,n} n! \frac{1}{m!n!} (\hat{a}^\dagger)^n |0\rangle \langle 0| \hat{a}^m = \sum_n \frac{1}{n!} (\hat{a}^\dagger)^n |0\rangle \langle 0| \hat{a}^n \quad (2.43)$$

It is now straightforward to prove that the expression above is the identity operator:

$$\langle i| \mathbb{1} |j\rangle = \sum_n \langle i| \frac{1}{n!} (\hat{a}^\dagger)^n |0\rangle \langle 0| \hat{a}^n |j\rangle = \sum_n \frac{1}{n!} \langle i \,|\, n \rangle \langle 0 \,|\, j-n \rangle \frac{j!}{(j-n)!} = \quad (2.44)$$

$$\frac{j!}{i!(j-i)!} \langle 0 \,|\, j-i \rangle = \delta_{i,j} = \langle i \,|\, j \rangle \quad (2.45)$$

So far we have been dealing with a system with only one lattice site. In order to be as general as possible we will derive the field theory with an arbitrary number of sites in the lattice. In this case the choerent states take the form:

$$|\{\phi\}\rangle = e^{-\frac{1}{2}\sum_{\mathbf{m}} |\phi(\mathbf{m})|^2} e^{\sum_{\mathbf{m}} \phi(\mathbf{m})\hat{a}^\dagger(\mathbf{m})} |0\rangle = |\phi(\mathbf{m})\rangle \otimes |\phi(\mathbf{n})\rangle \otimes \ldots \quad (2.46)$$

The expression for the identity that we will employ is the following:

$$\mathbb{1} = \int_{\mathbb{C}} \prod_{\mathbf{m}} \frac{d\phi^*(\mathbf{m}) d\phi(\mathbf{m})}{\pi} e^{-\sum_{\mathbf{m}} \phi^*(\mathbf{m})\phi(\mathbf{m})} e^{\sum_{\mathbf{m}} \phi(\mathbf{m})\hat{a}^\dagger(\mathbf{m})} |0\rangle \langle 0| e^{\sum_{\mathbf{m}} \phi^*(\mathbf{m})\hat{a}(\mathbf{m})} \quad (2.47)$$

Given the decomposition (trotter's formula) of the temporal evolution operator:

$$e^{-\hat{H}t} = \lim_{\Delta t \to 0} (1 - H\Delta t)^{t/\Delta t} = (1 - H\Delta t) \dots (1 - H\Delta t) \qquad (2.48)$$

we can insert the identity between each slice of the decomposition:

$$e^{-Ht} = \lim_{\Delta t \to 0} \dots (1-H\Delta t) \int \Big(\prod_{\mathbf{m}} \frac{d\phi^*(\mathbf{m},t)d\phi(\mathbf{m},t)}{\pi}\Big) e^{-\frac{1}{2}\sum_{\mathbf{m}}\phi^*(\mathbf{m},t)\phi(\mathbf{m},t)} e^{\sum_{\mathbf{m}}\phi(\mathbf{m},t)\hat{a}^\dagger(\mathbf{m})} |0\rangle$$

$$\underbrace{\Bigg(\langle 0| \, e^{\sum_{\mathbf{m}}\phi^*(\mathbf{m},t)\hat{a}(\mathbf{m}) - \frac{1}{2}\sum_{\mathbf{m}}|\phi(\mathbf{m},t)|^2} (1 - H\Delta t) \int \prod_{\mathbf{m}} \frac{d\phi^*(\mathbf{m},t-\Delta t)d\phi(\mathbf{m},t-\Delta t)}{\pi}\Bigg)}_{\bigcirc}$$

$$\underbrace{e^{-\frac{1}{2}\sum_{\mathbf{m}}|\phi(\mathbf{m},t-\Delta t)|^2} e^{\sum_{\mathbf{m}}\phi(\mathbf{m},t-\Delta t)\hat{a}^\dagger(\mathbf{m})} |0\rangle}_{\bigcirc} \Bigg) \langle 0| \dots \quad (2.49)$$

In the term between bracket there are two real factors that can be taken out of the sandwich:

$$\bigcirc = e^{-\frac{1}{2}|\phi(\mathbf{m},t)|^2 - \frac{1}{2}|\phi(\mathbf{m},t-\Delta t)|^2} \langle 0| \, e^{\phi^*(\mathbf{m},t)\hat{a}(\mathbf{m})} (1 - H\Delta t) e^{\phi(\mathbf{m},t-\Delta t)\hat{a}^\dagger(\mathbf{m})} |0\rangle \quad (2.50)$$

We are now going to consider the terms between braket separately. To make the procedure as clear as possible we start from the easiest one, which is the one without pseudo-Hamiltonian:

$$\langle 0| \, e^{\phi^*(\mathbf{m},t)\hat{a}(\mathbf{m})} e^{\phi(\mathbf{m},t-\Delta t)\hat{a}^\dagger(\mathbf{m})} |0\rangle = \sum_{i,j} \langle 0| \, \frac{\phi^{*i}(\mathbf{m},t)\hat{a}^i(\mathbf{m})}{i!} \frac{\phi^j(\mathbf{m},t-\Delta t)\hat{a}^{\dagger j}(\mathbf{m})}{j!} |0\rangle =$$

$$(2.51)$$

$$\sum_{i,j} \frac{1}{j!} \langle i| \, \phi^{*i}(\mathbf{m},t)\phi^j(\mathbf{m},t-\Delta t) |j\rangle = e^{\phi^*(\mathbf{m},t)\phi(\mathbf{m},t-\Delta t)} \quad (2.52)$$

The second term require more attention. The pseudo-Hamiltonian is normal ordered and it always appear as a product of creation and annihilation operators. Thus we can consider a generic term of the form $\hat{a}^{\alpha\dagger}\hat{a}^\beta$ as the computation of all the other terms that appear in $\hat{H}$ is the same.

$$\langle 0| e^{\phi^*(\mathbf{m},t)\hat{a}(\mathbf{m})} \hat{a}^{\dagger\alpha}(\mathbf{m}) \hat{a}^{\beta}(\mathbf{m}) e^{\phi(\mathbf{m},t-\Delta t)\hat{a}^{\dagger}(\mathbf{m})} |0\rangle =$$

$$= \sum_{i,j} \langle i|\phi^{*i}\hat{a}^{\dagger\alpha}(\mathbf{m})\hat{a}^{\beta}(\mathbf{m})\frac{\phi^j}{j!}!j\rangle =$$

$$= \sum_{i,j} \frac{1}{j!} \langle i-\alpha| \, \phi^{*i}(\mathbf{m},t)\phi^j(\mathbf{m},t-\Delta t)\frac{j!}{(j-\beta)!} |j-\beta\rangle \quad (2.53)$$

We can take ϕ and ϕ^* out of the summation multiplying by $\phi^{\alpha-\alpha}$ and $\phi^{*\beta-\beta}$:

$$\sum_{i,j} \frac{1}{j!} \langle i-\alpha| \, \phi^{*i}(\mathbf{m},t)\phi^j(\mathbf{m},t-\Delta t)\frac{j!}{(j-\beta)!} |j-\beta\rangle =$$

$$= \phi^{*\alpha}(\mathbf{m},t)\phi^{\beta}(\mathbf{m},t-\Delta t) \sum_{i,j} \langle i-\alpha| \frac{\phi^{*(i-\alpha)}(\mathbf{m},t)\phi^{j-\beta}(\mathbf{m},t-\Delta t)}{(j-\beta)!} |j-\beta\rangle \quad (2.54)$$

In the sum on the right hand side we can shift the indeces i and j and perform the summation, i.e.:

$$\phi^{*\alpha}(\mathbf{m},t)\phi^{\beta}(\mathbf{m},t-\Delta t) \sum_{i,j} \langle i-\alpha| \frac{\phi^{*(i-\alpha)}(\mathbf{m},t)\phi^{j-\beta}(\mathbf{m},t-\Delta t)}{(j-\beta)!} |j-\beta\rangle =$$

$$= \phi^{*\alpha}(\mathbf{m},t)\phi^{\beta}(\mathbf{m},t-\Delta t) \sum_{j} \frac{\phi^{*j}(\mathbf{m},t)\phi^j(\mathbf{m},t-\Delta t)}{j!} \quad (2.55)$$

Which is:

$$\langle 0| e^{\phi^*(\mathbf{m},t)\hat{a}(\mathbf{m})} \hat{a}^{\dagger\alpha}(\mathbf{m}) \hat{a}^{\beta}(\mathbf{m}) e^{\phi(\mathbf{m},t-\Delta t)\hat{a}^{\dagger}(\mathbf{m})} |0\rangle = \phi^{*\alpha}(\mathbf{m},t)\phi^{\beta}(\mathbf{m},t-\Delta t)e^{\phi^*(\mathbf{m},t)\phi(\mathbf{m},t-\Delta t)}$$
$$(2.56)$$

As the very same calculations can be performed for each term in the quasi-Hamiltonian, the latter is now a function of $\phi^*(\mathbf{m},t)$, $\phi(\mathbf{m},t-\Delta t)$, i.e. $H : H(\phi^*(\mathbf{m},t),\phi(\mathbf{m},t-\Delta t))$[1].

Now we can insert these terms in the decomposition of the evolution operator:

---

[1]Note the time difference between the two fields

$$e^{-Ht} = \lim_{\Delta t \to 0} \int_{\mathbb{C}} \Big(\prod_{\mathbf{m},t'=(0,\Delta t,...,t)} \frac{d\phi^*(\mathbf{m},t')d\phi(\mathbf{m},t')}{\pi} \Big) e^{-\frac{1}{2}\sum_{\mathbf{m}}\phi^*(\mathbf{m},t)\phi(\mathbf{m},t)} e^{\sum_{\mathbf{m}}\phi(\mathbf{m},t)\hat{a}^\dagger(\mathbf{m})}$$

$$(1-H\Delta t)\,|0\rangle\, [\prod_{\mathbf{m},t'=\Delta t}^{t} e^{\phi^*(\mathbf{m},t')\phi(\mathbf{m},t'-\Delta t)} e^{-\frac{1}{2}|\phi(\mathbf{m},t')|^2 - \frac{1}{2}|\phi(\mathbf{m},t'-\Delta t)|^2}$$

$$(1-\Delta t H(\phi^*(\mathbf{m},t'),\phi(\mathbf{m},t'-\Delta t)))]\,\langle 0|\,e^{\sum_{\mathbf{m}}\phi^*(\mathbf{m},0)\hat{a}(\mathbf{m})-\frac{1}{2}\sum_{\mathbf{m}}|\phi(\mathbf{m},0)|^2}(1-H\Delta t)$$

$$(2.57)$$

In contrast with the term in round brackets, the product over t' in the square braket runs from $t' = \Delta t$, as the term $t' = 0$ has been taken into account separately. The former can be rewritten as follow (the summation over the lattice sites in the exponential has been omitted for the sake of clarity):

$$e^{\phi^*(\mathbf{m},t')\phi(\mathbf{m},t'-\Delta t)} e^{-\frac{1}{2}|\phi(\mathbf{m},t')|^2 - \frac{1}{2}|\phi(\mathbf{m},t'-\Delta t)|^2} =$$

$$e^{-\phi^*(\mathbf{m},t')[\phi(\mathbf{m},t')-\phi(\mathbf{m},t'-\Delta t)]} e^{\frac{1}{2}|\phi(\mathbf{m},t')|^2 - \frac{1}{2}|\phi(\mathbf{m},t'-\Delta t)|^2} \quad (2.58)$$

This term is included in the product of a sequence that run from Δt to t. The polar opposite terms of the second exponential[2] are the only ones that survive after having performed such a product and we will consider them later on.
All the other second exponentials cancelled and the product can be rewritten as:

$$\prod_{\mathbf{m},t'=\Delta t}^{t} e^{-\phi^*(\mathbf{m},t')[\phi(\mathbf{m},t')-\phi(\mathbf{m},t'-\Delta t)]} = \prod_{\mathbf{m},t'=\Delta t}^{t} e^{-\phi^*(\mathbf{m},t')\frac{d\phi(\mathbf{m},t')}{dt}\Delta t + O(\Delta t^2)} \quad (2.59)$$

The limit of $\Delta t \to 0$ of this expression has an important physical consequence, but let us proceed step by step.

Following [39], in order to find the action we will consider the espression of the expectation value for a generic observable $\hat{O}$:

$$\langle 0|\,e^{\sum_{\mathbf{m}}\hat{a}(\mathbf{m})}\hat{O}\,|\Psi(t)\rangle = \langle P|\,\hat{O}e^{-Ht}\,|\Psi(0)\rangle \quad (2.60)$$

---

[2]i.e. the one at time $t = 0$ and $t = t_f$: $e^{-\frac{1}{2}|\phi(\mathbf{m},0)|^2}$ and $e^{\frac{1}{2}|\phi(\mathbf{m},t_f)|^2}$

Which explicitly is:

$$\langle \hat{O} \rangle = Z^{-1} \lim_{\Delta t \to 0} \int \Big(\prod_{\mathbf{m}, \tau \in \{t, \Delta t, ..., 0\}} \frac{d\phi^*(\mathbf{m}, \tau) d\phi(\mathbf{m}, \tau)}{\pi} \Big) \langle P | \hat{O} | \{\phi_t\} \rangle$$

$$\Big(\prod_{\tau = \Delta t}^{t} \langle \{\phi_\tau\} | (1 - H\Delta t) | \{\phi_{\tau - \Delta t}\} \rangle \Big) \langle \{\phi_0\} | | \Psi(0) \rangle \quad (2.61)$$

The last terms that has to be evaluated now are the initial and final overlap (which, as detailed above have to be multiplied for the terms that not cancelled in the products). The operator $\hat{O}$, as outlined in the previous section, is assumed to be a function of the annihilation operator only, so we are left with the evaluation of (for sake of clarity in the following calculations we will omit the product over the lattice sites):

$$\langle P | \{\phi_t\} \rangle \, e^{\frac{1}{2}|\phi(\mathbf{m},t)|^2} = \langle 0| \, e^{\hat{a}} e^{\phi(\mathbf{m},t)\hat{a}^\dagger} |0\rangle = \sum_{i,j} \langle 0| \frac{a^i}{i!} \frac{\phi^j a^{\dagger j}}{j!} |0\rangle =$$

$$= \sum_{i,j} \langle i | \frac{\phi^j}{j!} | j \rangle = e^{\phi(\mathbf{m},t)} \quad (2.62)$$

And the term at $t = 0$:

$$\langle \{\phi_0\} | \Psi(0) \rangle \, e^{-\frac{1}{2}|\phi(\mathbf{m},0)|^2} = \langle 0| \, e^{\phi^*(\mathbf{m},0)\hat{a} - \frac{1}{2}|\phi(\mathbf{m},0)|^2 - \frac{1}{2}|\phi(\mathbf{m},0)|^2} e^{n_0(\hat{a}^\dagger - 1)} |0\rangle =$$

$$= e^{-|\phi(\mathbf{m},0)|^2 - n_0} \sum_{i,j} \langle 0| \frac{\phi^{*i} \hat{a}^i}{i!} \frac{n_0^j \hat{a}^{\dagger j}}{j!} |0\rangle = e^{-|\phi(\mathbf{m},0)|^2 - n_0} \sum_{i,j} \langle i | \phi^{*i} \frac{n_0^j}{j!} | j \rangle =$$

$$= e^{(n_0 \phi^*(\mathbf{m},0) - |\phi(\mathbf{m},0)|^2 - n_0)} \quad (2.63)$$

We recall that the initial state is assume to be $|\Psi(0)\rangle = e^{n_0 \sum_{\mathbf{m}} (\hat{a}^\dagger(\mathbf{m}) - 1)} |0\rangle$ as the initial distribution is Poissonian[39].

We can now perform the limit $\Delta t \to 0$ and the product over the time variable (see equation (2.59)):

$$\lim_{\Delta t \to 0} e^{-\phi^*(\mathbf{m},t') \frac{d\phi(\mathbf{m},t')}{dt} \Delta t + O(\Delta t^2)} = e^{-\int dt (\phi^*(\mathbf{m},t) \partial_t \phi(\mathbf{m},t))} \quad (2.64)$$

It is important to notice the physical implication of this limit. Before taking the

limit the quasi-Hamiltonian was a function of $\phi^*(x, t)$ and $\phi(x, t - \Delta t)$, the $O(\Delta t)$ difference between the two fields is dropped but it has to be remind that the field ϕ^* follow the field ϕ in time. This limit set a particular direction for the time variable, in particular it is interesting to note that in a perturbative approach such a limit exclude the presence of diagram like:
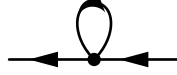
which would contribute to the renormalisation of the propagator but here are excluded in order to guarantee causality [35]. Also, the time limit will play an important rule in the action below.

Putting all the pieces togheter we finally have an expression for the expectation value of a general observable and for the Doi-Peliti action:

$$\langle \hat{O(t)} \rangle = Z^{-1} \int (\prod_{\mathbf{m}} \mathcal{D}\phi\mathcal{D}\phi^*)\hat{O}(\{\phi_t\})e^{-S(\{\phi^*\},\{\phi\})_0^t} \qquad (2.65)$$

Where the functional integral $\mathcal{D}\phi\mathcal{D}\phi^*$ stands for $\prod_{t' \in \{0, \Delta t, \dots t_f\}} d\phi d\phi^*$ in the limit $\Delta t \to 0$.

The *Doi-Peliti* action reads:

$$S[\{\phi^*\}, \{\phi\}]_0^t = \sum_{\mathbf{m}} [(-\phi(\mathbf{m}, t_f) - n_0\phi^*(\mathbf{m}, 0) + |\phi(\mathbf{m}, 0)|^2 + n_0 +$$
$$+ \int_0^{t_f} dt(\phi^*(\mathbf{m}, t)\partial_t\phi(\mathbf{m}, t) + H(\{\phi^*\}, \{\phi\}))] \quad (2.66)$$

Imposing that the identity operator average to one, determinates the normalisation factor Z:

$$Z = \int (\prod_{\mathbf{m}} \mathcal{D}\phi\mathcal{D}\phi^*)e^{-S[\{\phi^*\},\{\phi\}]_0^t} \qquad (2.67)$$

In order to deal with a genuine field theory we take the continuum limit in the space variable as well as the one in the time variable: $\sum_{\mathbf{m}} \to a_0^{-d} \int d^d x$, where a_0 is the lattice constant [39, 45].
The product of integrals becomes a functional integral over the fields $\phi^*(x, t) \to \bar{\phi}(x, t)$, $\phi(x, t) \to \phi(x, t)a^d$. Where the substitution $\phi^*(x, t) \to \bar{\phi}(x, t)$ has been

made because now we will threat $\bar{\phi}(x,t)$ and $\phi(x,t)$ as two independent variables [46].

At this stage it is convinient to introduce a shift of the field $\bar{\phi}(x,t)$: $\bar{\phi}(x,t) \to \tilde{\phi}(x,t) + 1$, in the literature such an operation is refered to as the *Doi-Shift*.
The Doi-shift allow a semplification of the analytical expression of the action without changing the value of the integral and, as we shall see later, this can be seen as a shift about the solution of the classical field equation $\frac{\delta S[\phi^*,\phi]}{\delta \phi^*} = 0$.
Note that this is the same shift that we could have made at the operator level and it encodes *probability conservation* (see discussion at the end of section 2.2.1).
Performing the shift the action reads:

$$S[\{\tilde{\phi}\},\{\phi\}] = [\int d^d x \int_0^{t_f} dt(\tilde{\phi}(x,t)\partial_t\phi(x,t) + H(\{\tilde{\phi}\},\{\phi\}))+$$
$$+ \phi(x,t_f) - \phi(x,0) - \phi(x,t_f) + \tilde{\phi}(x,0)(\phi(x,0) - n_0) + \phi(x,0) + n_0 - n_0] =$$
$$= [\int d^d x \int_0^{t_f} dt(\tilde{\phi}(x,t)\partial_t\phi(x,t) + H(\{\tilde{\phi}\},\{\phi\})) + \tilde{\phi}(x,0)(\phi(x,0) - n_0)] \quad (2.68)$$

The last term is a constrain that impose that the system has a random Poissonian distribution a $t = 0$ with denisty n_0. The term $\tilde{\phi}(x,0)\phi(x,0)$ drops as, in the time limit we have taken before, the fields $\tilde{\phi}$ follow in time the field ϕ and their product in $t = 0$ will give zero in a perturbative expansion.
Finally, the general form of the Doi-Peliti action is:

$$S[\{\tilde{\phi}\},\{\phi\}] = [\int d^d x \int_0^{t_f} dt(\tilde{\phi}(x,t)\partial_t\phi(x,t) + H(\{\tilde{\phi}\},\{\phi\})) - \tilde{\phi}(x,0)n_0)] \quad (2.69)$$

We now have a formal method to extract the expectation value of the observables, for example, recalling equation (2.37), we are able to write down the expectation value of the density in the path integral picture:

$$\langle\phi\rangle = \frac{\int\int \mathcal{D}\phi\mathcal{D}\tilde{\phi}\phi e^{-S[\tilde{\phi},\phi]}}{\int\int \mathcal{D}\phi\mathcal{D}\tilde{\phi} e^{-S[\tilde{\phi},\phi]}} \quad (2.70)$$

i.e. $\bar{n} = \langle\phi\rangle$ but it has to be remarked that ϕ as a fluctuating quantity is not the same as the denisty (i.e. $n \neq \phi$).
Another quantity interesting to calculate is $\bar{n^2}$:

$$\bar{n^2} = \langle 0|e^{\hat{a}}\hat{a}^\dagger\hat{a}\hat{a}^\dagger\hat{a}|\Psi(t)\rangle = \langle 0|e^{\hat{a}}\hat{a}\hat{a}^\dagger\hat{a}|\Psi(t)\rangle = \langle 0|e^{\hat{a}}\hat{a}^\dagger\hat{a}^2|\Psi(t)\rangle +$$
$$+ \langle 0|e^{\hat{a}}\hat{a}|\Psi(t)\rangle = \langle\phi^2\rangle + \langle\phi\rangle \quad (2.71)$$

From this it follows that, if the quantity $\langle\phi^2\rangle - \langle\phi\rangle^2$ vanishes then $\bar{n}$ has a Poissonian

distribution. In fact, the variance of $\bar{n}$ is $\bar{n^2} - \bar{n}^2 = \langle \phi^2 \rangle + \langle \phi \rangle - \langle \phi \rangle^2$ which is equal to the mean if $\langle \phi^2 \rangle - \langle \phi \rangle^2$ vanishes.

Since the mean particle density is the one point function: $\langle \phi(x,t) \rangle$, in a perturbative expansion one needs diagram with a single field at time t which terminate the graph on the left. Summing the diagrams in the perturbation series that contribute to $\langle \phi(x,t) \rangle$ but contain no loops yields the solution to the equations described as mean field theory (tree level). Incorporating higher-order effects is a matter of including diagrams with some number of loops [49].

In this chapter we have given an overview of the Doi-Peliti formalism, we have recovered the master equation for the model under investigation and we have performed the mapping of the latter into the imaginary time Schrödinger equation. On the other hand, the calculation of the last section are general and the results can be used as a starting point for the investigation of any model.
Now that we have all the necessary tools we can finally move on and perform field-theoretic calculations.

APPENDIX

2.A   The Detailed Balance

Before going into the details of the perturbative expansion it is worthwhile to make some considerations about the *detailed balance* and the non-equilibrum nature of the model.

Recalling the discussion in chapter 1, non-equilibrium statistical mechanics is characterised by a lack of detailed balance, i.e. lack of equilibrium between two pairs of states.
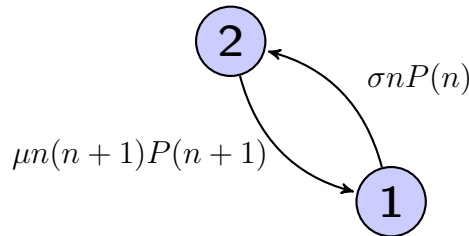

Figure 2.A.1: The two nodes in the graph represent the system in a configuration with n (node 1) and $n+1$ (node 2) particles. Only the case with $\epsilon = 0$ has been considered.

In the figure above we are considering only branching and coagulation as systems with an absorbing state are necessary out of equilibrium because of the presence of a configuration (the absorbing one) from which the system has not rate of escape, see section 1.2.2.

In the absence of the spontaneous extinction process, the system still reach a stationary state (for any value of the parameters) but the dynamics does not have any absorbing configuration as the coagulation process always requires the presence of two particles and always remove only one of them from the lattice.

To prove that the system, with $\epsilon = 0$, reaches an equilibrium stationary state, we need to prove that the detailed balance condition is satisfied between two states

of the system, e.g. a configuration with n particles and $n+1$ particels as depicted
in figure (2.A).

$$\sigma n P(n) = \mu n(n+1)P(n+1) \tag{2.72}$$

By defining $Q(n) = n!P(n)$ the equation above can be rewritten as:

$$\sigma Q(n) = \mu Q(n+1) \tag{2.73}$$

Solving the equation above we easily obtain the expression for the probability distribution:

$$P(n) = \frac{\frac{1}{n!}\left(\frac{\sigma}{\mu}\right)^n}{e^{\frac{\sigma}{\mu}} - 1}(1 - \delta_{n,0}) \tag{2.74}$$

Where the denominator is the normalisation and the term $(1 - \delta_{n,0})$ come from the
boundary condition $P(0) = 0$. The latter impose that the probability of reaching a
system with no particles on the lattice, starting from a non-zero initial distribution,
is zero.

Fragmentation-aggregation processes[3] without diffusion reach a stationary state in
which the detailed balance is restored. This is not surprising as it is clear that,
in the absence of other reactions, the branching and the coagulation processes
balance each others at stationarity.

On the other hand, adding on top of such a system a spontaneous extinction
of particles, would break this equilibrium taking the system out and far from
equilibrium statistical mechanics where new fascinating and still poorly understood
phenomena, such as absorbing phase transitions, occur.

---

[3] $A \to A + A$ i.e. Fragmentation
$A + A \to A$ i.e. Aggregation

CHAPTER 3

THE STATIONARY STATE

In this chapter we will go into the details of the field theory of the reaction-diffusion model described in the previous chapter.
By means of a diagrammatic expansion we will study non-universal properties of the stationary state in the active phase. The analytical results will be compared with numerical simulations in two and three dimensions.
In the last part of the chapter we will focus on another model which is particularly interesting for its biological applications: *the Brusselator*.

3.1   Setting Up The Perturbative Expansion

Following the prescriptions of the previous chapter we can now map the out of equilibrium problem originally described by a master equation into a field theory. The procedure is now straightforward: we introduce creation and annihilation operators, the probability distribution becomes a vector in an abstract Fock space and the master equation will be rewritten as a imaginary time Schrödinger equation with a quasi-Hamiltonian that is a function of $\hat{a}, \hat{a}^\dagger$:

$$\hat{H} = \frac{h}{q} \sum_{\langle \mathbf{m}, \mathbf{n} \rangle} (\hat{a}^\dagger(\mathbf{m}) - \hat{a}^\dagger(\mathbf{n}))(\hat{a}(\mathbf{m}) - \hat{a}(\mathbf{n}))$$
$$+ \mu \sum_{\mathbf{m}} (\hat{a}^\dagger(\mathbf{m})\hat{a}^\dagger(\mathbf{m})\hat{a}(\mathbf{m})\hat{a}(\mathbf{m}) - \hat{a}^\dagger(\mathbf{m})\hat{a}(\mathbf{m})\hat{a}(\mathbf{m}))$$
$$+ \sigma \sum_{\mathbf{m}} (\hat{a}^\dagger(\mathbf{m})\hat{a}(\mathbf{m}) - \hat{a}^\dagger(\mathbf{m})\hat{a}^\dagger(\mathbf{m})\hat{a}(\mathbf{m}) + \epsilon \sum_{\mathbf{m}} \hat{a}^\dagger(\mathbf{m})\hat{a}(\mathbf{m}) - \hat{a}(\mathbf{m})) \quad (3.1)$$

Annihilation and creaction operators are replaced by real fields: $\hat{a}(\mathbf{m}) \to \phi(x,t)$ and $\hat{a}^\dagger(\mathbf{m}) \to \phi^*(x,t)$. In order to simplifiy the expression of the action we shift the field ϕ^* about 1: $\phi^* \to \tilde{\phi} + 1$ (Doi-shift). Inserting the quasi-Hamiltonian (3.1) expressed in terms of $\phi, \tilde{\phi}$ into equation (2.69) we obtain the Doi-Peliti action

49

which fully captures the microscopic reactions:

$$S[\tilde{\phi}, \phi] = \int d^d x \int_0^{t_f} dt [\tilde{\phi}(\partial_t - D\nabla^2 + (\epsilon - \sigma))\phi + \mu\tilde{\phi}^2\phi^2 + \mu\tilde{\phi}\phi^2 - \sigma\tilde{\phi}^2\phi - n_0\tilde{\phi}\delta(t)]$$

(3.2)

Where D is the diffusion constant that on a d-dimensional regular lattice is $D = \frac{ha^2}{2d}$ where a is the lattice constant and $2d$ is the number of nearest neighbours. Following [44] we can drop the initial term $n_0\tilde{\phi}(x,t)\delta(t)$ and extend the integral over t between $-\infty$ and $+\infty$ as the system quickly forget about the initial conditions because of the contiuous production and destruction of particles.

The time-dependent correlation and response functions of the theory are denoted by:

$$G^{[n,m]}(x_1, \ldots, x_n; t_1, \ldots, t_n) =$$
$$= \frac{\int\int \mathcal{D}\phi\mathcal{D}\tilde{\phi}\phi(x_1, t_1)\ldots\phi(x_n, t_n)\tilde{\phi}(x_{n+1}, t_{n+1})\ldots\tilde{\phi}(x_{n+m}, t_{n+m})e^{-S[\tilde{\phi},\phi]}}{\int\int \mathcal{D}\phi\mathcal{D}\tilde{\phi}e^{-S[\tilde{\phi},\phi]}}$$

(3.3)

and can be calculated by introducing a generating functional:

$$Z[J, \tilde{J}] = \int \mathcal{D}\phi\mathcal{D}\tilde{\phi}e^{-S[\phi,\tilde{\phi}]+\int d^d x dt J\phi + \tilde{J}\tilde{\phi}}$$

(3.4)

where $J(x, t), \tilde{J}(x, t)$ are the source functions; correlation functions are then obtained by functional derivation with respect to $J, \tilde{J}$.

The generating functional contains all of the statistical information about the system and in principle in order to extract observables it would be enough to calculate $Z[J, \tilde{J}]$. However, this would be an insurmountable task for any not trivial system, thus Z is usually evaluated by means of a perturbation series [49].

The connected correlation and response functions of the theory are obtained by taking functional derivatives of the logarithm of the generating functional and we will denote them by:

$$G_c^{[n,m]}(x_1, \ldots, x_n; t_1, \ldots, t_n; x_{n+1}, \ldots, x_{n+m}; t_{n+1}, \ldots, t_{n+m}) =$$
$$= \langle\phi(x_1, t_1)\ldots\phi(x_n, t_n)\tilde{\phi}(x_{n+1}, t_{n+1})\ldots\tilde{\phi}(x_{n+m}, t_{n+m})\rangle_c \quad (3.5)$$

In term of functional derivative the connected functions are [39]:

$$G_c^{[n,m]}(x_1,\ldots,x_n;t_1,\ldots,t_n;x_{n+1},\ldots x_{n+m};t_{n+1},\ldots,t_{n+m}) = \langle \prod_i^n \phi(x_i,t_i) \prod_j^m \tilde{\phi}(x_j,t_j) \rangle_c =$$

$$= \prod_i^n \frac{\delta}{\delta J(x_i,t_i0)} \prod_j^m \frac{\delta}{\delta \tilde{J}(x_j,t_j)} \ln Z[J,\tilde{J}]|_{\tilde{J}=J=0} \quad (3.6)$$

All of the following calculations will be performed in Fourier space where is much more convinient and clear evaluate Feynman diagrams, the connected functions will be functions of k and ω:

$$G_c^{[n,m]}(k_1,\ldots,k_n;\omega_1,\ldots,\omega_n;k_{n+1},\ldots,k_{n+m};\omega_{n+1},\ldots,\omega_{n+m}) =$$

$$= \langle \phi(k_1,\omega_1)\ldots\phi(k_n,\omega_n)\tilde{\phi}(k_{n+1},\omega_{n+1})\ldots\tilde{\phi}(k_{m+n},\omega_{m+n}) \rangle_c \quad (3.7)$$

In the rest of the work we will use the following sign and notational convenction for the integrals and the Fourier transforms:

$$\phi(x,t) = \int \frac{d^d k}{(2\pi)^d} \frac{d\omega}{2\pi} \phi(k,\omega) e^{i(kx-\omega t)} = \int đ^d k đ\omega \phi(k,\omega) e^{i(kx-\omega t)} \quad (3.8)$$

$$\phi(k,\omega) = \int d^d x dt \phi(x,t) e^{-i(kx-\omega t)} \quad (3.9)$$

Following standard techniques, [15, 51, 44], the action is separeted into two parts: a bilinear term in ϕ and $\tilde{\phi}$ which is the one that can be integrated by means of Gaussian integration and a *interaction* terms which will be treated perturbatively:

$$S[\phi,\tilde{\phi}] = S_0[\phi,\tilde{\phi}] + S_i[\phi,\tilde{\phi}] \quad (3.10)$$

In order to extract the bare propagator which is the two point function:

$$G_0^{[1,1]}(k,k';\omega,\omega') = \langle \phi(k,\omega)\tilde{\phi}(k',\omega') \rangle_0 \quad (3.11)$$

we need to take the Fourier transform of the bilinear part in equation (3.2)

$$S_0[\phi, \tilde{\phi}] = \int đ^d k đ \omega đ^d k' đ \omega' d^d x dt \tilde{\phi}(k, \omega)(-i\omega + Dk^2 + r_0)\phi(k', \omega')e^{i(kx-\omega t)}e^{i(k'x-\omega't)} =$$

$$= \int đ^d k đ \omega đ^d k' đ \omega' d^d x dt \tilde{\phi}(k, \omega)(-i\omega + Dk^2 + r_0)\phi(k', \omega')e^{i(k+k')x}e^{-i(\omega+\omega')t} =$$

$$= \int đ^d k đ \omega đ^d k' đ \omega' \tilde{\phi}(k, \omega)(-i\omega + Dk^2 + r_0)\phi(k', \omega')\check{\delta}(k + k')\check{\delta}(\omega + \omega') =$$

$$= \int đ^d k' đ \omega' \tilde{\phi}(-k', -\omega')(-i\omega + Dk^2 + r_0)\phi(k', \omega') \quad (3.12)$$

where r_0 is the bare mass which shall remain unspecified for the time being. The notation adopted for the delta functions is: $\check{\delta}(\omega+\omega') = \delta(\omega+\omega')2\pi$ and $\check{\delta}(k+k') = \delta(k + k')(2\pi)^d$

The propagator is a two point response function[1] and will be depicted by a straight line with an arrow that indicates the direction of time. Taking the second functional derivative of the generating functional with respect to the sources, the bilinear part of the path integral will produce:

$$\frac{\check{\delta}(\omega+\omega')\check{\delta}(k+k')}{-i\omega+Dk^2+r_0} = \underleftarrow{\qquad\qquad}$$

$$(3.13)$$

In the space (k, t) the propagator assume the form:

$$\int đ \omega \frac{1}{-i\omega + Dk^2 + r_0}e^{-i\omega t} = e^{-(Dk^2+r_0)t}\theta(t) \quad (3.14)$$

where the integral has been evaluated with the help of the residue theorem (the pole is in $\omega = -i(Dk^2 + r_0)$) and the factor 2π cancel with the one that sit under $d\omega$. The *Heaviside's theta function* on the rigth hand side has a twofold meaning: physically, it expresses causality: the propagator only connects earlier $\tilde{\phi}$ fields to later ϕ fields (see the time limit taken in the previous chapter). Mathematically the sign of t specify whether the integration contour has to be closed in the upper or lower frequency half plane [44].

---

[1]This can be easily seen thinking in terms of numerical simulations: the response function is the response of the system in (x, t) to an external perturbation in (x', t'). Let us consider a system in a stationary state, we add a particle in a given point in space and time and we measure the density in another point in space and time given the presence of the perturbation (subtracting the stationary density), this is: $\langle \phi(x, t)\phi^\dagger(x', t') \rangle - \langle \phi(x, t) \rangle = \langle \phi(x, t)\tilde{\phi}(x', t') \rangle$.

3.2   Feynman Diagrams

The diagrammatic expansion for performing the calculations of the correlation and response functions of the theory is constructed in the usual way: all the terms that are not bilinear in $\phi, \tilde{\phi}$ are evaluated perturbatively by expanding the exponential in the path integral and taking averages with statistical weight e^{S_0}. These averages decompose into product of pair correlation functions that are depicted by Feynman diagrams, which are a pictorial, and elegant, way of keeping track of the various terms in the perturbative expansion [50].

The non linear couplings can be eaily read from the action (3.2) and are grafically representeted as follow:
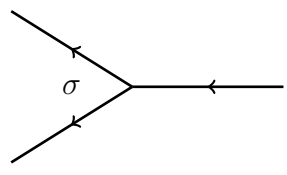

$$(3.15)$$
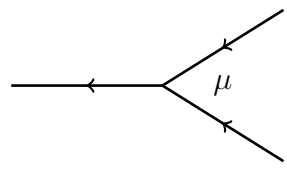
$$(3.16)$$
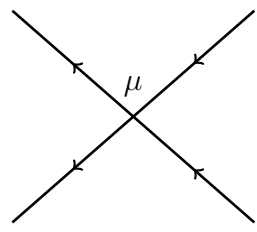
$$(3.17)$$

The first diagram is the symbolic representation of the term $-\sigma\tilde{\phi}^2\phi$, the second diagram is the symbolic representation of the coagulation process and correspond to the term $\mu\tilde{\phi}\phi^2$ and the third corresponds to $\mu\tilde{\phi}^2\phi^2$.

Note that, even if one would be tempted to read the first diagram as the contribution from the branching process to the number of particles, it has to be remembered that, as stated at the end of section (2.3), the contribution to the density is given from diagrams that end with a single line on the left. The branching process enter in the calculation of the density through the mass of the propagator.

If we were to consider the contribution from the initial conditions we would have to take into account another diagram, namely:
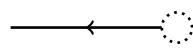
$$(3.18)$$

where the little bubble on the right of the diagram represent the initial distribution. However, such a diagram does not appear in the following calculations as we have extended the temporal limit to all the real axis getting rid of this term.

The independence of the stationary density from the initial condition can be understood by looking at the term in Fourier space:

$$\int đ^d k đ \omega d^d x dt n_0 \tilde{\phi}(k,\omega)\delta(t)e^{i(kx-\omega t)} = \int đ^d k đ \omega n_0 \tilde{\phi}(k,\omega)\delta(k) \qquad (3.19)$$

thus in k space the initial state diagram will be of the form:

$$\longleftarrow \cdots = \frac{n_0 \delta(k)}{-i\omega + Dk^2 + r_0} \qquad (3.20)$$

which goes to zero in the limit of $t \to \infty$, which is the case we are interested in.

3.3   Mean-Field Theory and Langevin Equation

The *mean field theory* is the first and easiest approach to the model and gives us an idea, even if fairly wrong, of the qualitative behaviour of the system under investigation.
The rate equations are obtained by taking the rate of change of the density or concentration to be proportional to the appropriate product of the reactant densities and the reaction rates. This corresponds to a factorization of higher-order correlation functions and thus it is the equivalent of a mean field approximation [44].
The rate equations read:

$$\partial_t \phi(x,t) = D\nabla^2 \phi(x,t) - (\epsilon - \sigma)\phi(x,t) + \mu\phi^2(x,t) \qquad (3.21)$$

In the stationary state $\partial_t \phi(x,t) = 0$ and the density is homogeneously distribuited so that $\nabla^2 \phi(x,t)$ is zero as well. This gives us immediately the stationary solutions:

$$\langle \phi \rangle_s = \begin{cases} \frac{\sigma - \epsilon}{\mu} \\ 0 \end{cases} \qquad (3.22)$$

Obviously the steady state solution $\langle \phi \rangle_s = 0$ corresponds to the absorbing state, the mean field approach predicts a phase transition between an active and an absorbing state for $\epsilon = \sigma$ which as we shall see later is quite far from being the case. However, the mean field solutions are expected to be valid in sufficiently high space dimensions where diffusive mixing is strong enough to suppress correlations [8]. In particular mean field holds above the *upper critical dimension* which is $d_c = 4$ in

the present case (this is a well knonw result in the literature, see [44, 8, 34].
Note that the rate equations can be found directly from the action by taking the
classical field equations which are given by functional derivative with respect to
the fields ϕ and ϕ^*.
The first one to consider is:

$$\frac{\delta S}{\delta \phi} = 2\mu\phi^{*2}\phi - 2\mu\phi^*\phi + \sigma\phi^* - \sigma\phi^{*2} + D\nabla^2\phi^* - \partial_t\phi^* + \epsilon\phi^* - \epsilon = 0 \qquad (3.23)$$

is always solved by $\phi^* = 1$ which ensure probability conservation[2]. Inserting the
uniform solutions in the second one:

$$\frac{\delta S}{\delta \phi^*} = 0 \qquad (3.24)$$

one obtains the reaction-diffusion equations (3.21).

From the action it is possible to obtain a *Langevin equation* which is a stochas-
tic partial differential equation (SPDE). The Langevin equation can be written by
adding a stochastic forcing to the reaction diffusion equations (3.21). In the case
of an action which is at most quadratic in the field $\tilde{\phi}$ the Langevin equation is
easily obtained by taking the noise term be proportional to the $\tilde{\phi}^2$ terms:

$$\partial_t\phi(x,t) = D\nabla^2\phi(x,t) - (\epsilon - \sigma)\phi(x,t) + \mu\phi^2(x,t) + \eta(x,t) \qquad (3.25)$$

The stochastic noise is $\eta(x,t) = 2i\sqrt{\phi(\mu\phi - \sigma)}\kappa$ where κ represents a stochastic
Gaussian variable with zero mean and unit variance.
However, even if in the present case it is trivial to obtain the SPDE, the corre-
spondence between the Doi-Peliti action and the Langevin equation is not always
so straightforward.
An even more significant observation is that only two-particle reactions can straight-
forwardly be cast in the form of an SPDE, since the operation requires that the
field $\tilde{\phi}$ appears at most quadratic in the action [44].

3.4   Perturbative Expansion

The aim of the present work is to characterise the stationary state in the active
phase.
The mean field theory results obtained in the previous section must be recovered
at *tree level* (i.e. no loops) in the diagrammatic expansion. At this stage, in order
to performe a perturbative expansion, we need to consider the explicit form of the
bare mass r_0: $r_0 = \epsilon - \sigma$.
Recalling that ϵ is the rate at which particles are removed from the system and

---

[2]Note that functional derivative are taken with respect to the field ϕ^* and not with respect
to the Doi-shifted field

σ is the rate at which particle reproduce, it is clear that the bare mass would be negative in the active phase which is the phase of the system we are interested in. This would make the Gaussian integral on which we base any perturbative expansion non convergent and the perturbation theory would break down from the very beginning. Also, a negative mass would correspond to a non-physical, negative correlation length and the theory would predict an explosion in the number of particles which is obviously not the case.

In order to avoid divergences of the theory we perform a *shift* to the field $\phi(x,t)$ about a generic constant ζ, the only constrain that we impose on the shift is that has to be big enough to make the mass of the bare propagator positive in the active phase.

The reason why a generic shift of the fields can be performed without having to worry about ending up on a different field theory lies on the fact that in the construction of the field theory we could have used a different representation for the Identity operator which is constructed by shifting the complex numbers ϕ, ϕ^* in equation (2.40) by two different amount. This is also the reason why the Gaussian integral can be performed also after having applied the Doi-shift of the field $\tilde{\phi}$ without shifting the field ϕ.

All the observables that we will measure will have to be independent of the shift but as we shall see there is a particular choice for ζ that has some interesting features.

Applying the shift $\phi(x,t) \to \phi'(x,t)+\zeta$, the action (3.2) in the (x,t) space becomes

$$S[\phi', \tilde{\phi}] = \int d^d x dt \{\tilde{\phi}(x,t)(\partial_t - D\nabla^2 + (\epsilon + 2\mu\zeta - \sigma))\phi'(x,t) + \mu\tilde{\phi}^2(x,t)\phi'^2(x,t) +$$
$$+ \mu\tilde{\phi}(x,t)\phi'^2(x,t) - (\sigma - 2\mu\zeta)\tilde{\phi}^2(x,t)\phi'(x,t) +$$
$$+ \zeta(\mu\zeta - \sigma)\tilde{\phi}^2(x,t) + \zeta(\mu\zeta + \epsilon - \sigma)\tilde{\phi}(x,t)\} \quad (3.26)$$

Where the integral over time have been extended to the entire real axis and the intial term has been dropped.

The term $2\mu\zeta$ that shows up in the new bare mass, that from now on will be denoted by $r_0 = \epsilon + 2\mu\zeta - \sigma$ without any ambiguities, allows us to perform Gaussian integrations.

The new terms that appear in the action are symbolically represented by the two Feynman diagrams:

$$(3.27)$$
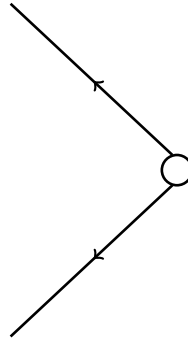
$$(3.28)$$

Diagram (3.27) represents spontaneous and continuum creation of particles whereas diagram (3.28) is the noise vertex and represents spontaneous creation of correlations. By *continuum* we mean that such a diagram does not correspond to diagram (3.18).

As usual the analytical expression of the diagram can be better appreciated in Fourier space:

$$\int đ^d k đ\omega d^d x dt \zeta(\mu\zeta+\epsilon-\sigma)\tilde{\phi}(k,\omega)e^{i(kx-\omega t)} = \int đ^d k đ\omega \zeta(\mu\zeta+\epsilon-\sigma)\tilde{\phi}(k,\omega)đ(k)đ(\omega)$$

$$(3.29)$$

note that the difference between (3.29) and (3.19) lies in the $đ(\omega)$ that makes the former finite in the long time limit.

In fact:

 $= \dfrac{\zeta(\mu\zeta+\epsilon-\sigma)đ(\omega)đ(k)}{-i\omega+Dk^2+r_0}$

$$(3.30)$$

in order to take the long time limit we have to perform a Fourier transform in ω which in this case corresponds to consider an integral of the kind:

$$\lim_{t\to\infty} \int đ\omega f(\omega)đ(\omega)e^{-i\omega t} = f(0)$$

$$(3.31)$$

given that $f(\omega)$ has no pole in the origin the value of the integral is finite (or zero) also for $t \to \infty$.

Note that this makes perfect sense as the stationary density is obviously influenced by spontaneous creation of particles whereas it does not depend upon the initial condition.

The noise term is:

$$\int \mathrm{d}^d k \mathrm{d}\omega \mathrm{d}^d k' \mathrm{d}\omega' d^d x dt \zeta(\mu\zeta - \sigma)\tilde{\phi}(k,\omega)\tilde{\phi}(k',\omega')e^{i(k+k')x}e^{i(\omega+\omega')t} =$$

$$= \int \mathrm{d}^d k \mathrm{d}\omega \mathrm{d}^d k' \mathrm{d}\omega' \zeta(\mu\zeta - \sigma)\tilde{\phi}(k,\omega)\tilde{\phi}(k',\omega')\delta(k+k')\delta(\omega+\omega') =$$

$$= \int \mathrm{d}^d k \mathrm{d}\omega \zeta(\mu\zeta - \sigma)\tilde{\phi}(k,\omega)\tilde{\phi}(-k,-\omega) \quad (3.32)$$

Also, there is a shift of the coupling constant of the branching vertex which do not introduce new diagrams and for the time being is not relevant.

3.4.1   Tree-Level

Before performing the perturbation expansion we need to provide a definition of stationarity. Let us consider an empty lattice on which we place a particle in a random position. If the parameters of the model are such that the system ends up in an active stationary state, its density can be recovered by measuring the number of particles[3] in the limit of $t \to \infty$.

In a field theoretical formulation, given that $\hat{a}^\dagger\hat{a}$ is the number operator and that, once the operators are normal ordered, we are free to use ϕ and $\phi^\dagger$ instead of $\hat{a}$ and $\hat{a}^\dagger$, we have:

$$\lim_{t\to\infty}\langle\phi^\dagger(x,t)\phi(x,t)\phi^\dagger(x_0,t_0)\rangle = \lim_{t\to\infty}\langle\phi(x,t)\phi^\dagger(x_0,t_0)\rangle = \bar{\zeta} \quad (3.33)$$

where $\bar{\zeta}$ stand for the stationary density. If we place a particle in an empty system in presence of spontaneous extinction there is always a finte proability that the particle will die before the system reaches its stationary state. To avoid this problem we place a seed in a background density ζ[4]:

$$\lim_{t\to\infty}\langle(\phi'(x,t)+\zeta)\phi^\dagger(x_0,t_0)\rangle = \bar{\zeta} \quad (3.34)$$

Where ζ is the same constant about which we have shifted the field ϕ in the previous section and assume now the role of a background density.

$$\lim_{t\to\infty}\langle\phi'(x,t)\phi^\dagger(x_0,t_0)\rangle + \langle\phi^\dagger(x_0,t_0)\rangle\zeta = \bar{\zeta} \quad (3.35)$$

By means of the Doi-shift this is:

$$\lim_{t\to\infty}\langle\phi'(x,t)\tilde{\phi}(x_0,t_0)\rangle + \langle\phi'(x,t)\rangle + \langle\tilde{\phi}(x_0,t_0)\rangle\zeta + \zeta = \bar{\zeta} \quad (3.36)$$

---

[3]With an appropriate average

[4]The fact that the shift of the field ϕ corresponds to a different initialisation of the processes can be seen by recovering the field theory starting from a shifted annihilation operator

Let us examine the terms that appear on the left hand side: the first term is the propagator and goes to zero in the limit of $t \to \infty$ if $r_0 \geq 0$ otherwise blow up, see equation (3.14). The third term goes to zero as the expectation of the field $\tilde{\phi}$ is zero for any x, t. The last term is simply ζ which is a constant and is not affected by the limit.

The second term is the expected density given that we have not created any particle, which diagrammatically is depicted as:

$$\langle \phi' \rangle = \; \begin{array}{c}\longrightarrow\!\!\!\!\!\!\!\!\leftarrow\!\!\!\oslash\end{array} \tag{3.37}$$

This is the diagram we are after, namely we want to show that:

$$\langle \phi \rangle_s = \lim_{t \to \infty} \langle \phi'(x, t) \rangle + \zeta = \bar{\zeta} \tag{3.38}$$

and that such a value does not depend upon the particular choice of the shift ζ.

In the following we will denote by $\gamma^{[n,m]}$ the tree level coupling of the proper vertex of the correlation function:

$$G_c^{[n,m]}(k_1, \omega_1, \ldots, k_n, \omega_n; k_{n+1}, \omega_{n+1}, \ldots, k_{n+m}, \omega_{n+m}) =$$
$$= \langle \phi(k_1, \omega_1), \ldots, \phi(k_n, \omega_n)\tilde{\phi}(k_{n+1}, \omega_{n+1}), \ldots, \tilde{\phi}(k_{n+m}, \omega_{n+m}) \rangle_c \quad (3.39)$$

In order to evaluate the diagram (3.37) we need to evaluate:

$$\gamma^{[1,0]} = \; \begin{array}{c}-\!\!\oslash\end{array} \tag{3.40}$$

.

Simbolically all the corrections to the proper vertex $\gamma^{[1,0]}$ are depicted by the following diagrams:


$$\tag{3.41}$$

The expansion continues by adding a source term to each leg in such a way that each new term in the summation reproduce a coagulation vertex, i.e. two incoming and one outgoing legs.

The entire summation above can be rewritten as a reccurence relation which is diagrammatically depicted as follow:
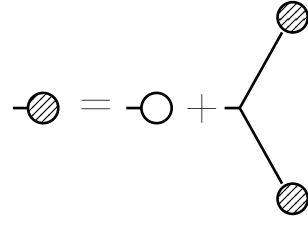
$$(3.42)$$

For ease of notation we call the proper vertex S (where S stands for source term) and the first term on the right hand side $s_0 = \zeta(\mu\zeta + \epsilon - \sigma)$. With this notation we have:
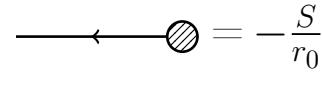
$$= -\frac{S}{r_0}$$

$$(3.43)$$

The minus sign in front of the right hand side comes from the expansion of the exponential in the path integral.
The diagram can be evaluated at $k = 0$ and $\omega = 0$, this reduce to solve the equation:

$$S = s_0 + \mu \frac{1}{r_0^2} S^2 \qquad (3.44)$$

which solution is:

$$S = \frac{1 \pm \sqrt{1 - 4\frac{\mu}{r_0^2} s_0}}{2\frac{\mu}{r_0^2}} \qquad (3.45)$$

The expression for diagram (3.43) is then:

$$\frac{S}{r_0} = \frac{1}{2\mu}(r_0 \pm \sqrt{r_0^2 - 4\mu s_0}) \qquad (3.46)$$

We now recall that $r_0 = \epsilon + 2\mu\zeta - \sigma$, expanding the term under the square root we get: $\sqrt{r_0^2 - 4\mu s_0} = \sqrt{(\sigma - \epsilon)^2}$, which gives us:

$$\frac{S}{r_0} = \frac{\epsilon + 2\mu\zeta - \sigma \pm (\sigma - \epsilon)}{2\mu} \qquad (3.47)$$

The density of the stationary state at tree level is then easily obtained by summing ζ to such a diagram (equation (3.38))

$$\langle \phi \rangle_s^{tree} = \quad \text{———————} \bullet \quad = \zeta + \quad \text{———————} \oslash \qquad (3.48)$$

Which is:

$$\langle\phi\rangle_s^{tree} = \lim_{t\to\infty}\langle\phi(x,t)\phi^\dagger(x_0,t_0)\rangle = \zeta - \frac{S}{r_0} = \begin{cases} \frac{\sigma-\epsilon}{\mu} \\ 0 \end{cases} \tag{3.49}$$

As expected there are two possible stationary densities, namely an active stationary state with a finite number of particles and an absorbing state with no particles. As in the mean field theory the phase transition at the tree level occurs at $\epsilon_c = \sigma$.

We can now proceed and correct higher order correlation functions, in the following calculation we want to show that the mass of the propagator and all the other vertices of the theory are ζ−independent.

We start with the response function $G^{[1,1]} = \langle\phi(k,\omega)\tilde{\phi}(k',\omega')\rangle$ which is the propagator of the field theory. To do so we need to consider all the diagrams with one incoming and one outgoing leg:

$$\tag{3.50}$$

Where the thick line represents the tree level full propagator, this is a Dyson sum and can be rewritten in a more suggestive way as follow:

$$\tag{3.51}$$

which, in a more compact form, is:

$$\tag{3.52}$$

The term in brackets in equation (3.51) is a geometric sum:

$$1 + \text{(diagrams)} + \cdots = \frac{1}{1 - 2\mu \frac{S}{r_0} \frac{1}{-i\omega + Dk^2 + r_0}} \tag{3.53}$$

Where the factor 2 in front of the coupling μ is the symmetry factor of the diagram which take into account the possible ways of connecting the *mistletoe* diagram[5] to the propagator.

Multiplying out the propagator in front of the bracket in equation (3.51) we obtain the expression for the tree-level full propagator:

$$\text{(diagram)} = \frac{\bar{\delta}(k+k')(\omega+\omega')}{\underbrace{-i\omega + Dk^2 + r_0 - 2\mu\frac{S}{r_0}}_{= r_t}} \tag{3.54}$$

Where r_t stands for *tree level mass*. Recalling equation (3.46) we find that:

$$r_t = \pm\sqrt{r_0^2 - 4\mu s_0} = |\sigma - \epsilon| \tag{3.55}$$

The tree-level mass is, as expected, $\zeta-$independent and positive in the active phase.

The other vertices that get tree-level corrections are the two point function with proper vertex $\bar{n} = \gamma^{[2,0]}$:

$$\gamma^{[2,0]} = \text{(diagrams)} \tag{3.56}$$

Note that the thick line is the tree level full propagator which includes all the corrections from the mistletoe diagram (which in turn is made of all the correction to the source term).

Recalling that $\hat{\mu}$ is the coupling of the four point vertex that now, to avoid abiguities, has to be considered as being different from the coupling of the couagulation

---

[5]The mistletoe diagram is the tree level summation of the source term

diagram[6], we obtain:

$$\bar{n} = \zeta(\mu\zeta - \sigma) - (2\hat{\mu}\zeta - \sigma)\frac{S}{r_0} + \hat{\mu}(\frac{S}{r_0})^2 = \hat{\mu}(\zeta - \frac{S}{r_0})^2 - \sigma(\zeta - \frac{S}{r_0}) \qquad (3.57)$$

Which is $\zeta-$independent as the terms between brackets is the stationary density which as shown above is independent of ζ.
The two point function: $C_t(k,\omega) = G^{[2,0]}(k,\omega) = \langle\phi(k,\omega)\phi(k',\omega')\rangle$ can now be written explicitly $\forall\, k, \omega$:

$$C_t(k,\omega) = \bar{n}\frac{1}{\omega^2 + (Dk^2 + r_t)^2} = \bar{n}|G_t^{[1,1]}(k,\omega)|^2 \qquad (3.58)$$

The correlation function at tree level is proportional to the absolute square of the response function.

The last vertex to be corrected is $\bar{\sigma} = \gamma^{[2,1]}$

$$(3.59)$$

The second diagram on the right hand side has a symmetry facor of 2 which come from the two possible ways to attach the source diagram. Note that the upper leg on the right han side of the last diagram is a tree level full propagator which includes all the milstletoe corrections:

$$(2\hat{\mu}\zeta - \sigma) - 2\hat{\mu}\frac{S}{r_0} = 2\hat{\mu}(\zeta - \frac{S}{r_0}) - \sigma \qquad (3.60)$$

The tree level reproduces the mean field theory results found in the previous section but is still far from reproducing the numerical simulations (see figure 3.1). In order to obtain more accurate results we need to take into account fluctuations in a systematic way.

However, before going into the details of the loop expansion it is interesting to make some observations about the shift that we have performed. The original field theory was ill-defined in the active phase, i.e. divergent bilinear action $S_0[\tilde{\phi}, \phi]$. The divergence has been *cured* by means of a shift of the field $\phi(x, t)$ and, as a result of this operation, we have ended up with a theory which has a bare level different from its tree-level.

---

[6]This is because the two couplings, μ and $\hat{\mu}$ have different scaling dimension.

The upper critical dimension is left unchanged after the shift and the tree level is ζ−independent for what concern the mass of the propagator, density of the stationary state and coupling constants. This is encouraging as we have not introduced any alteration to the underlying physics of the system and we are not limited by any constrain when we apply the shift, some choice are more convinient then others and we are free to make any of them.

Also, looking at equations: (3.26), (3.55), (3.57) and (3.60) it appears clear that the bare level and the tree level coincide when the shift ζ is taken to be ugual to the mean field density which, as stated in the previous section, is the solution of the classical field equation $\frac{\delta S}{\delta \phi^*} = 0$.

This is particularly interesting because it remind us of the Doi-shift which, as stressed at the end of the previous chapter, is a shift about the solution of the other classical equation $\frac{\delta S}{\delta \phi} = 0$.
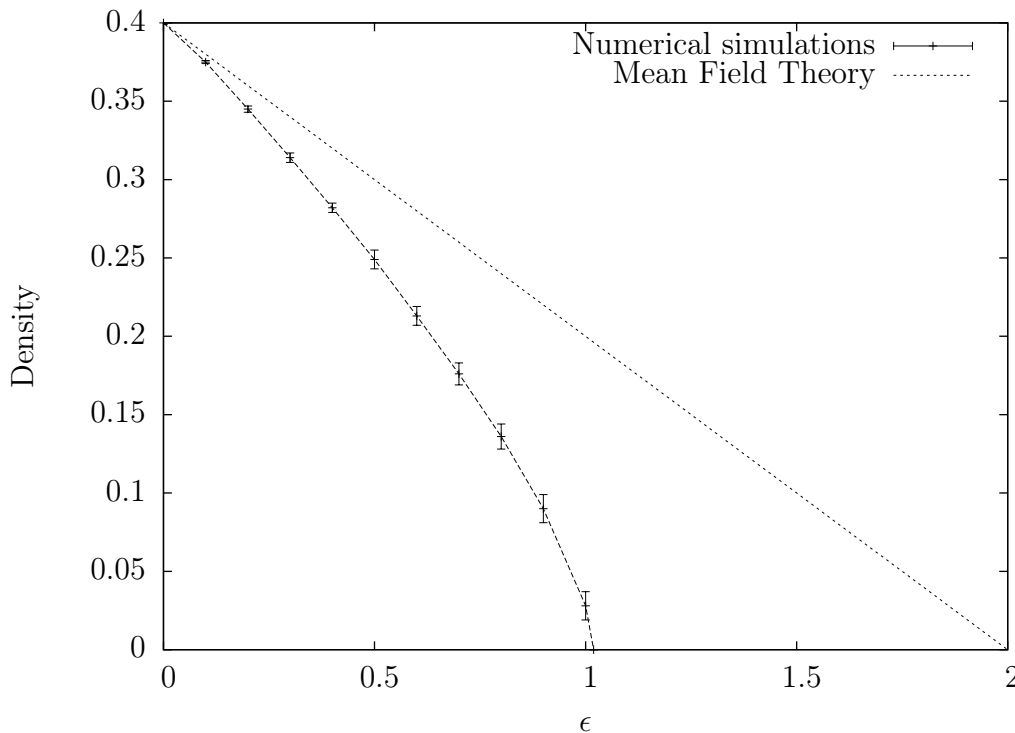
Figure 3.1: Density as a function of extinction rate. Numerical simulations in comparison to the prediction of the mean field theory. The simulations have been performed in two dimensions on a initially fully occupied lattice of linear size L=128. The other parameters has been kept fixed at $\sigma = 2$, $\mu = 5$ and $h = 10$.

3.4.2   One Loop

Fluctuations are ubiquitous in nature and they can drammatically influence the behavior of a system, this is particularly important and interesting in systems that

undergo a second-order phase transitions where fluctuactions of the order parameter exhibit long range correlations.

In systems made of many interacting units, such as for example living systems, fluctuations can led to novel emergent behavior on a macroscopic scale. Intrinsic and large fluctuations make the characterisation of the system under investigation a challanging task. When the size of the system (its volume or number of particles) is really small standard techniques for solving the chemical master equation, such as Van Kampen's system size expansion and the Kramers-Moyal expansion, do not capture properly the boundary conditions and fluctuations can lead to negative populations [57]. The Doi-Peliti formalism do not suffer from these problems as the vacuum state set a lower bound in the number of particles.

In order to systematically take into account fluctuations effects we need to go beyond the tree level and consider a loop expansion. This is a reorganisation of the perturbative expansion according to the topology of the graphs in each term [49]. Following the *Feynman rules* to each directed line corresponds a response propagator and to each closed loop corresponds an integral over internal wavevectors and frequencies. The propagator that has to be used in the loops is the tree level corrected propagator with mass r_t.

In the following we will calculate all the integrals for the loops making use of countor integration for the integral over ω and Feynman integrals for the integrals over k.

The first two loops to consider are the ones that contribuite to the correction of the propagator, namely the one formed by diagram (3.15) and diagram (3.16) and the one form by diagram (3.28) and the propagator.

$$a = \;\vcenter{\hbox{\includegraphics{loop}}}\; = 2\mu\bar{\sigma} \int đ^d k\, đ\omega' \frac{1}{-i\omega' + Dk^2 + r_t} \frac{1}{-i(\omega - \omega') + D(q-k)^2 + r_t} =$$

$$= 2\mu\bar{\sigma} \int đk^d \frac{1}{-i\omega + D(q-k)^2 + Dk^2 + 2r_t} =$$

$$2\mu\bar{\sigma} \int đk^d \frac{1}{-i\omega + D(\frac{q}{2} - k)^2 + D(\frac{q}{2} + k)^2 + 2r_t} \quad (3.61)$$

Where the factor 2 sitting in front of the integral is the symmetry factor. The integral in ω has been evaluated with the pole $\omega' = \omega + i(D(q-k)^2 + r_t)$.

$$= 2\mu\bar{\sigma} \int đk^d \frac{1}{2Dk^2 \underbrace{-i\omega + D\frac{q^2}{2} + 2r_t}_{m}} =$$

By means of the identity:

$$\int d^d x \frac{1}{x^2 + a} = K_d \int dx \frac{x^{d-1}}{x^2 + a} \tag{3.62}$$

with K_d volume of a d-dimensional sphere, the integral above become:

$$= \frac{2\mu\bar{\sigma} K_d}{(2\pi)^d} \int dk \frac{k^{d-1}}{2Dk^2 + m} = \frac{4\mu\bar{\sigma}}{(4\pi)^{d/2}\Gamma(\frac{d}{2})2D} \int dk \frac{k^{d-1}}{k^2 + \frac{m}{2D}} =$$
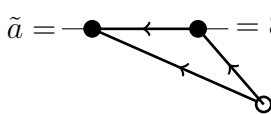
With the help of the integral [15]:

$$\int_0^\infty du \frac{u^\alpha}{(u + m)^\beta} = m^{\alpha-\beta+1} \frac{\Gamma(\beta - 1 - \alpha)\Gamma(\alpha + 1)}{\Gamma(\beta)} \tag{3.63}$$

the integral above become:

$$= \frac{2\mu\bar{\sigma}}{(4\pi)^{d/2}2D} \Big(\frac{2r_t + D\frac{q^2}{2} - i\omega}{2D}\Big)^{\frac{d}{2}-1} \Gamma\Big(\frac{2 - d}{2}\Big)$$

The second diagram to consider is the *shark fin* diagram:

$$\tilde{a} = \underbrace{} = 8\mu^2\bar{n} \int đ^d k\, đ\omega' \frac{1}{-i\omega' + Dk^2 + r_t} \frac{1}{i\omega' + Dk^2 + r_t} \frac{1}{-i(\omega - \omega') + D(q-k)^2 + r_t} =$$

$$\tag{3.64}$$

Where 8 is the symmetry factor of the diagram. The poles are in $\omega' = \pm i(Dk^2 + r_t)$ and $\omega' = -i(D(q-k)^2 + r_t)$, performing the integral over ω' one obtaines:

$$= 8\mu^2\bar{n} \int đ^d k \frac{1}{2(Dk^2 + r_t)} \frac{1}{-i\omega + Dk^2 + D(q-k)^2 + 2r_t} =$$

This integral can be evaluated for vanishing external momenta and frequencies (i.e. $q = 0$, $\omega = 0$) as it is a contribution to the correction of the mass:

$$= 8\mu^2\bar{n} \int đ^d k \frac{1}{4(Dk^2 + r_t)^2} = \frac{16\mu^2\bar{n}}{4(4\pi)^{\frac{d}{2}}\Gamma(\frac{d}{2})} \int dk \frac{k^{d-1}}{(Dk^2 + r_t)^2} =$$

$$= \frac{16\mu^2\bar{n}}{4D^2(4\pi)^{\frac{d}{2}}\Gamma(\frac{d}{2})} \int dk \frac{k^{d-1}}{(k^2 + \frac{r_t}{D})^2} = \frac{8\mu^2\bar{n}}{4D^2(4\pi)^{\frac{d}{2}}\Gamma(\frac{d}{2})} \int du \frac{u^{\frac{d-2}{2}}}{(u^2 + \frac{r_t}{D})^2} =$$

$$= \frac{8\mu^2\bar{n}}{4D^2(4\pi)^{\frac{d}{2}}\Gamma(\frac{d}{2})} \Big(\frac{r_t}{D}\Big)^{\frac{d-4}{2}} \frac{\Gamma(\frac{4-d}{2})\Gamma(\frac{d}{2})}{\Gamma(2)} = \frac{8\mu^2\bar{n}}{4D^2(4\pi)^{\frac{d}{2}}} \Big(\frac{r_t}{D}\Big)^{\frac{d-4}{2}} \Gamma\Big(\frac{4 - d}{2}\Big)$$

We are now left with the calculation of the two loops made by diagram (3.16) and diagram (**??**).

The first one will contribute the correction to the source term:

$$b = \quad \raisebox{-0.5em}{\includegraphics[width=1cm]{}} \quad = 2\mu\bar{n} \int \bar{d}^d k \bar{d}\omega' \frac{1}{-i\omega' + Dk^2 + r_t} \frac{1}{i\omega' + Dk^2 + r_t} = \tag{3.65}$$

$$= 2\mu\bar{n} \int \bar{d}^d k \frac{1}{2(Dk^2 + r_t)} = \frac{2\mu\bar{n}}{(4\pi)^{\frac{d}{2}}\Gamma(\frac{d}{2})D} \int dk \frac{k^{d-1}}{k^2 + \frac{r_t}{D}} =$$

$$= \frac{2\mu\bar{n}}{(4\pi)^{\frac{d}{2}}\Gamma(\frac{d}{2})2D} \int dk \frac{u^{\frac{d-2}{2}}}{u^2 + \frac{r_t}{D}} = \frac{\mu\bar{n}}{(4\pi)^{\frac{d}{2}}\Gamma(\frac{d}{2})D}\left(\frac{r_t}{D}\right)^{\frac{d-2}{2}}\Gamma\left(\frac{2-d}{2}\right)$$

The two diagrams quoted above but with a different topology give rise to another loop, namely:

$$\tilde{b} = \quad \raisebox{-1em}{\includegraphics[width=1.5cm]{}} \quad = \tag{3.66}$$

$$= 2\mu^3\bar{n} \int \bar{d}^d k \bar{d}\omega \frac{1}{-i\frac{\omega}{2} + D(\frac{k}{2})^2 + r_t} \frac{1}{i\frac{\omega}{2} + D(\frac{k}{2})^2 + r_t} \frac{1}{-i\frac{\omega}{2} + D(\frac{k}{2})^2 + r_t} \frac{1}{i\frac{\omega}{2} + D(\frac{k}{2})^2 + r_t}$$

There are two poles, namely: $\omega = \pm 2i(D(\frac{k}{2})^2 + r_t)$, the integral over ω gives us:

$$= 2\mu^3\bar{n} \int \bar{d}^d k \frac{1}{(2D(\frac{k}{2})^2 + 2r_t)^2} = \frac{2\mu^3\bar{n}}{\frac{D^2}{4}} \int \bar{d}^d k \frac{1}{(k^2 + \frac{4r_t}{D})^2} =$$

$$= \frac{2\mu^3\bar{n}}{\frac{D^2}{4}} \frac{2}{(4\pi)^{\frac{d}{2}}\Gamma(\frac{d}{2})} \int dk \frac{k^{d-1}}{(k^2 + \frac{4r_t}{D})^2} = \frac{2\mu^3\bar{n}}{\frac{D^2}{4}} \frac{1}{(4\pi)^{\frac{d}{2}}\Gamma(\frac{d}{2})} \int du \frac{u^{\frac{d}{2}-1}}{(u + \frac{4r_t}{D})^2} =$$

$$= \frac{8\mu^3\bar{n}}{D^2(4\pi)^{\frac{d}{2}}}\left(\frac{4r_t}{D}\right)^{\frac{d-4}{2}}\Gamma\left(\frac{4-d}{2}\right)$$

The branching and the coagulation vertex give rise to:

$$t = \qquad\qquad\qquad\qquad =$$

(3.67)

$$4\bar{\sigma}^2\mu \int \dj^dk \dj\omega \frac{1}{-i\omega + Dk^2 + r_t}\frac{1}{i\omega + Dk^2 + r_t}\frac{1}{-i\omega + Dk^2 + r_t} =$$

$$= 4\bar{\sigma}^2\mu \int \dj^dk \frac{1}{4(Dk^2 + r_t)^2} = \frac{4\bar{\sigma}^2\mu}{4D^2}\int \dj^dk \frac{1}{(k^2 + \frac{r_t}{D})^2} =$$

$$= \frac{2\bar{\sigma}^2\mu}{(4\pi)^{\frac{d}{2}}\Gamma(\frac{d}{2})D^2}\int dk \frac{k^{d-1}}{(k^2 + \frac{r_t}{D})^2} = \frac{2\bar{\sigma}^2\mu}{(4\pi)^{\frac{d}{2}}\Gamma(\frac{d}{2})2D^2}\int du \frac{u^{\frac{d}{2}-1}}{(u + \frac{r_t}{D})^2} =$$

$$= \frac{\bar{\sigma}^2\mu}{(4\pi)^{\frac{d}{2}}D^2}(\frac{r_t}{D})^{\frac{d}{2}-2}\Gamma(\frac{4-d}{2})$$

The one made of three coagulation vertices and one noise vertex is a contribution to the correction of the coagulation vertex:

$$q = \qquad\qquad\qquad\qquad =$$

(3.68)

$$= 16\mu^3\bar{n} \int \dj^dk \dj\omega \frac{1}{-i\omega + Dk^2 + r_t}\frac{1}{i\omega + Dk^2 + r_t}\frac{1}{i\omega + Dk^2 + r_t}\frac{1}{i\omega + Dk^2 + r_t} =$$

$$= \frac{16\mu^3\bar{n}}{8D^3}\int \dj^dk \frac{1}{(k^2 + \frac{r_t}{D})^3} = \frac{4\mu^3\bar{n}}{(4\pi)^{\frac{d}{2}}\Gamma(\frac{d}{2})D^3}\int dk \frac{k^{d-1}}{(k^2 + \frac{r_t}{D})^3} =$$

$$= \frac{2\mu^3\bar{n}}{(4\pi)^{\frac{d}{2}}\Gamma(\frac{d}{2})D^3}\int du\frac{u^{\frac{d}{2}-1}}{(u+\frac{r_t}{D})^3} = \frac{2\mu^3\bar{n}}{(4\pi)^{\frac{d}{2}}D^3}(\frac{r_t}{D})^{\frac{d-6}{2}}\frac{\Gamma(\frac{6-d}{2})}{2}$$

The last loop to consider is a contribution to the correction of the branching vertex:

$$\tilde{q} =$$

$$\tag{3.69}$$

$$8\bar{n}\bar{\sigma}\mu^2\int đ^dk đ\omega\frac{1}{-i\omega+Dk^2+r_t}\frac{1}{i\omega+Dk^2+r_t}\frac{1}{-i\omega+Dk^2+r_t}\frac{1}{i\omega+Dk^2+r_t} =$$

$$8\bar{n}\bar{\sigma}\mu^2\int đ^dk\frac{1}{4(Dk^2+r_t)^2} = \frac{16\bar{n}\bar{\sigma}\mu^2}{4(4\pi)^{\frac{d}{2}}\Gamma(\frac{d}{2})}\int dk\frac{k^{d-1}}{(Dk^2+r_t)^2} =$$

$$\frac{8\bar{n}\bar{\sigma}\mu^2}{4D^2(4\pi)^{\frac{d}{2}}\Gamma(\frac{d}{2})}\int du\frac{u^{\frac{d}{2}-1}}{(u+\frac{r_t}{D})^2} = \frac{2\bar{n}\bar{\sigma}\mu^2}{D^2(4\pi)^{\frac{d}{2}}}(\frac{r_t}{D})^{\frac{d-4}{2}}\Gamma(\frac{4-d}{2})$$

We now have all the ingredients to perform a loop expansion. The main task is to find the stationary ($t \to \infty$) density and compare it with the numerical results. In order to find the correct expression we begin with an analysis of the loop expansion for the response propagator i.e. we have to find all the topologically different graphs with one leg sticking in and one sticking out of a loop.
As we did at tree level, the full (loop corrected) propagator $G(k,\omega)$ can be written as a series of tree level propagators and a complet set of *one particle irriducible* diagrams (figure 3.70). A 1PI graphs is a diagram that cannot be separated into two independent parts by cutting just one internal line [15].
The contributions to the correction of the propagator are depicted diagrammatically as:

$$\text{(3.70)}$$

This is again a *Dyson sum* that reproduces completely the perturbation expansion at one loop order for the response propagator. Analytically, equation (3.70), becomes the *Dyson's equation* [39]:

$$G^{[1,1]}(k,\omega) = G_t^{[1,1]}(k,\omega)(1 + \Sigma(k,\omega)G_t^{[1,1]}(k,\omega)+$$
$$+ \Sigma(k,\omega)G_t^{[1,1]}(k,\omega)\Sigma(k,\omega)G_t^{[1,1]}(k,\omega) + \dots) =$$
$$= G_t^{[1,1]}(k,\omega)(1 + \Sigma(k,\omega)G^{[1,1]}(k,\omega)) \quad \text{(3.71)}$$

Which is the equivalent at one loop level of equation (3.51).
The exact expression for the full propagator is easily found:

$$G^{[1,1]}(k,\omega) = \frac{G_t^{[1,1]}(k,\omega)}{1 - \Sigma(k,\omega)G_t^{[1,1]}(k,\omega)} \quad \text{(3.72)}$$

All we have to do now is to calculate the *self energy* $\Sigma(g,\omega)$ from which we obtain the one loop-corrected mass **r** that will be used for the evaluation of the density. The one particle irriducible diagrams that contribute to the self energy are the first two loops in the integrals above:

$$\text{(3.73)}$$

Note that the 1PI diagrams have been drawn with amputated external legs to highlight the fact that the corresponding analytical expression do not include external propagators. An emphasis has been given to the vertices. As always the vertex depicted as a white circle is the noise vertex.
From equation (3.72) we obtain the new mass **r**:

$$\text{(3.74)}$$

The full propagator is:

$$\longleftarrow = \frac{\bar{\delta}\left(k+k'\right)\bar{\delta}\left(\omega+\omega'\right)}{-i\omega+Dk^2+\mathbf{r}}$$

(3.75)

Diagrammatically one has to immagine the propagator as a straigth line with all the sources sticking in (i.e. tree level corrections) and dressed with the loops (3.61),(3.64) which in turn incorporate the tree level corrections.

In order to find the density we need to consider the loop corrections to the source term. Using the mass **r** in the integral for the loops we include all the corrections due to trees and loops to the propagator, as a consequence the equation to recover the density will have the same structure as the one at tree level.
Thus the procedure will be the same, we need to find the correction to the source itself and then stick in it a propagator, summing this diagram to the mean field theory will give us the one loop correction to the density.
The summation we are after is given by the following recurrence relation:

(3.76)

Where the dotted circle stands for the correction to the coagulation vertex. As usual the one loop correction to the proper vertex with amputated legs, with m incoming legs and n outgoing legs is denoted by $\Gamma^{[n,m]}$:

$$\Gamma^{[1,2]} = \quad (3.77)$$

The corrections to the branching vertex are:

$$\Gamma^{[2,1]} = \quad (3.78)$$

Denoting the loop-corrected source by $\bar{S}$, and the one loop-corrected coagulation vertex (which in turn include the loop-corrected branching vertex) by $\tilde{\mu}$, equation (3.76) correspond to:

$$\bar{S} = b + \tilde{\mu}\frac{\bar{S}^2}{\mathbf{r^2}} \tag{3.79}$$

which has the same form of (3.44). We strees again that the integrals in the loops have to been calculated with the new loop-corrected mass $\mathbf{r}$ in order to take into account the corrections due to the other loops.

The solution of the equation above gives us the new loop-corrected source term $\bar{S}$ which as to be multiplied by the full propagator to obtain:

$$\frac{\bar{S}}{\mathbf{r}} = \frac{\mathbf{r} \pm \sqrt{\mathbf{r} - 4\tilde{\mu}b}}{2\tilde{\mu}} \tag{3.80}$$

The delta functions that come with the source term take care of ω and k in the propagator.

Diagrammatically the stationary density at one loop level is depicted as follow:

$$\langle \phi \rangle_s^{\text{One loop}} = \quad \rule{3cm}{0.4pt}\!\!\bullet \quad = \zeta + \quad \rule{2cm}{0.4pt}\!\!\oslash \quad + \quad \rule{1.5cm}{0.4pt}\!\!\bullet\!\!\bigcirc \tag{3.81}$$

All the observables are $\zeta-$independent as all the dependence from the shift ζ has been cancelled by the tree level summation.

To check the quality of the approximation above we need to compare it with the results obtained in numerical simulations.
The integrals in equation (3.61) and (3.65) are clearly divergent for d=2 and thus the field theory cannot be defined by the straightforward perturbative expansion without some modification [51]. In order to make the Feynman diagrams well defined finite quantities we need to introduce some kind of regularisation.

There is a vast literature ([15, 51, 52], to quote some of them) regarding *regularisation methods* in quantum field theory and critical phenomena. The main ones are [15]:

- Strong cut-off: integrals over k are restricted to $|k| < \Lambda$.

- Pauli-Villars:The propagator is modified in such a way that decreas faster for large momentum.

- Lattice regularisation: the theory is 'placed' on a lattice so that the space is discretized and the spatial derivative is replaced by the finite difference.

Every technique has its advantage and disadvantage. The strong cut-off technique is obviously the most intuitive one and is the most easy to deal with, particularly in the field description of condensed matter systems where Feynman diagrams are naturally regularised at length scale a [52]. Nevertheless, the strong cut-off Λ has the big disadvantage to break traslational invariance of the system.
In the comparison with the numerics we have adopted a *lattice regularisation* which is the most suitable when the aim is to compare with numerical simulations where integrations, even in high dimensions, are easily implemented by means of Monte Carlo methods. Also, non-universal properties, such as the phase diagram and the density, depend upon the form of the theory at small distances (the specific

form of the lattice) [58]. Away from the critical domain, the continuum limit is not necessary well-defined, thus in order to compare with the numerical simulation one has to deal with a field theory, defined on a lattice, in which we keep the same terms that we had in the continuum theory.

The comparison between the loop expansion and the Monte Carlo simulations has been implemented by means of the following procedure: in lattice regularisation techniques on an hyper-cubic lattice the propagator in the intergals of the loops is replaced by [51]:

$$G^{[1,1]}(k,\omega) \rightarrow G^{[1,1]}(k,\omega) = \frac{1}{-i\omega + \frac{2D}{a^2}\sum_{i=1}^{d}(1 - cos(ak_i)) + \mathbf{r}} \tag{3.82}$$

Which is obtained by discretizing the continuum derivative [53]. The lattice spacing a is set equal to one and the diffusion constant is $D = \frac{ha^2}{2d\Delta t}$, where $2d$ is the number of nearest neighbours in a d-dimensional regular lattice and Δt has been set equal to one.

The integral over ω can be performed in the usual way by means the theorem of residues and the remaining integral over k is calculated numerically, in the first Brillouine zone, taking great care of signs and prefactors.

The results in figure 3.2 show the comparison between numerics, mean field theory (tree level approximation) and one loop approximation in two and three dimensions.

As one can easily see in three dimensions there is much more agreement between numerics and calculations, this is because fluctuactions play a much less important role in higher dimensions (note that the upper critical dimension of the theory is four).

The position of the critical point is: $\epsilon_t^c = 1.06$, $\epsilon_n^c = 1.019$ in two dimensions and $\epsilon_t^c = 1.3, \epsilon_n^c = 1.275$ in three dimensions, where the subscripts t and n stand for theory and numerics.

Other results, for different value of the parameters, in three dimensions have been shown in the following page.

Fluctuactions have been taken into account by means of the loop expansion. The continuum theory has been placed on a lattice by using a lattice regularisation technique, at one loop level the theory is able to predict the evolution of the density as a function of the parameters and it is able to localise the position of the critical point with great accurancy for different value of the parameters. We want to stress that the one developed in this chapter is an uncontrolled approximation scheme, i.e. in order to obtain accurate results one has to choose the most relevant diagrams but this operation normally relies on the intuition of the researcher.

A particular attention has to be given to the continuum limit. Even though the latter has been formally taken during the mapping of the master equation into a field theory, in order to evaluate non-universal properties, away from the critical domain, the FT has been placed on a discrete lattice. This procedure allow us to compare the analytical results with Monte Carlo simulations.
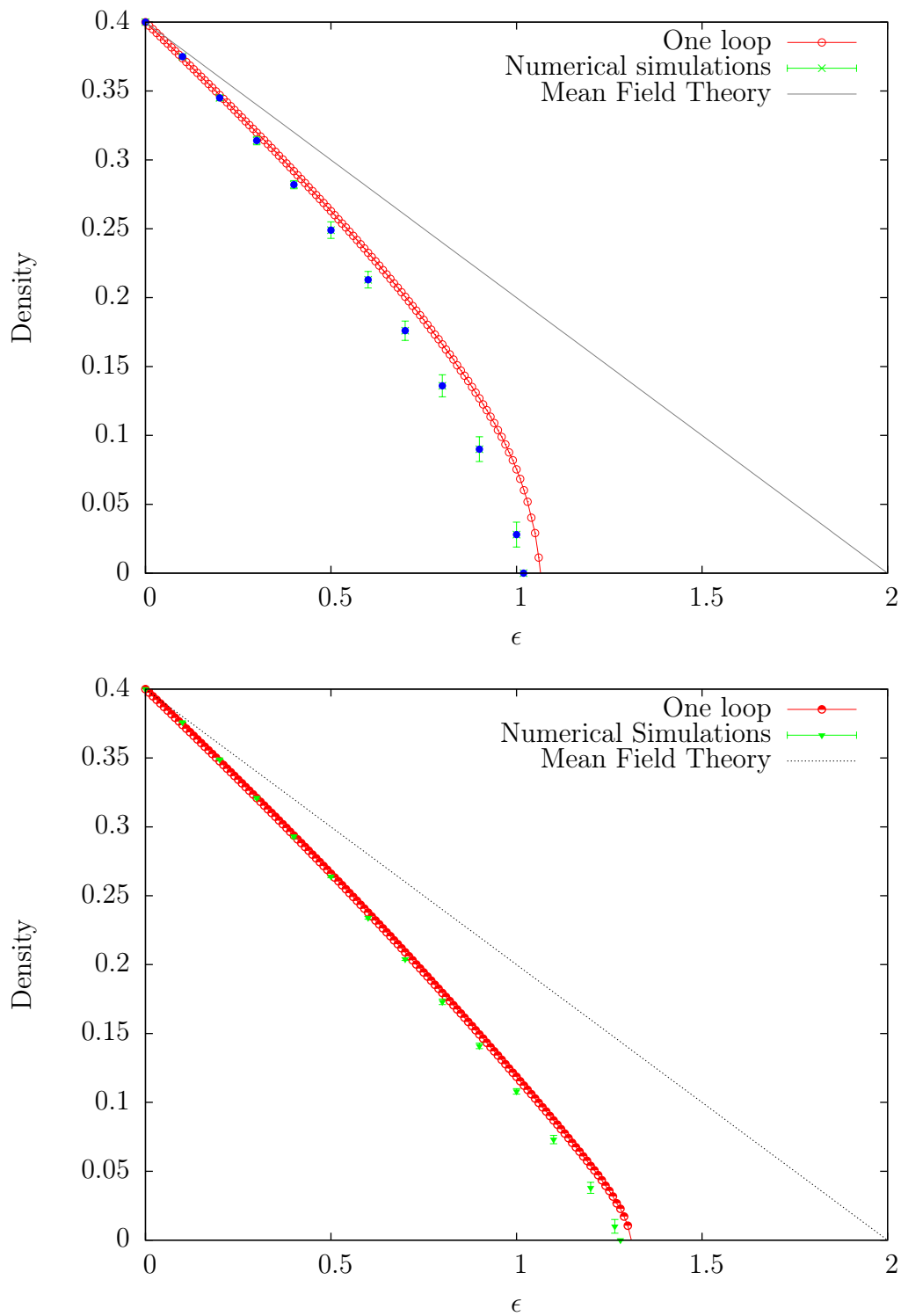
Figure 3.2: Comparison between numerical simulations and analytical calculations in two (L=128) and three (L=30) dimensions. Parameter: $\sigma = 2, \mu = 5, h = 10$. The data are the results of averaging over 100 realisations of the process for the first points and 800 realisations of the process nearby the critical point.
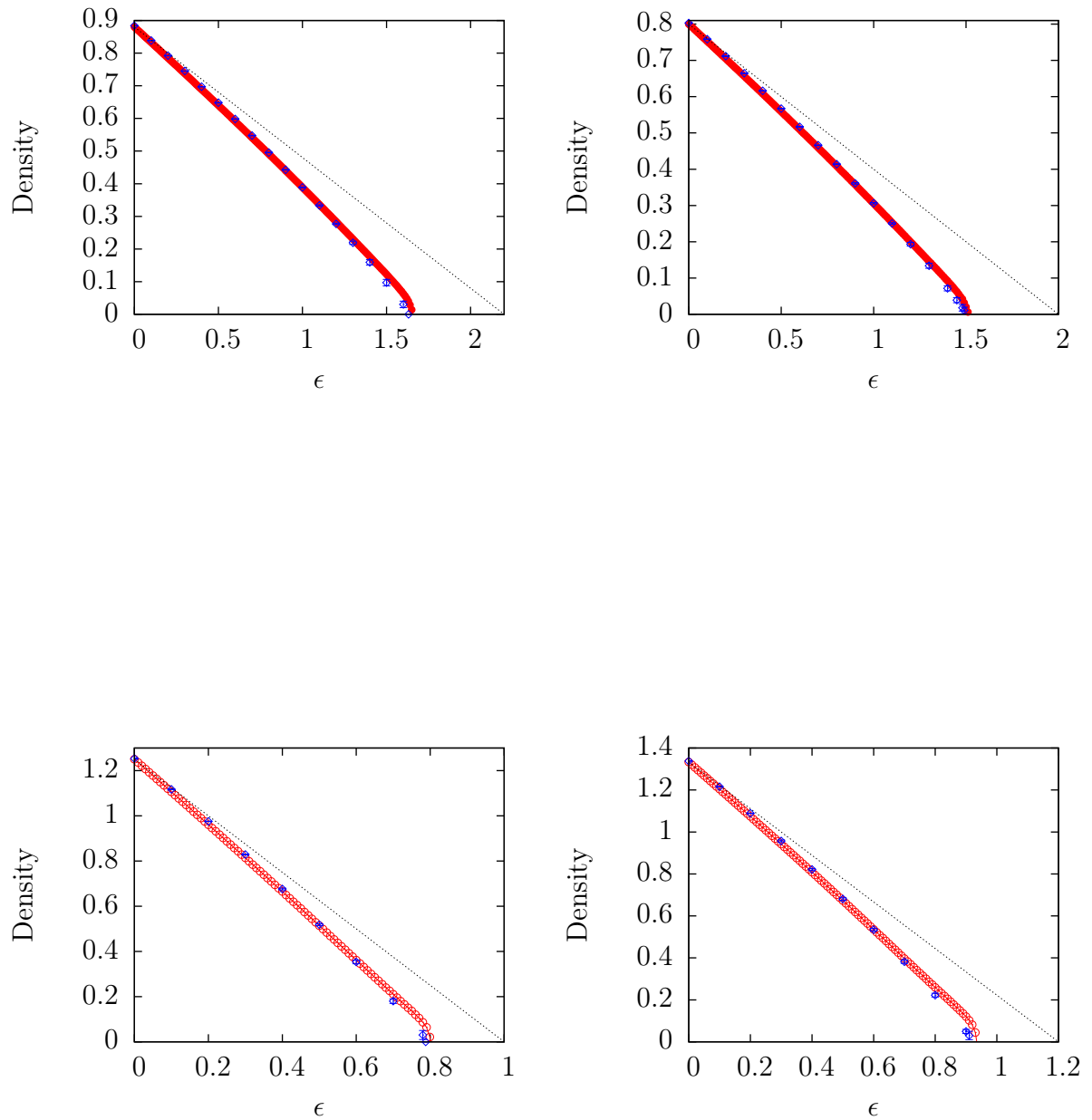
Figure 3.3: Blue points: numerical simulations, red points: one loop approximation, line: mean field theory. Three dimensions, parameters from top left: $\sigma = 2, \mu = 2.5, h = 10$; $\sigma = 2.2, \mu = 2.5, h = 10$; $\sigma = 1, \mu = 0.8, h = 5$; $\sigma = 1.2, \mu = 0.9, h = 5$.

3.5   The Brusselator

In the last part of this project we moved our attention to a two species reaction diffusion process particularly important because of its biological applications: *the Brusselator* [54]. The following calculation are the starting point for future works, in which we want to apply the techniques developed so far to a model which has been deeply investigated by means of other methods.

The Brusselator is an *auto-catalytic*[7] process defined by the following reactions:

$$A \xrightarrow{\epsilon} \emptyset \qquad\qquad \emptyset \xrightarrow{\sigma} A$$

$$A \xrightarrow{\tau} B \qquad\qquad 2A + B \xrightarrow{\mu} 3A$$
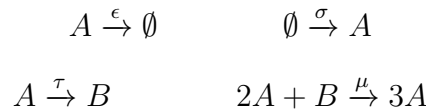
Where spontaneous extinction occours with rate ϵ, spontaneous creation occurs with rate σ, transmutaion with rate τ and the last reaction occurs with rate μ.
In some variant of the process the empty set is replaced by an inert species which population do not form degrees of freedom (see for example [55]).
The state of the system at any time is described by the number of reactants A,B whereas the size of the system in a zero dimensional model, which is the one under investigation in this project, is set by the spontaneous creation rate[8] or, equivalently, by the number of inert particles in the system [55].

The master equation that describe the time evolution of the probability distribution is again mapped into a field theory by means of the Doi-Peliti formalism. To this end we need to introduce a pair of creation and annihilation operators for species A: $\hat{a}^\dagger, \hat{a}$ and a pair of creation and annihilation operators for species B: $\hat{b}^\dagger \hat{b}$. Given the absence of space the imaginary time Schrdinger equation is easily obtained by looking at the reactions (see note at the end of section 2.2).

$$\frac{\partial \, |\Psi(t)\rangle}{\partial t} = -[\epsilon(\hat{a}^\dagger\hat{a}-\hat{a})+\sigma(1-\hat{a}^\dagger)+\tau(\hat{a}^\dagger\hat{a}-\hat{b}^\dagger\hat{a})+\mu(\hat{b}^\dagger\hat{a}^{2\dagger}\hat{b}\hat{a}^2-\hat{a}^{3\dagger}\hat{b}\hat{a}^2)] \, |\Psi(t)\rangle \quad (3.83)$$

Repeating the procedure of the last chapter we replace the operators by fields: $\hat{a} \to \phi(t)$, $\hat{a}^\dagger \to \phi^*(t)$, $\hat{b} \to \psi(t)$ and $\hat{b}^\dagger \to \psi^*(t)$, we apply the Doi-shift $\phi^*(t) \to \tilde{\phi}(t) + 1$ and $\psi^*(t) \to \tilde{\psi}(t) + 1$ and we plug the quasi-Hamiltonian into the the Doi-Peliti action (2.69) with the additional time derivative for $\psi(t)$.

---

[7]An auto-catalytic reaction is a process in which the presence of a given reactant acts to increase the rate of its own production [55]. Examples of auto-catalytic reactions in cell biology are: activation of the M-phase promoting factor in cell-cycle control Belousov-Zhabotinsky reaction [56]

[8]This can be seen by a dimensional analysis of the rate equations, see the following footnote

$$S[\phi, \tilde{\phi}, \psi, \tilde{\psi}] = \int dt [\tilde{\phi}(t)(\partial_t + \epsilon + \tau)\phi(t) + \tilde{\psi}(t)\partial_t\psi(t) - \tau\tilde{\psi}(t)\phi(t) - \sigma\tilde{\phi}(t) +$$
$$+ \mu\tilde{\psi}(t)\tilde{\phi}^2(t)\psi(t)\phi^2(t) + \mu\tilde{\psi}(t)\psi(t)\phi^2(t) + 2\mu\tilde{\phi}(t)\tilde{\psi}(t)\phi^2(t)\psi(t) +$$
$$- 2\mu\tilde{\phi}^2(t)\psi(t)\phi^2(t) - \mu\tilde{\phi}(t)\psi(t)\phi^2(t) - \mu\tilde{\phi}^3(t)\psi(t)\phi(t)] \quad (3.84)$$

Where again we have omitted the initial term and extended the temporal integral over the entire real axis.

3.5.1   Tree-level

Taking the Fourier transform of the bilinear part and the second derivative of the generating functional we can extract the propagators of the theory

$$\frac{\tilde{\delta}(\omega_1 + \omega_2)}{-i\omega_1 + r_0} = \underset{\longleftarrow}{\rule{3cm}{0.4pt}}$$

$$\lim_{m' \to 0}\frac{\tilde{\delta}(\omega_1 + \omega_2)}{-i\omega_1 + m'} = \sim\!\sim\!\sim\!\sim\!\sim$$

Where the mass m' has been introduce in order to mantain causality.
The other vertices with the relative coupling constants have been listed below:
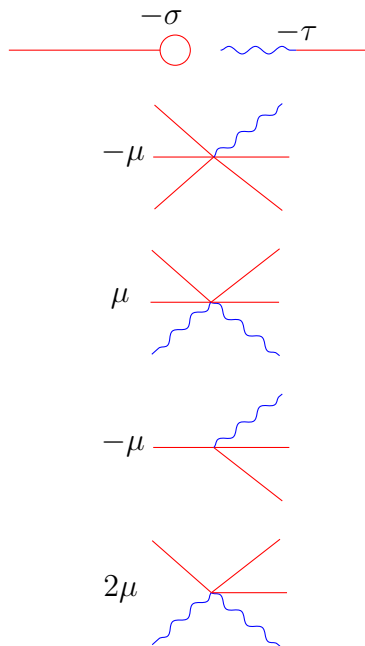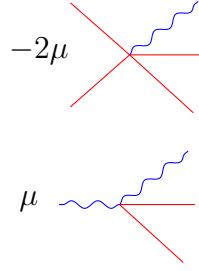
In the following we want to exploit the same shift we have applied in the previous model in order to characterise the proprieties of the stationary state.

The stationary state is defined as before by the limit:

$$\lim_{t\to\infty}\langle\phi^\dagger(t)\phi(t)\phi^\dagger(t_0)\rangle = \lim_{t\to\infty}\langle\phi(t)\tilde{\phi}(t_0)\rangle + \langle\phi(t)\rangle = \bar{\zeta}_A \tag{3.85}$$

for species A and by the limit:

$$\lim_{t\to\infty}\langle\psi^\dagger(t)\psi(t)\phi^\dagger(t_0)\rangle = \lim_{t\to\infty}\langle\psi(t)\tilde{\phi}(t_0)\rangle + \langle\psi(t)\rangle = \bar{\zeta}_B \tag{3.86}$$

Where the difference between the two comes from the fact that we are interested in measuring the density of the stationary state given that we have created something on the lattice. Particles of species B are created by mutation of species A, thus in order to observe a finite density of species B we need to place on the lattice a particle of species A.

To be precise, given that particles of species A are spontaneously created at rate σ we wouldn't need to put anything on the lattice in order to observe a finite density of both A and B. This is not relevant to the end of the calculations so we are free to take the identites above as definition of the stationary state.

For what concerns the tree-level density it is convenient to shift only one of the fields. Shifting the field $\phi(t)$ about a generic ζ, i.e. $\phi \to \hat{\phi} + \zeta$, and taking the limit of $t \to \infty$ the stationary density for A reads:

$$\langle\phi\rangle_s = \lim_{t\to\infty}\langle\hat{\phi}\rangle + \zeta \tag{3.87}$$

and for B:

$$\langle\psi\rangle_s = \lim_{t\to\infty}\langle\psi\rangle \tag{3.88}$$

For notational semplicity we drop the little hat in top of the field $\hat{\phi}$, i.e. $\hat{\phi} = \phi$, the *shift-dependent* part of the action is:

$$S_\zeta[\phi, \tilde{\phi}, \psi, \tilde{\psi}] = \int dt[\zeta(\epsilon + \tau)\tilde{\phi}(t) - \tau\zeta\tilde{\psi}(t) + \mu\zeta^2\tilde{\phi}^2(t)\tilde{\psi}(t)\psi(t)+$$

$$+ 2\mu\zeta\tilde{\psi}(t)\tilde{\phi}^2(t)\psi(t)\phi(t) + \mu\zeta^2\tilde{\psi}(t)\psi + 2\mu\zeta\tilde{\psi}(t)\phi(t)\psi(t)+$$

$$+ 2\mu\zeta^2\tilde{\phi}(t)\tilde{\psi}(t)\psi(t) + 4\mu\zeta\tilde{\psi}(t)\tilde{\phi}(t)\psi(t)\phi(t) - 2\mu\zeta^2\tilde{\phi}^2(t)\psi(t)+$$

$$-4\mu\zeta\tilde{\phi}^2(t)\psi(t)\phi(t)-\mu\zeta^2\tilde{\phi}(t)\psi(t)-2\mu\zeta\tilde{\phi}(t)\phi(t)\psi(t)-\mu\zeta^2\tilde{\phi}^3(t)\psi(t)-2\mu\zeta\tilde{\phi}^3(t)\psi(t)\phi(t)]$$

$$(3.89)$$

After the shift the massless propagator of B get a mass term: $r_b = \mu\zeta^2$, the source term for A is shifted by $+\zeta(\epsilon+\tau)$ and a number of completely new coupling appear:

$$(3.90)$$

The diagrams that contribute to the correction of the source terms are the ones, in the two jungles above, that end with one line on the left hand side.
The entire summation that one should perform to derive the correction of the source terms can again be rewritten as a recurrence relation. As the source term of species A get corrections from the source term of species B (and *vice versa*) the two recurrence relations have to be considered togheter. We are left with the system:

$$(3.91)$$

Denoting the source term of species A by A and the source term of species B by B we can write the system of diagrams above as:

$$\begin{cases} A = -\bar{\sigma} + \mu\frac{A^2 B}{\mu\zeta^2 r_a^2} + 2\mu\frac{AB}{\mu\zeta^2 r_a} + \frac{\mu\zeta^2 B}{\mu\zeta^2} \\ B = \tau\zeta - \mu\frac{A^2 B}{\mu\zeta^2 r_a^2} - 2\mu\frac{AB}{\mu\zeta^2 r_a} + \frac{\tau A}{r_a} \end{cases} \tag{3.92}$$

where $\bar{\sigma} = \zeta(\epsilon + \tau) - \sigma$.

Summing the first with the second line we obtain:

$$A = -\bar{\sigma} + \tau\zeta + \frac{\tau A}{r_a} \implies A(1 - \frac{\tau}{r_a}) = -\bar{\sigma} + \tau\zeta \tag{3.93}$$

The corrected A-source is:

$$A = -\zeta r_a + \frac{\sigma}{\epsilon}r_a \tag{3.94}$$

Which is:

 $= \frac{A}{r_a} = -\zeta + \frac{\sigma}{\epsilon}$

$$(3.95)$$

Inserting this expression in equation (3.87) we find the tree-level (mean field) stationary density for species A:

$$\langle\phi\rangle_s^{\text{tree level}} = \underline{\quad\quad\quad}\bullet = \zeta + \frac{A}{r_a} = \frac{\sigma}{\epsilon} \tag{3.96}$$

Which is the correct mean field density for species A[9]

It is now straightforward to find the stationary density for species B:

$$B = \tau\zeta - \frac{B}{\zeta^2}(\frac{A}{r_a})^2 - 2\frac{B}{\zeta}(\frac{A}{r_a}) + \tau\frac{A}{r_a} \implies B(1 + \frac{(A/r_a)^2}{\zeta^2} + 2\frac{A/r_a}{\zeta}) = \tau\zeta + \tau\frac{A}{r_a} \tag{3.97}$$

Given the expression above for $\frac{A}{r_a}$:

$$B(1 + \frac{1}{\zeta}(\frac{\sigma}{\epsilon} - \zeta))^2 = \tau\frac{\sigma}{\epsilon} \implies B = \tau\frac{\sigma}{\epsilon}\frac{\zeta^2}{(\zeta + \frac{\sigma}{\epsilon} - \zeta)^2} = \tau\frac{\epsilon}{\sigma}\zeta^2 \tag{3.98}$$

Recalling equation (3.88) we have:

$$\langle\psi\rangle_s^{\text{tree level}} = \sim\sim\sim\sim\bullet = \frac{B}{\mu\zeta^2} = \frac{\tau\epsilon}{\mu\sigma} \tag{3.99}$$

The mean field theory results have been recovered by means of a tree level expansion of the source terms.

In a future work it will be interesting to carry on with the perturbative expansion, correct the tree level vertices and perform a loop expansion in order to compare the results obtained by means of the Doi-Peliti formalism with, for example, the one obtained by means of a Van Kampen's system size expansion (Linear noise approximation, see for example [48]).

We belive that the present approach leads to better results, particularly in the biological relevant case of low density systems where standard techniques for solving the chemical master equation fail as they do not properly capture the boundary conditions [57]. In fact, the Van Kampen's system size expansion and the Kramers-Moyal expansion fail if the system size is small (low number of particles in the zero dimensional case), population can become negative because of the large fluctuations leading to misleading, non-physical results [57].

---

[9]By *correct mean field density* we mean that is the same as the one that can be found from the rate equations:

$$\frac{\partial}{\partial t}[a] = \sigma - \epsilon[a] - \tau[a] + \mu[a]^2[b]$$

$$\frac{\partial}{\partial t}[b] = \tau[a] - \mu[a]^2[b]$$

where $[a]$ and $[b]$ are the concentration of species A and B

CHAPTER 4

NUMERICAL SIMULATIONS

In this final chapter we will discuss the way we have implemented numerical simulations for the model that was under investigation in this project.
All the simulations have been performed in C and all the figures have been generated with gnuplot.

4.1 Stationary Density

Numerical simulations are a necessary and extremely useful tool in theoretical physics. The reasons why simulations are so important are quite obvious, for example they are the means by which we can check the conlusions of analytic proofs, they can do hard computations which cannot be done analytically and they give an hint on how the system behave, expecially when real experiments are difficult to perform [59] and, finally, it's fun.

Non-equilibrium phase transitions of non-integrable models, such as the one that was under investigation in this thesis, are particularly interesting to investigate by means of Monte Carlo simulations.
Numerical simulations are limited by the finiteness of computer memory, thus when one approach the problem, differences between finite and infinte systems, have always to be considered.
The stationary state of an infinite system in the active phase is characterised by a stationary density that does not fluctuate about a mean value [8]. On the other hand, in a finite system fluctuations are always present and their intensity depend upon the system size and the dimensionality of the system (see figure 4.1).
Obvioulsy, fluctuactions can be reduced either by taking a large number of realisations of the process and measuring the average over all of them or by taking large systems. In both cases the execution time increase rapidly thus the code must be written in the most efficent way.
Another difference between finite and inifinte systems is the probability of reaching the absorbing state: in a *finte* system there is always a non-zero probability to

reach the empty state and such a probability depends upon the size L of the system [8], on the other hand, in a infinte system, the stationary state is an attractor of the dynamics and thus once has been reached cannot be left.

In numerical simulations the actual realisation of the dynamics rely on the possibility to produce very long sequences of random numbers identically distribuited and mutually independent.
It is clear that in a computer simulation it is impossible to generate *truly* random numbers; however, it is possible to generate numbers that are random for all pratical purposes [59]. An ideal set of pseudo-random numbers should have the following features: the set must be *uniformly distribuited*, the set must have uncorrelated members, each number must be quickly generated.
In the present simulation we have used the *Mersenne Twister* random number generator MT19937 which generates pseudorandom integers uniformly distributed in $[0, (2^{32} - 1)]$ and has a period of $2^{19937} - 1$[1].

The simulations have been implemented as follow: we create a list where we continuously store active particles (i.e. we store the position on the lattice of each particle), the lattice is a d-dimensional array and we have imposed *periodic boundary conditions*.
Once a suitable initial configuration have been selected (see below) we set $t = 0$ and start to run the simulation. The rate that have been inserted from terminal (σ, μ, ϵ and h) are converted in probabilities, i.e. we compute the total rate, which is $R = \sum_i r_i$ where r_i is the rate of the particular process, and each event take place with probability $\frac{r_i}{R}$.[2]
At each time step all the particles on the list have the possibility to get extinct, branch, hop on a nearest neighbour or coagulate with another particle (each particle can undergoes to more then one event, coagulation assume the role of carrying capacity limiting the number of particles for each site). The decision whether a reaction occours or not is made by extracting a random number between zero and one and comparing it with the proability of the reaction. Once all the observable of interest have been recorded time is incremented by Δt until $t = t_f$. This corresponds to one realisation of the process, the number of realisations that have to be run depends upon the size of the system and the observable that has to be recordered.

For continuous time simulations at the end of each time step we draw a random number η from a uniform distribution, the waiting time dt between two consecutive events is calculated by:

$$dt = \frac{1}{R} log(\frac{1}{\eta}) \implies t \to t + dt \tag{4.1}$$

---

[1]As steated in the preamble of the file the version we have used is a recode by Shawn Cokus on March 8, 1998 of a version by Takuji Nishimura.
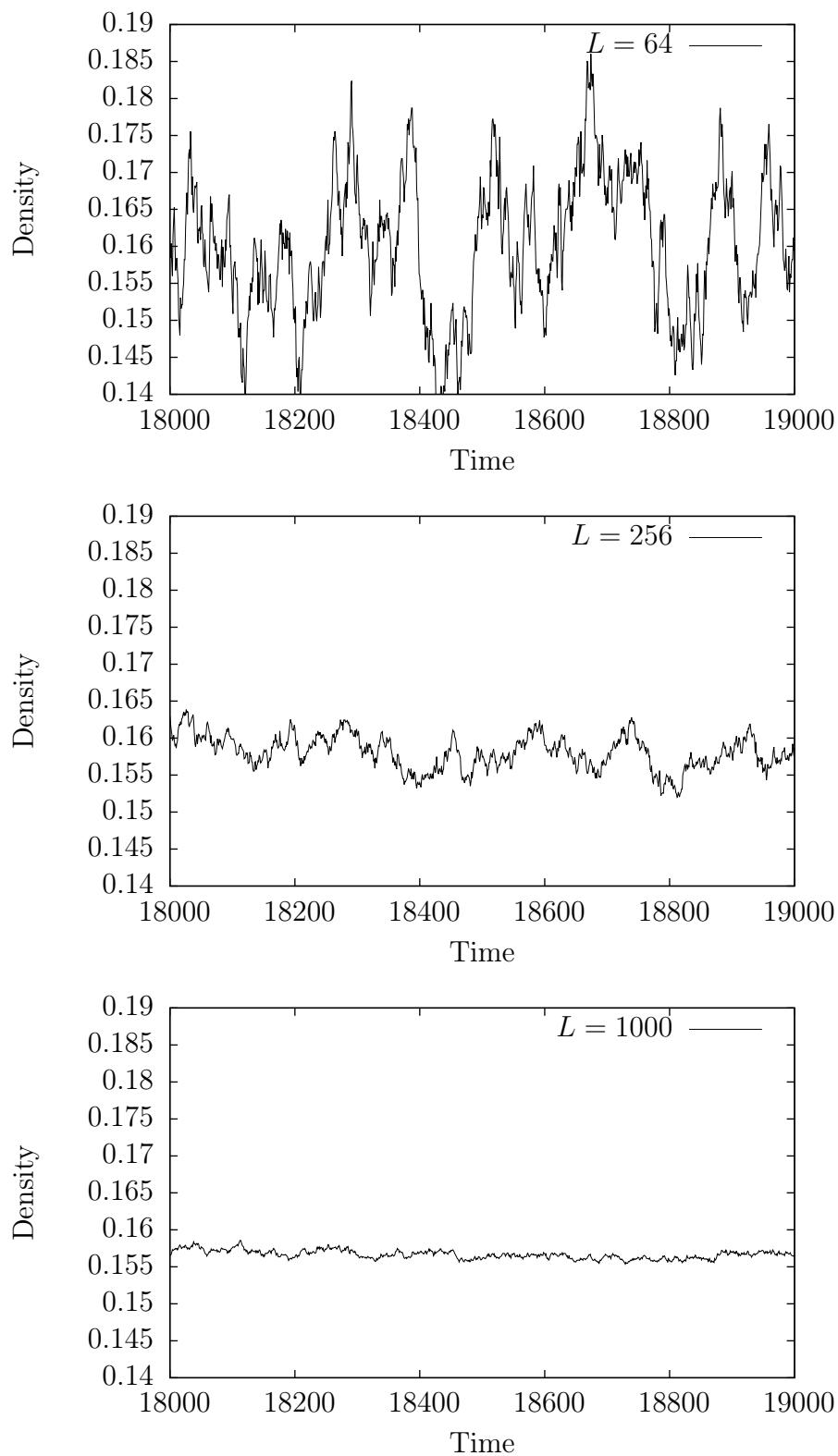[2]This is a rescale of the time scale

Figure 4.1: Role of system size:one realisation of the process on a two-dimensional square lattice with periodic boundary conditions. Parameters: $\sigma = 2, \mu = 5, \epsilon = 0.75, h = 10$
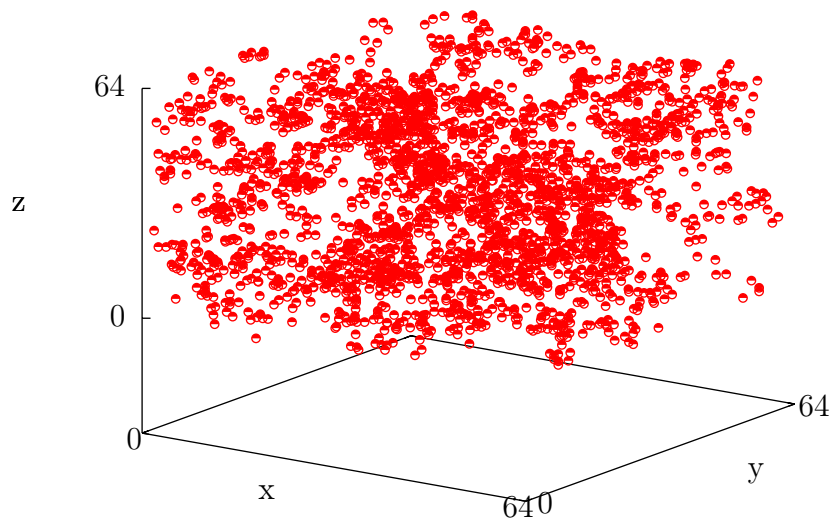
Figure 4.2: Process on a three dimensional lattice. Parameters: $L = 64, \sigma = 2, \mu = 5, \epsilon = 1.15, h = 10$

where R is the total rate.

In the theory of absorbing phase transitions simulations are usually implemented using two different initial conditions [8]:

- Homogeneous initial conditions i.e. completely full lattice.

- Single seed placed on a random position on the lattice.

the choice between the two depends upon the particular observable we are interested in.

The first observable that we need to measure is the position of the critical point as a function of ϵ keeping σ, μ and h fixed. Or equivalently the stationary density as a function of ϵ.
To this end the suitable initial codition is a fully occupied lattice; starting at t=0 we measure the decay of the *order parameter* (the density) as a function of time fine tuining the control parameter (ϵ in the present case).
In order to reduce fluctuctions as much as possible and avoid finite size effects we have two possibilities: we either run the code on a fairly big lattice, e.g. $L > 128$ and we take average over many realisations, or we run the code on a very big lattice, e.g. $L > 1000$ and take average over few realisations.
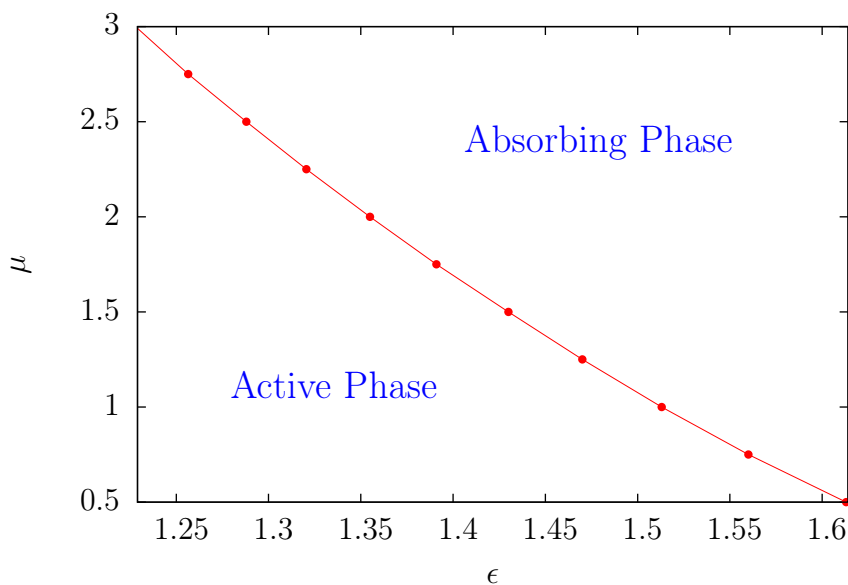
Figure 4.3: Phase diagram at $\sigma = 2$ and $h = 10$.

Figure 4.4 shows the decay of the density at the critical point in the sub- and super-critical regime, the exponent of the power law at the critical point has been measured and its value is $\delta = 0.487 \pm 0.003$.

Repeating the procedure for many values of the parameter we can draw the phase diagram with the curve that separetes the absorbing phase from the active phase (see figure 4.3).

Note that the diffusion constant D play a fundamental role in the evolution of the system in fact if one increase the hopping rate up to really big value (*e.g.*>1000) one would recover the results of the mean field theory. This feature is what in the literature is normally refered to as *well-mixing.*
This make sense looking at the diagrammatic expansion as well, the diffusion constant always appear in the denominator of the loops, if one take the limit of $D \to \infty$ the contribution of the loops would be minimum and one would recover the tree level.

4.2   Correlation Functions

Correlations play a fundemental role in systems that undergo a phase transition. A particular attention has to be given to temporal correlations as an increasing correlation time τ has drammatic consequeces on the extimation of statistical error.
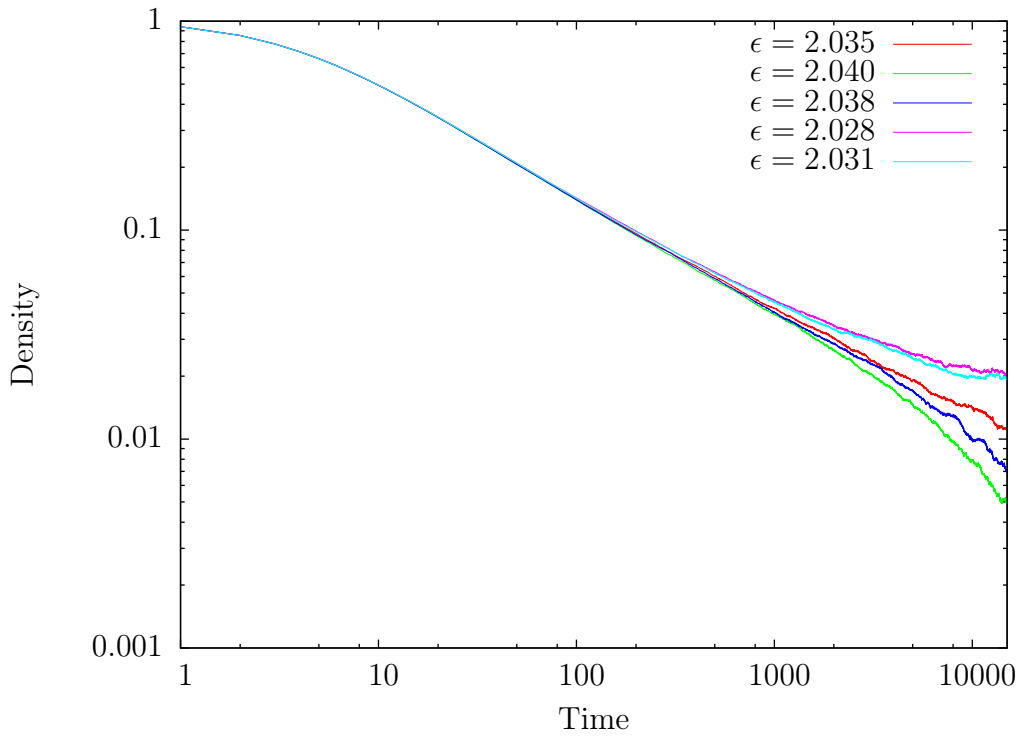
Figure 4.4: Critical decay of the density as a function of time, the critical point is at $\epsilon = 2.035$ (Green line). Parameters: $\sigma = 4$, $\mu = 5$, h=10, L=256, 100 realisations of the process.

In fact, let us consider the mean value of the density $\langle n \rangle$:

$$\langle n \rangle = \frac{1}{T} \sum_{t=t_0}^{t=t_f} n_r \tag{4.2}$$

where n_r stands for the average of the density over many realisations of the process. If the configurations at two consecutive times are correlated the statistical error cannnot be estimated simply by taking:

$$\sigma^2 \sim \frac{\langle n^2 \rangle - \langle n \rangle^2}{T} \tag{4.3}$$

because this relation requires that the measures at two consecutive times are completely uncorrelated [60], thus a more efficient techinque has to be found.

Introducing the quantity [60]:

$$\phi(\Delta t) = \frac{\sum_{t=t_0}^{t_f - \Delta t} n_t n_{t+\Delta t}}{t_f - \Delta t} - \frac{\sum_{t=t_0}^{t_f - \Delta t} n_t}{t_f - \Delta t} \frac{\sum_{t=t_0}^{t_f - \Delta t} n_{t+\Delta t}}{t_f - \Delta t} \tag{4.4}$$

the connected temporal autocorrelation function is defined as:

$$C(\Delta t) = \frac{\phi(\Delta t)}{\phi(0)} \tag{4.5}$$

In the previous definition t_0 is the time at which we start to measure correlations which is generally taken to be the time when we are sure that the system has reached a stationary state.

From figure 4.1 it appears clear that the time needed to make two measure scorrelated increase when we are near the critical point. The correlation time can be easily extrapolated by fitting with [60]:

$$C(\Delta t) \sim e^{-\frac{\Delta t}{\tau}} \tag{4.6}$$

The correlation time has a maximum at the critical point and it diverges in the thermodynamic limit ($L \to \infty$). The divergence of the autocorrelation time is an hallmark of what in dynamical system's theory is known as *critical slowing down*. One of the consequences of having a slower dynamics is that the system will need more time to recover from an external perturbation (see the response function below), for this reason critical slowing down is frequently used as an *early-warning* signal for *critical transitions*, such as earthquakes financial crisis and climate change [61].

Once one has measured the autocorrelation time by fitting the data or evaluating the integral:

$$\tau \sim \int_0^\infty C(\Delta t) \Delta t \tag{4.7}$$

the statistical error can then be evaluated by taking:

$$\sigma^2 \sim 2\tau \frac{\langle n^2 \rangle - \langle n \rangle^2}{T} \tag{4.8}$$

Note that the two definition of correlation time (4.6) and (4.7) coincide if the correalation function is exponential [60].

The one described above is not the only method to estemate the statistical error in situations where consecutive measures are correlated. Another efficient method is make use of *chunks* which are made of measurement over many iterations and realisations of the process and then bin them together. The magnitude of the error will increase increasing the number of bin, b until it saturate and this is the value that one has to choose.
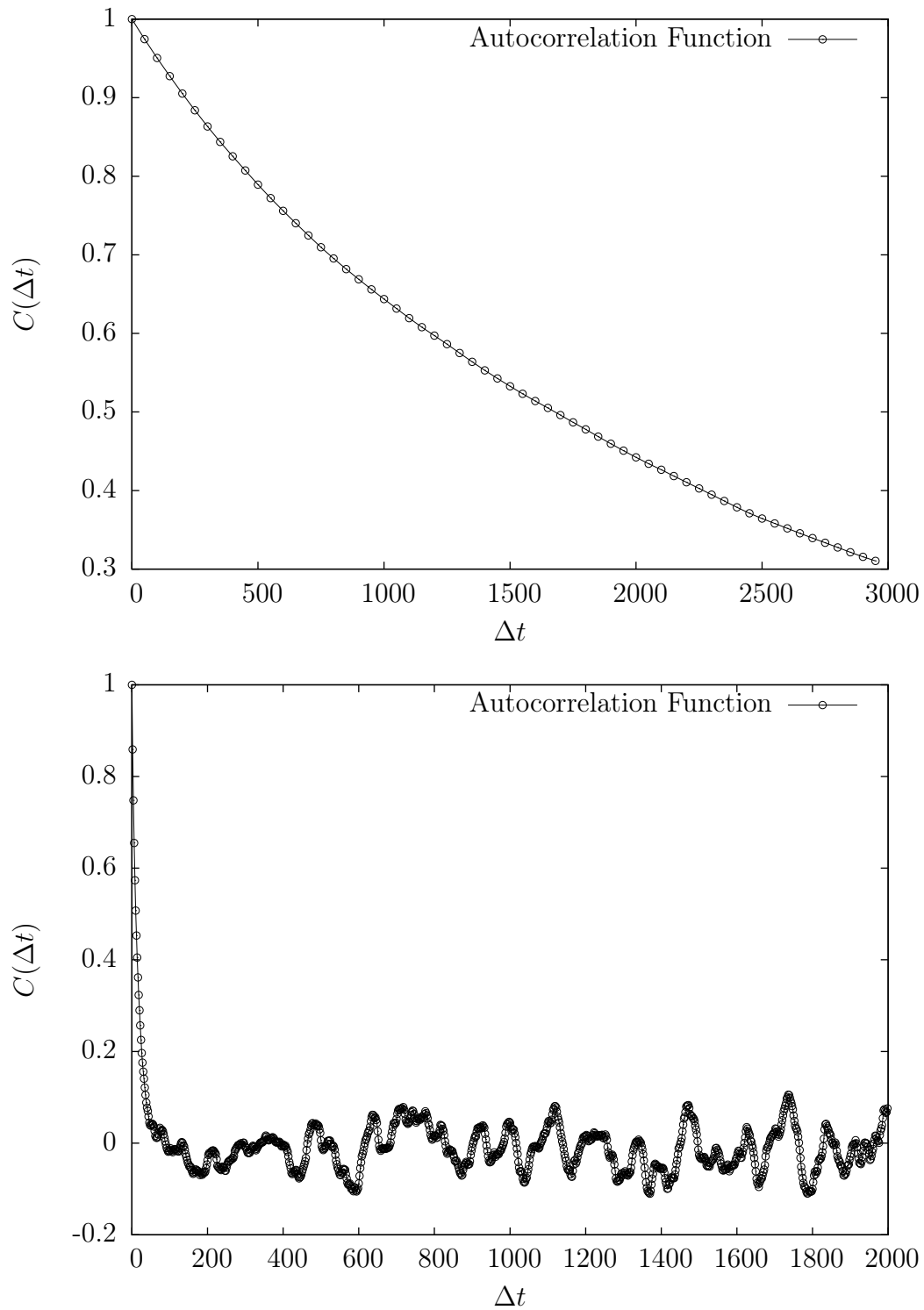
Figure 4.1: Connected temporal autocorrelation function at the critical point ($\epsilon_c - \epsilon = 0.005$) and away from criticality ($\epsilon_c - \epsilon = 0.8$). Two dimensional lattice of linear size $L = 256$.

4.3   Response Function

The response function is a measure of the averaged response of the system at site $(\mathbf{r}_1, t_1)$ to a local perturbation by an external field at point $(\mathbf{r}_0, t_0)$ [62]. Nearby a critical transition, given to the growth of the autocorrelation time the system's response to an external perturbation is way slower than the response that the system would have away from the critical point (this is another consequence of the critical slowing down, see discussion above).

Numerically the response function is measured as follow: the simulation starts with a fully occupied lattice and the system is left to reach the stationary state. At a given point in space and time $(\mathbf{r}_0, t_0)$, either random or not, a local perturbation is introduced by creating one single particle, the response function is then measured by measuring the difference between the density at point $(\mathbf{r}_1, t_1)$ with and without the perturbation at $(\mathbf{r}_0, t_0)$. This is done by measuring the density given the presence of the perturbation and subtracting the stationary density. A large amount of realisations has to be taken, normally more than 40 000, as the perturbation introduced in the system is fairly small, this makes this kind of simulation quite challanging as the measurements have to be really precise in order to observe a measurable response of the system.

In the following figures we show the response function near and away from the critical point, the evolution of the perturbation has been measured placing the perturbation in the middle of the lattice and taking measures from the perturbated point to the border of the lattice.
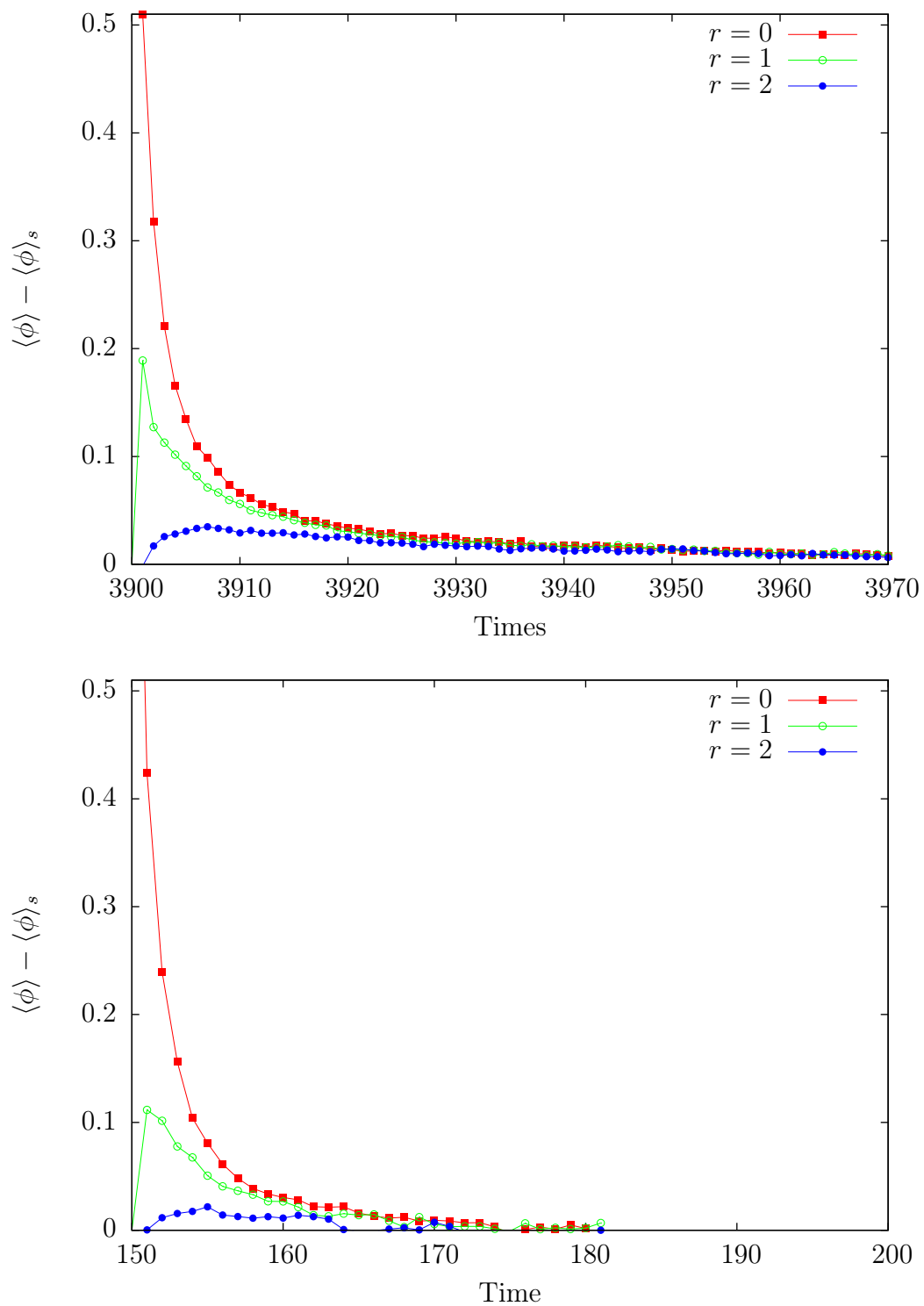
Figure 4.1: Response function as a function of time in different positions of the lattice, $r = 0$ correspond to the site that has been perturbated. $\epsilon_c - \epsilon = 0.04$ (upper figure) $\epsilon_c - \epsilon = 0.8$ (lower figure). A one can see away from the critical point really few MCS are enough to forget about the perturbation.

CONCLUSIONS

Reaction-diffusion processes can be employed to describe an immense variety of different phenomena *"... The potential applications of these ideas to systems in chemistry, biology and physics are limited only by the imagination of the reader ... "* [33].

If one goes through the literature one will immediately realise the truth of the above mentioned quote and will find tons of fantastic ideas in disparate disciplines[3].

However, although one can write down a model which is able to give an accurate description of the system under investigation, the actual solution is a challenging task because of the intrinsic stochasticity and the strength of fluctuation effects in RD systems. The integration of the master equation is generally infeasible and a straightforward approach to the problem, which consist in neglecting fluctuations and correlations (mean field theory), is not able to give a quantitative description of the process even far away from the critical domain.

In this contest the Doi-Peliti formalism supplies an elegant method which enable one to include the effects of fluctuations in the analytical description of the process. However, as outlined in [57], the Doi-Peliti formalism provides an exact description of the problem as long as one is able to sum all the involved Feynman's diagrams, an operation which is in general quite unwieldy.

In this work, field theoretical techniques, usually used for the computation of universal quantities at criticality, have been employed for the characterisation of the system's behaviour away from the critical domain. This is of particular interest in biological systems with low number of molecules where standard techinques, such as Van Kampen system size expansion or the Kramers-Moyal expansion, fail.

In order to deal with a well-defined field theory we have performed a generic shift of the field $\phi(x,t)$. The results obtained from a perturbative expansion have been explicitly proved to be independent from the particular shift that one adopt.

---

[3]The interested reader will find the following references particularly enlightening [30, 34, 35, 39, 57]

93

Furthermore, we have shown that some choices are more convenient then others and we are now free, in future works, to pick up the shift that is more suitable for the particular observable that we want to calculate.

A general definition of the stationary state in terms of a field theory has been given, equation (3.33), and a strong agreement between field theoretical calculations and Monte Carlo simulations has been found, near and away from the critical domain.
As stated in chapter 3, the one developed in this thesis is an *uncontrolled approximation scheme*, i.e. in order to obtain accurate results one has to choose the most relevant diagrams. This operation normally relies on the intuition of the researcher as we cannot know *a priori* which diagrams contain the leading contribution.

In future works we will pursue the perturbative expansion for the *brusselator*. We will include loops to extract time-dependent observables, such as correlation and response function, away from the critical domain. This will be done in small systems (low number of particles per cell) as, in this case, we will be able to compare our methods with the existing literature.

BIBLIOGRAPHY

[1] H. Hinrichsen: *Nonequilibrium Critical Phenomena and Phase Transitions into Absorbing States.* Adv. Phys. 49, 815–958, (2000)

[2] R.A. Blythe: *Nonequilibrium Phase Transitions and Dynamical Scaling Regimes.* Doctoral dissertation. The University of Edinburgh, September (2001).

[3] P. Buttá, P. Negrini: *Note del corso di sistemi dinamici.* Dipartimenti di Matematica Guido Castelnuovo, "Sapienza", Roma (2008)

[4] F. Kelly: *Reversibility and stochastic networks.*
http://www.statslab.cam.ac.uk/ frank/BOOKS/book/whole.pdf

[5] H. Hinrichsen: *Physics of Complex Systems.* Lecture notes, Theoretische Physik III Lehrstuhl fur Physik und Astronomie Fakultat fur Universitat Wurzburg (2015).

[6] N.G. Van Kampen : *Stochastic Processes in Physics and Chemistry.* Third edition. North Hollan Personal Library (1981).

[7] H.J. Jensen,P. Sibani: *Stochastic Dynamics of Complex Systems. From Glasses to Evolution.* Series on Complexity Science-Vol. 2. Imperial College Press (2013).

[8] M. Henkel,H. Hinrichsen,S. Lubek:*Non-Equilibrium Phase Transitions. Volume I:Absorbing Phase Transitions.* Springer Theoretical and Mathematical Physics (2008)

[9] P. Calabrese and A. Gambassi: *Ageing Properties of Critical Systems.* J. Phys. A: Math. Gen. **38** R133 (2005).

[10] K. Huang: *Meccanica statistica.* Zanichelli editore (1997).

[11] K.A. Takeuchi,M. Kuroda,H. Chaté and M. Sano: *Experimental realization of directed percolation criticality in turbulent liquid crystals.* Phys. Rev. E **80**, 051116 (2009).

[12] G. Pruessner:*Self Organised Criticality. Theory Models and Characterisation.* Cambridge, Cambridge University Press (2012).

[13] G. Grinstein and M.A. Mufioz: *The Statistical Mechanics of Absorbing States.* Fourth Granada Lectures in Computational Physics Lecture Notes in Physics Volume 493, pp 223-270, (1997).

[14] C. R. Doering and D. Avraham: *Interparticle distribution functions and rate equations for diffusion-limited reactions* Phys. Rev. A 38, 3035 (1988)

[15] M. Le Bellac: *Quantum and Statistical Field Theory.* Oxford University Press (1991).

[16] M.E.J. Newman: *Power laws, Pareto Distribution and Zipf's Law.* Contemporary Physics 46 (2005)

[17] Ma Shang-Keng: *Modern Theory of Critical Phenomena.* Reading, Mass: W.A. Benjamin, Advanced Book Program, (1976).

[18] R. K. P. Zia and B. Schmittmann: *A possible classification of non-equilibrium steady states.* J.Phys. A: Math. Gen. **39** L407-L413 (2006).

[19] J. Cardy: *Scaling and Renormalisation in Statistical Physics.* Cambridge, Cambridge University Press, (1996)

[20] P. Clifford and A. Sudbury: *A model for spatial conflict.* Biometrika 60(3), 581, (1973).

[21] R. Holley and T. M. Liggett: *Ergodic Theorems for Weakly Interacting Infinite Systems and the Voter Model.* Ann. Probab, vol 3, No. 4, 643-663, (1975).

[22] T.E. Harris: *Contact interactions on a lattice.* Ann. Probab. Volume 2, Number 6, 969-988 (1974).

[23] J. Marro,R. Dickman: *Nonequilibrium Phase Transitions in Lattice models.* Cambridge University Press, (1999)

[24] T.M. Ligget: *Interacting particle systems.* Springer-Verlag, New York (1985).

[25] R. Durret: *Lecture Notes on Particle Systems and Percolation.* Wadsworth and Brooks/Cole, PacificGrove, CA (1988).

[26] C. Bezuidenhout, G. Grimmett: *The Critical Contact Process Die Out.* Ann.Probab. **18**,1462 (1990).

[27] I. Jensen: *Critical Behaviour of the Pair-Contact Process.* Phys. Rev. Lett., 70:1465, (1993).

[28] T. Vojta, A. Farquhar and J. Mast: *Infinite-Randomness Critical Point in the Two-Dimensional Contact Process.* Phys.Rev.E **79**, 011111 (2009).

[29] M.A. Munoz, G. Grinstein and Y. Tu: *Survival probability and field theory in systems with absorbing states.* Phys. Rev E V. 56, N. 5 (1997).

[30] E. Frey: *Evolutionary game theory: Theoretical concepts and applications to microbial communities.* Physica A 389 (2010)

[31] A. Szolnoki, M. Mobilia, L.L.Jiang, B. Szczesny, A. M. Rucklidge, M. Perc: *Cyclic dominance in evolutionary games: a review* Downloaded from http://rsif.royalsocietypublishing.org on the 2nd of July 2015.

[32] H. Cheng,N. Yao,G.Huang,J. Park and Y.-C.Lai: *Mesoscopic Interactions and Species Coexistence in Evolutionary Game Dynamics of Cyclic Competitions.* Scientific Reports | 4 : 7486 | DOI: 10.1038/srep07486 (2014)

[33] J. Cardy: *Renormalisation Group Approach To Reaction-Diffusion Problems.* arXiv:cond-matter9607163v2, (1996).

[34] J. Cardy: *Field theory and nonequilibrium statistical mechanics* (1999). URL http://www-thphys.physics.ox.ac.uk/people/JohnCardy/notes.ps.

[35] A. Winkler: *Analytic Approaches to Stochastic Many-Particle Systems Scaling and Renormalization in Microbial Communities and in Chemical Kinetics.* Doctoral dissertation Munich (2012)

[36] M.Doi: *Stochastic theory of diffusion-controlled reaction.* J . Phys. A: Math. Gen., Vol. 9.. No. 9, (1976)

[37] M. Doi: *Second quantization representation for classical many-particle system.* J. Phys. A:Math. Gen. Vol. 9 No. 9 (1976).

[38] L. Peliti: *Path integral approach to birth-death processes on a lattice.* J. Phys. (Paris) **46**, 1469-1483 (1985).

[39] U.C. Tauber: *Critical Dynamics*, Cambridge University Press, Cambridge, UK (2014)

[40] C.F. Lee: *Stochastic dynamics of reaction-diffusion systems: An epidemic model case study.* Talk at the Complexity Forum, Warwick University (2013)

[41] J. Cardy:*Introduction to Quantum Field theory.* Michaelmas Term 2010 – Version 13/9/10.

[42] S. Nekovar,G. Pruessner: *Field Theory of the Wiener Sausage.* arXiv: 1407.7419 [cond-mat.stat-mech] (2014).

[43] B.P. Lee: *Critical Behavior in Nonequilibrium Systems* PhD Thesis: University of California at Santa Barbara 1994; URL: http://www.eg.bucknell.edu/bvollmay/leethesis.pdf

[44] U.C. Tauber,M. Howard,B.P. Vollmayr-Lee: *Applications of Field-Theoretic Renormalization Group Method to Reaction-Diffusion Problems*, J. Phys. A 38,R 79(2005)

[45] U.C. Tauber: *Population oscillations in spatial stochastic Lotka–Volterra models: a field-theoretic perturbational analysis.* J. Phys. A: Math. Theor. **45** 405002 (2012).

[46] U.C. Tauber: *Field-Theoretic methods.* arXiv 0707.0794v1. [cond-math.stat-mech] (2007).

[47] M. Beccaria, B. Alles and F. Farchioni: *Coherent-state path-integral simulation of many-particle systems.* Phys. Rev. E **55** 3870 (1997).

[48] P. Thomas, C. Fleck, R. Grima and N. Popović: *System size expansion using Feynman rules and diagrams.* J. Phys. A: Math. Theor. 47 (2014).

[49] A.M. Buice,J.D. Cowan:*Field-theoretic approach to fluctuation effects in neural networks.* Phys.Rev. E 75, 051919 (2007)

[50] P. Sollich: *Diagrams for dynamics: some basis.* Short course in "Diagrammatic methods for dynamics", King's College London (2001).

[51] J. Zinn-Justin: *Quantum Field Theory and Critical Phenomena.* Clarendon Press-Oxford (1993).

[52] H. Kleinert, V. Schulte-Frohlinde: *Critical Properties of ϕ^4 Theories.* Freie Universitt Berlin (2001).

[53] U.J. Wiese: *An introduction to lattice field theory.*Background Material for Lectures presented at the Summer School for Graduate Students "Foundations and New Methods in Theoretical Physics" in Saalburg, Septem- ber 7 – 11, 2009

[54] I. Prigogine, R. Lefever, A. Goldbeter and M.H. Kaufman: *Symmetry Breaking Instabilities in Biological Systems.* Nature **223**, 913-916 (1969).

[55] R.P. Boland,T. Galla, A.J. McKane: *How Limit Cycles and Quasi-Cycles are Related in Systems With Intrinsic Noise.* Journal of statistical Mechanics: Theory and Experiment (2008).

[56] R. Ramaswamy and I. F. Sbalzarini: *Intrinsic noise alters the frequency spectrum of mesoscopic oscillatory chemical reaction systems.* Scientific Reports | 1 : 154 | DOI: 10.1038/srep00154 (2011).

[57] F. Peruani and C.F. Lee: *Fluctuations and the role of collision duration in reaction-diffusion systems.* EPL, 102 (2013)

[58] F. Benitez, N. Wschebor: *Branching and annihilating random walks: Exact results at low branching rate.* Phys. Rev. E **87**, 052132 – Published 28 May 2013

[59] G. Parisi: *Principles of Numerical Simulations*. E.Brézin and J.Zinn-Justin, eds. Les HouchesmSession XLIX (1988).

[60] L.M. Barone,E. Marinari,G. Organtini,F. Ricci-Tersenghi: *Programmazione Scientifica. Linguaggio C, Algoritmi e Modelli nella Scienza*. Pearson Education Italia (2006).

[61] M. Scheffer,J. Bascompte,W.A. Brock,V. Brovkin,S.R. Carpenter,V. Dakos,H. Held,E.H. Van Nes,M. Rietkerk,G. Sugihara: *Early Warning Signal for Critical Transitions*. Nature **461**, 53-59 (2009)

[62] H.Hinrichsen: *Is local scale invariance a generic property of ageing phenomena?*. Journal of Statistical mechanics:theory and experiments (2006).